Spring 6-21-2019

The Role of MRGPRX2/Mrgprb2 in Regulating Mast Cell Function

Ibrahim S. Alkanfari
aibra@upenn.edu

The Role of MRGPRX2/Mrgprb2 in Regulating Mast Cell Function

Abstract
Mast"cells"(MCs)"are"derived"from"bone"marrow"pluripotent"hematopoietic" stem" cells" and" are" located" in" close" proximity" to" the" external" environment." MCs" expresses"several"receptors"on"their"surface"such"as"the"high"affinity"IgE"receptor" (Fc!RI)"and"G"ProteinECoupled"Receptors"(GPCRs)."MRGPRX2"is"a"GPCR,"which" consists"of"seven"transmembrane"domains"and"is"expressed"exclusively"in"MCs" but" no" other" immune" cells." This" receptor" is" activated" by" multiple" amphipathic" ligands" including" neuropeptides," US" Food" and" Drug" Administration" (FDA)E approved"peptidergic"drugs"and"host"defense"peptides"such"as"LL_37."HDPs"also" known" as" antimicrobial" peptides" (AMPs)" have" been" investigated" in" depth" as" an" alternative"to"overcome"antibiotic"resistance"crisis."However,"their"susceptibility"to" degradation,"cytotoxicity"and"high"production"expenses"have"limited"their"use."To" overcome" these" limitations," nonEpeptide" small" molecule" HDP" mimetics" (smHDPMs)" that" structurally" resemble" the" AMPs" properties" but" have" better" stability"and"less"cytotoxicity"have"been"developed."We"utilized"five"smHDPMs"and" found" that" these" compounds" demonstrated" its" ability" to" activate" MCs" via" MRGPRX2."This"raises"an"interesting"possibility"that"its"function"as"antimicrobial" agent"could"be"as"a"result"of"harnessing"MCs"host"defense"functions"beside"their" antimicrobial"activities.""

MCs" can" also" participate" in" chronic" inflammatory" diseases" when" innate" immunity" is" dysregulated." Rosacea" is" a" chronic" skin" disease" that" is" common" among"middle"aged"Caucasians."Human"rosacea"skin"samples"exhibited"higher"

number"of"MCs"compared"to"normal"subjects."AMP"LL37"and"neuropeptide"(NP)" substance"P"(SP)"are"upregulated"in"rosacea."LL37"and"SP"activate"MCs"through" MRGPRX2"in#vitro.#Utilizing"Mrgprb2"knockout"mice"(Mrgprb2E/E)"we"demonstrated" a" reduction" in" erythema" presentation," inflammatory" cell" recruitment," MMP+9" and" CXCL+2"mRNA"expression"compared"to"WT"mice"following"intradermal"injection" of" LLE37" and" SP" to" rosacea" model." Calcium" signaling" is" essential" for" MC" degranulation" and" function." In" this" dissertation" we" present" an" evidence" that" STIM1/Orai1" plays" an" important" role" in" MRGPRX2" mediated" calcium" influx" and" mediators"release"when"stimulated"with"LLE37"and"SP.""

Moreover,"this"dissertation"showed"naturally"occurring"missense"mutations" of" MRGPRX2" both" within" and" outside" the" receptor's" predicted" ligand" binding" pocket" (G165E," D184H," W243R" and" H259Y)" renders" it" unresponsive" neuropeptides," HDPs" and" peptidergic" drugs" for" MC" degranulation." Thus," individuals" harboring" these" mutations" may" develop" resistance" to" drugEinduced" allergic"reactions"and"rosacea"but"may"display"increased"susceptibility"to"microbial" infection.""

Degree Type
Thesis

The Role of MRGPRX2/Mrgprb2 in

Regulating Mast Cell Function

DScD candidate: Ibrahim Alkanfari

Mentor: Prof. Hydar Ali

Acknowledgments

I would like to express my sincere gratitude and appreciation to my mentor Dr. Hydar Ali for all of his support throughout this program. You have been a tremendous mentor to me and nothing would be possible without your guidance, positivity, and dedication.

My sincere appreciation extends to Dr. Jonathan Korostoff, Dr. Kathleen Boesze-Battaglia, and Dr. Faizan Alawi for serving as my committee members, and for taking the time out of their busy schedules to meet with me. Also for their guidance and valuable inputs.

I would also like to thank Dr. Dana Graves and Dr. Jordan-Sciutto for granting me acceptance into the DScD program.

I would like to thank Dr. Ali's lab members past and present who contributed directly to this work. It has been a privilege to work with you and learn from you all.

Last but not least, all the thanks to my family and friends for their unconditional support throughout this journey. Without you I would not be able to do this.

Abstract

Mast cells (MCs) are derived from bone marrow pluripotent hematopoietic stem cells and are located in close proximity to the external environment. MCs expresses several receptors on their surface such as the high affinity IgE receptor (FcεRI) and G Protein-Coupled Receptors (GPCRs). MRGPRX2 is a GPCR, which consists of seven transmembrane domains and is expressed exclusively in MCs but no other immune cells. This receptor is activated by multiple amphipathic ligands including neuropeptides, US Food and Drug Administration (FDA)-approved peptidergic drugs and host defense peptides such as LL_37. HDPs also known as antimicrobial peptides (AMPs) have been investigated in depth as an alternative to overcome antibiotic resistance crisis. However, their susceptibility to degradation, cytotoxicity and high production expenses have limited their use. To overcome these limitations, non-peptide small molecule HDP mimetics (smHDPMs) that structurally resemble the AMPs properties but have better stability and less cytotoxicity have been developed. We utilized five smHDPMs and found that these compounds demonstrated its ability to activate MCs via MRGPRX2. This raises an interesting possibility that its function as antimicrobial agent could be as a result of harnessing MCs host defense functions beside their antimicrobial activities.

MCs can also participate in chronic inflammatory diseases when innate immunity is dysregulated. Rosacea is a chronic skin disease that is common among middle aged Caucasians. Human rosacea skin samples exhibited higher

number of MCs compared to normal subjects. AMP LL37 and neuropeptide (NP) substance P (SP) are upregulated in rosacea. LL37 and SP activate MCs through MRGPRX2 *in vitro.* Utilizing Mrgprb2 knockout mice (Mrgprb2$^{-/-}$) we demonstrated a reduction in erythema presentation, inflammatory cell recruitment, *MMP-9* and *CXCL-2* mRNA expression compared to WT mice following intradermal injection of LL-37 and SP to rosacea model. Calcium signaling is essential for MC degranulation and function. In this dissertation we present an evidence that STIM1/Orai1 plays an important role in MRGPRX2 mediated calcium influx and mediators release when stimulated with LL-37 and SP.

Moreover, this dissertation showed naturally occurring missense mutations of MRGPRX2 both within and outside the receptor's predicted ligand binding pocket (G165E, D184H, W243R and H259Y) renders it unresponsive neuropeptides, HDPs and peptidergic drugs for MC degranulation. Thus, individuals harboring these mutations may develop resistance to drug-induced allergic reactions and rosacea but may display increased susceptibility to microbial infection.

Table of Contents

List of Abbreviations

. AD: Atopic dermatitis

. AMPs: Antimicrobial peptides

. APCs: Antigen presenting cells

. BMMCs: Bone marrow mast cells

. BSA: Bovine serum albumin

. CLP: Cecal Ligation and Puncture

. CP: Chronic periodontitis

. Cpd: Compound

. CTMCs: Connective tissue mast cells

. CU: Chronic urticaria

. EC: Extracellular

. ER: Endoplasmic reticulum

. FA: Facially amphiphilic

. GAPDH: glyceraldehyde 3-phosphate dehydrogenase

. GPCRs: G protein coupled receptors

. hBD3: human β-defensin 3

. HDPMs: Host defense peptidomimetics

. HDPs: Host defense peptides

. HK-1: Hemokinin-1

. HSCs: Homeiopotic stem cells

. IC: Intracellular

. IF: Immunofluorescence

. IHC: Immunohistochemistry

. IL-3: Interleukin-3

. KLK5: Kallikerin 5

. MCs: Mast cells

. MICs: Minimal inhibitory concentrations

. MMCs: Mucosal mast cells

. MMP-9: Matrix metalloproteinase- 9

. Mrgprb2$^{-/-}$: Mrgprb2 knockout

. Mrgprb2: Mas-related G protein coupled receptor b2

. MRGPRX2: Mas-related G protein coupled receptor X2

. NPs: Neuropeptides

. PMCs: Peritoneal mast cells

. PNAG: p-nitrophenyl-N-acetyl-β-D-glucosamine

. PTx: Pertussis toxin

. RT-PCR: Real time PCR

. SCF: Stem cell factor

. SOC: Store Operated Ca^{2+} channel

. SP: Substance P

. STIM1: Stromal interaction molecule 1

. TM: Transmembrane

. TNF: Tumor necrotic factor

. TRPV4: Transient receptor potential vanilloid 4

. VEGFs: vascular endothelial growth factors

. WT: Wild type

Chapter 1: Introduction

MCs originate from bone marrow hematopoietic stem cells (HSCs) and circulate in an immature form unlike most immune cells. The final differentiation of MCs take place in tissue and depends on activation of KIT by stem cell factors (SCF) [1]. Defective expression of KIT receptor results in a dramatic reduction in MC number in mice [2]. Other cytokines such as Interleukin-3 (IL-3) secreted by fibroblast cells and endothelial cells are also a key factor for MC progression into a mature form [2]. MCs reside in all vascularized tissue in close proximity to external stimuli such as skin and respiratory tract. They are long-lived cells that don't undergo further division in terminal tissue. However, MCs recruitment is increased in inflammatory conditions as a result of migration of the progenitor cells. This process is regulated by the expression of surface receptors such as integrin on MC progenitors and other surface proteins on the endothelium such as VCAM-1 [3].

MCs are known for their role in anaphylaxis reaction and allergic diseases. However, their role in innate and adaptive immunity has become a topic of interest for many researchers. Their strategic location allows MCs to be one of the first responders in innate defense to any pathogens, allergen or toxin encounter [4]. This location also enables the MCs to interact with blood vessels by releasing factors such as IL-8, TNF-α, histamine, and vascular endothelial growth factors (VEGFs) which contribute to the local vascular permeability and recruitment of

other immune cells at the infection site [5]. Echtenacher et al. [6], demonstrated that MC-deficient mice were less efficient in clearing enterobacteria and had greater morbidity than control mice. Moreover, TLR4 MC-deficient mice have been shown to have higher morbidity in Cecal Ligation and Puncture (CLP) model of innate immunity compared to WT mice. This was explained as MC TLR4 knockout mice lost their ability to recruit neutrophils in the peritoneal cavity [7]. In addition to innate immune cell recruitment, MCs can participate in innate defense through other mechanisms such as antimicrobial peptide (AMP) release. AMPs can directly kill microbes by disrupting their cell membrane [8]. Other mediators such as proteases can also help in breaking down microbial virulence factors or toxins such as snake venom toxin and neutralize it [9].

MC protective functions are not only limited to their role in innate immunity, but it also extends to their ability to induce adaptive immune response as well. A MC-deficient mouse model was used in many studies to elaborate MC role in adaptive immunity. Previous studies [10, 11], demonstrated that T cell activation was impaired in MC-deficient mice compared to controls. This was correlated with a reduction in dendritic cell migration to the lymph nodes [10, 11]. Also, the production of chemokines such as CCL20 by MCs probably contributes to DC progenitors recruitment into tissue [12]. Furthermore, MCs can act as antigen presenting cells (APCs) to T-cells as they express MHCI and co-stimulatory molecules. MHC I dependent cross-presentation of antigen to $CD8^+$ T-cells has been shown to promote $CD8^+$ T-cells activation and proliferation. This raises the

possibility that MCs play a role as APCs in inducing $CD8^+$ T cells function in infection [13].

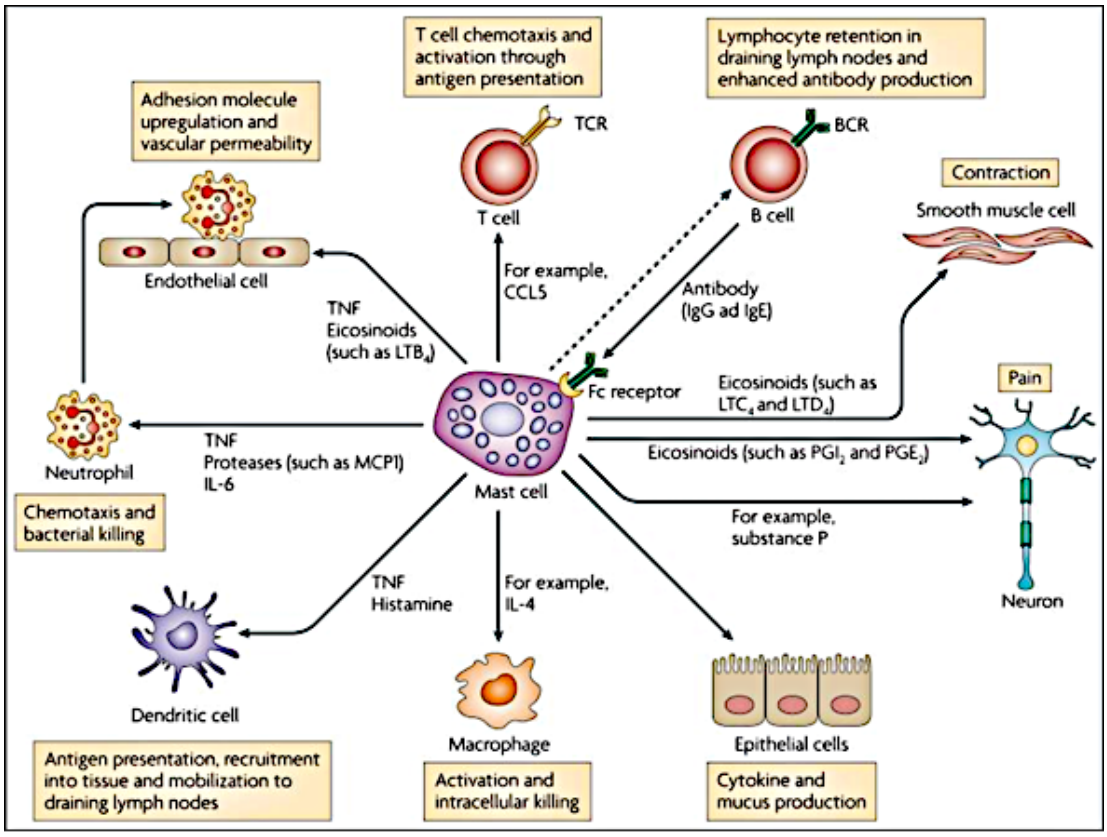

Fig 1: Mast cell role in host defense. (S.Abraham et al 2015)

MC also contributes to the pathogenesis of many diseases. As previously mentioned, MC are well-known for their role in anaphylaxis reaction and asthma, these occur when MCs respond inappropriately to innocuous antigens. Sensitization occurs with the initial exposure, but the clinical manifestations arise later after re-exposure to the same antigen. Moreover, MCs are involved in the pathogenesis of other chronic inflammatory diseases such as chronic periodontitis (CP), chronic urticaria (CU), and atopic dermatitis (AD). In CP, the

periodontopathogenic bacteria trigger the immunopathologic response which in conjunction with the bacterial virulence factors, results in the destruction of the periodontium. The number of MCs has been shown to be increased in CP patients compared to healthy or gingivitis patients [14]. Also, the severity of CP has been correlated to the degree of MC density and degree of degranulation [15]. Moreover, MC-deficient mice were protected against *Porphyromonas gingivalis*–induced alveolar bone loss compared to WT [16].

Similarly, the significant role of MCs in patients with CU and AD, was emphasized by the increase in number or activity in the affected tissue [17]; and utilizing anti-histamine and MC stabilizers helped in alleviating the signs and symptoms of CU and AD [18, 19]. One of the important aspects in the pathogenesis of AD and CU is the interaction between MCs and nerve fibers. It is now generally accepted that MC activation by neuropeptides (NPs) contributes to neurogenic inflammation, pain, and itch [20]. The increase in the activity of the MC results in the release of the proteases, leukotrienes, and histamine that in turn induce nerve endings to release neuropeptides and exacerbate the inflammation (Fig. 2) [21-24]. Moreover, the serum level of substance P (SP), a neuropeptide that has been implicated in several chronic inflammatory skin diseases such as rosacea, is increased and its level correlated with the disease activity in those patients [25, 26]. Therefore, besides the protective function of the MC, it has a role in chronic inflammatory diseases when inappropriately activated.

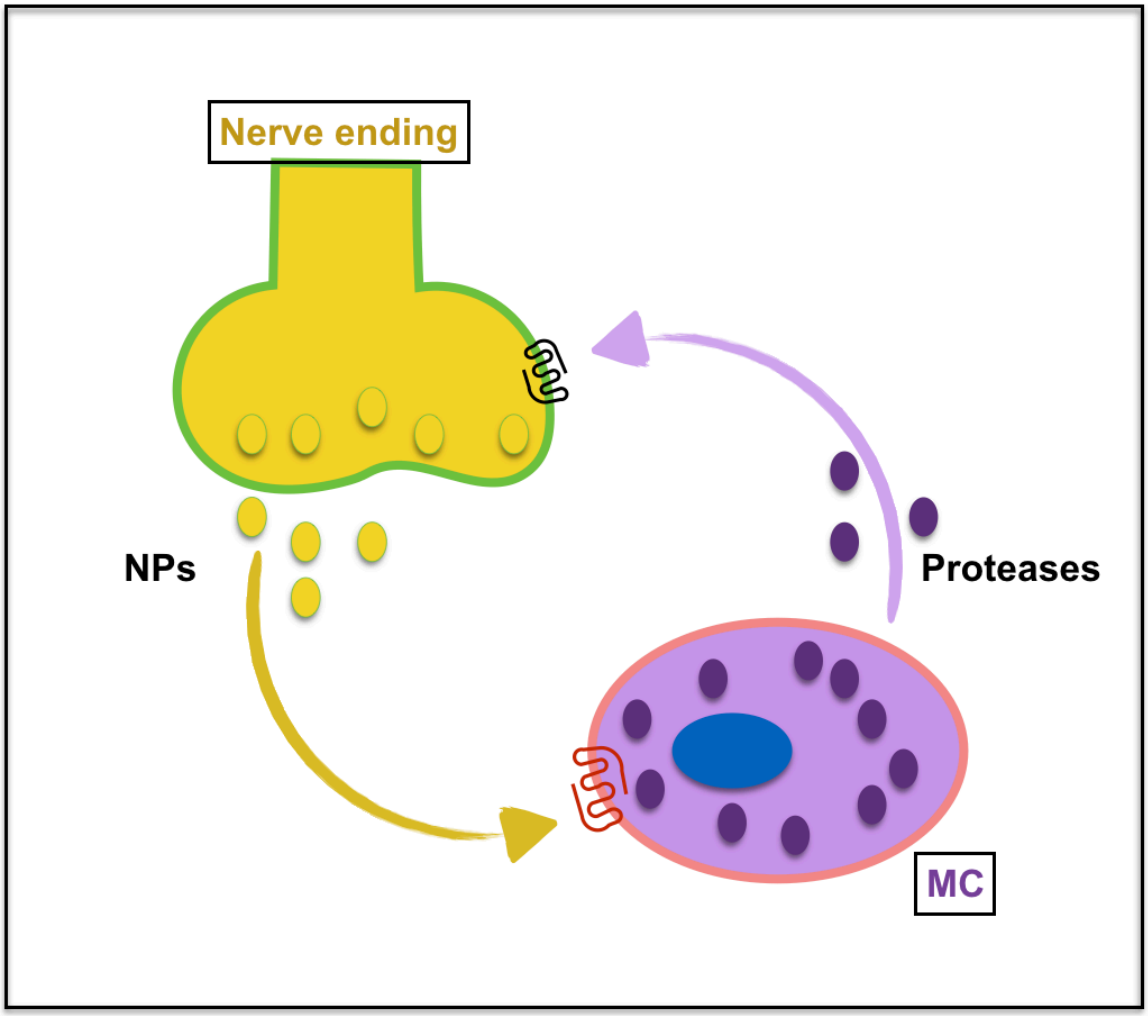

Fig 2: bidirectional interaction between nerve ending and MC.

The role of MCs in both normal and disease conditions is determined by mediators release and their abundance in the tissue. The release of different preformed granules or de novo production of mediators depends on several molecular pathways that are determined by the threshold and magnitude of MCs activation [27, 28]. The cytoplasmic granules contain biogenic amines (histamine), proteases (tryptase and chymase), lysosomal enzymes (β-hexosaminidase), cytokines (TNF and SCF), and proteoglycans (heparin and chondroitin sulfates) [28-32]. MCs express a vast array of cell surface receptors that regulate MC

activation, migration, and proliferation. At the initial activation of MCs, they release a large quantity of lipid-derived inflammatory mediators. Later after initial stimulation, activation of transcriptional factors result in enhancement of gene expression of a variety of cytokines that have different effects on the surrounding or distal environment [33].

However, the general concept that activation of the MC through those receptors only induces robust degranulation is only partially correct. This simplified view of MCs activation has been challenged by several studies. The outcome of the receptor activation could vary; for example, the outcome of MC activation via high-affinity IgE receptor (FcεRI) depends on the antigen concentration and affinity. In low concentration of antigen, it results in more chemokine production without degranulation. Whereas high antigen concentration or affinity results in both chemokine production and degranulation [34]. This is due to the ability of the MCs to trigger different signaling cascades based on the nature of the stimuli even with the same receptor. Therefore, the magnitude of the responses can be variable. Moreover, while MCs are well known for their proinflammatory properties, they can also have strong immunosuppressive effects directly or indirectly [35, 36]. Thus, MCs possess both proinflammatory and immunosuppressive effect which help in restoring homeostasis at the infection sites after pathogen clearance to prevent excessive inflammation and facilitate wound healing.

There are two categories of MCs based on their granule proteases content. The first type that is mostly found in skin is Tryptase and Chymase expressing

MCs also known as MC_{TC}. On the other hand, MCs that are found in the lung and respiratory tract are predominantly Tryptase-expressing mast cells (MC_T) [37]. In mice, there are two types of MCs: connective tissue type MCs (CTMCs) and mucosal type MCs (MMCs) that resemble MC_{TC} and MC_T, respectively. Although both types of MCs are activated through high-affinity IgE receptor; MC_{TC} and its mouse counterpart CTMCs showed to be activated in IgE-Independent manner by a wide variety of compounds such as C3a, C5a, Host Defense Peptides (HDPs) and 48/80 whereas MC_T and MMCs are not [38].

Besides FcεRI, MCs express several G proteins coupled receptors (GPCRs) which are characterized by seven transmembrane (7TM) domains, and as the name implies, are associated with heterotrimeric G proteins that coupled to the intracellular domains of the receptor. GPCRs constitute the largest class of receptors in eukaryote [39]. Recently it has been shown that a diverse group of amphipathic cationic peptides such as HDPs, NPs and FDA approved drugs activate MCs through a Mas-related GPCR known as MRGPRX2 [40-42]. As opposed to many other G protein-coupled receptors, MRGPRX2 has been shown to be predominantly expressed in MCs [43]. Among the five superfamilies of GPCRs, MRGPRX2 belong to the rhodopsin family, or class A, which comprises 85% of the entire superfamily [44].

In mice, there are 22 MRG GPCR possible coding genes, so it was challenging to identify the mouse ortholog of the human MRGPRX2. McNeil and his group [40] utilized a stringent reverse transcriptase polymerase chain reaction

in mouse peritoneal MCs (PMCs) and found that Mrgprb2 transcript was the only MRG GPCR detected. The same group was then conducted a series of functional experiments such as histamine release and calcium assays to confirm the genetic finding. The results showed that ligands which are known to activate human MCs through MRGPRX2 also activated the murine PMCs through this receptor but not in Mrgprb2 mutated PMCs [40]. Therefore, Mrgprbrb2 is considered to be the mouse ortholog of the human MRGPRX2.

MRGPRX2 and Mrgprb2 are expressed predominantly in MC_{TC} and CTMC, respectively. Although they are now considered as the basic secretagogue receptor in MCs, they do have differences with respect to agonist concentration required for their activation. EC_{50} values (concentration required to give 50% response) of most of the ligands are lower for MRGPRX2 than in the murine Mrgprb2. For instance, 48/80 EC_{50} value for human MC is 470 nM, whereas murine MC require 3.5 μM [40, 45]. This difference in concentration could be attributed to the difference in amino acid sequence between the two receptors. The overall sequence similarity is only ≈53%; with N-terminal and C-terminal sequence similarity at only ≈34% and ≈47% sequence similarity, respectively. According to homology modeling studies of different GPCR, extracellular (EC) and transmembrane extracellular domains (TM-EC) contribute to agonist binding whereas intracellular (IC) domains are involved in G protein coupling [46]. Thus, the variances in amino acids sequence between the two receptors might affect the ability of different ligands to activate both receptors equally.

In the following chapters, I will discuss the role of MRGPRX2 in host defense and the chronic inflammatory disease specifically, rosacea. I will also elaborate on how understanding the structure of this receptor can help further our understanding about its role in regulating MC activation.

Specific Aims

1-Specific Aim 1: To determine if non-cytotoxic synthetic smHDPMs that display antifungal and antibacterial activity promote human MC degranulation through MRGPRX2/Mrgprb2.

2-Specific Aim 2:

- **<u>2A:</u> To determine MRGPRX2 expression in human skin MCs in rosacea and to modulate experimental rosacea model by targeting Mrgprb2 *in vivo.***

- **<u>2B:</u> To determine the role of STIM1/Orai calcium channel on MRGPRX2 mediated mast cells activation and degranulation.**

3-<u>Specific Aim 3:</u> To identify the structural components of MRGPRX2 which interact with multiple ligands that induce pseudo-allergy and chronic diseases.

Chapter 2: Small-Molecule Host-Defense Peptide Mimetic antibacterial and antifungal agents activate human and mouse mast cells via Mas-Related GPCRs

Ibrahim Alkanfari [1], Katie B. Freeman [2], Saptarshi Roy [1], Tahsin Jahan [1], Richard W. Scott [2] and Hydar Ali [1,*]

[1] Department of Pathology, University of Pennsylvania, School of Dental Medicine, Philadelphia, PA-19104, USA; aibra@upenn.edu (I.A.); roysapta@upenn.edu (S.R.); Jtahsin@pennmedicine.upenn.edu (T.J.)

[2] Fox Chase Chemical Diversity Center, Doylestown, PA-18902, USA; kfreeman@fc-cdci.com (K.B.F.); rscott@fc-cdci.com (R.W.S.)

This chapter was published in Cells special issue (Mast cells in inflammation and immunity)

Abstract

Host-defense peptides (HDPs) have an important therapeutic potential against microbial infections but their metabolic instability and cellular cytotoxicity have limited their utility. To overcome these limitations, we utilized five small-molecule, nonpeptide HDP mimetics (smHDPMs) and tested their effects on cytotoxicity, antimicrobial activity, and mast cell (MC) degranulation. None of the smHDPMs displayed cytotoxicity against mouse 3T3 fibroblasts or human transformed liver HepG2 cells. However, one compound had both antifungal and antibacterial activity. Surprisingly, all five compounds induced degranulation in a human MC line, LAD2, and this response was substantially reduced in Mas-related G protein-coupled receptor-X2 (MRGPRX2)-silenced cells. Furthermore, all five compounds induced degranulation in RBL-2H3 cells expressing MRGPRX2 but this response was abolished in cells expressing naturally occurring loss-of-function missense variants G165E (rs141744602) and D184H (rs372988289). Mrgprb2 is the likely mouse ortholog of human MRGPRX2, which is expressed in connective tissue MCs (CTMCs) such as cutaneous and peritoneal MCs (PMCs). All five smHDPMs induced degranulation in wild-type PMCs but not in cells derived from Mrgprb2$^{-/-}$ mice. These findings suggest that smHDPMs could serve as novel agents for the treatment of drug-resistant fungal and bacterial infections because of their ability to harness CTMCs' host defense functions.

Introduction

MCs are granulated immune cells of hematopoietic origin that are widely distributed in tissues such as the skin and mucosal tissues that interact with the environment. Although MCs are best known for their roles in IgE-mediated allergic reactions, their most important functions likely include tissue homeostasis, host defense, and wound healing [47-50]. MCs display considerable heterogeneity based on their tissue localization, protease composition of their secretory granules, development pattern, and cell surface receptor expression. In humans, skin MCs are known as MC_{TC} because their secretory granules contain both tryptase and chymase but those present in the lung are known as MC_T because their secretory granules contain only tryptase [51]. In rodents, skin MCs resemble human MCTC and are referred to as connective tissue MCs (CTMCs) but lung MCs resemble human MCT and are known as mucosal MCs (MMCs). Interestingly, CTCMs contain abundant heparin in their granules but MMCs do not.

MCs are sometimes referred to as constitutive (innate) and mucosal (adaptive) not only based on their tissue distribution and granularity, but also on their development patterns and expression of cell surface receptors [52, 53].Thus, innate MCs (MC_{TC} and CTMCs) are present constitutively in connective tissues and are generally unaffected by T cells and express the cell surface receptor, Mas-related G protein-coupled receptor X2 (MRGPRX2 human) and Mrgprb2 (mouse) [40]. By contrast, adaptive MCs are found predominantly in intraepithelial tissues (lung, gut), are induced by T-cell-dependent inflammation, and do not express

MRGPRX2/Mrgprb2 [37, 40, 43]. It has been proposed that innate/constitutive MCs contribute to tissue homeostasis and host defense to bacterial infection through their degranulation and the subsequent recruitment of neutrophils and dendritic cells [6, 50, 54-56]

Infections by fungal organisms are associated with a wide spectrum of diseases ranging from acute self-limiting manifestations in immunocompetent individuals to allergy and severe life-threatening infections in immunocompromised patients [57]. Recently, there has been a tremendous increase in the incidence of fungal infection, which is attributed to the overuse of prophylactic antifungal therapy and increased resistance to these drugs [58-60]. Antibiotics have been used for treatment of bacterial infections since the early 1900s but the emergence of multidrug-resistant strains of microbes poses a tremendous public health concern globally [61]. Thus, there is an urgent need to develop a novel therapy for the treatment of fungal infection and infection caused by antibiotic-resistant bacteria.

Antimicrobial peptides (AMPs), also known as host-defense peptides (HDPs), represent an evolutionarily ancient mechanism of innate immunity found in both animal and plant kingdoms [62-64]. These peptides are cationic amphiphiles and provide protection against a variety of organisms including bacteria, fungi, and parasites [63, 65]. The cationic charge on HDPs provides electrostatic attraction with the anionic surface of microbial membrane and the hydrophobic surface mediates entry into the membrane leading to their death.

Selectivity of HDPs for microbial pathogens versus mammalian cells is attributed to differences in membrane charge, phospholipid composition, and the presence of unique cell membrane and cell wall protein components [66]. However, many HDPs that have antimicrobial activity *in vitro* have limited efficacy *in vivo*; this is likely due to the ability of negatively charged host proteins to neutralize the positive charges on these peptides [42].

Synthetic HDPs and those generated in transgenic plants harness MCs' innate immune function by promoting their degranulation through MRGPRX2 [42, 67]. HDPs also regulate angiogenesis and promote wound healing [68, 69]. These novel mechanisms of action are attributed to the low risk of developing resistance and thus appear to provide ideal therapeutic targets. However, chemical synthesis of HDPs is prohibitively expensive and postsynthetic modifications such as cyclization, disulfide bond formation, and folding may be inadequate for optimal antimicrobial activity [70]. In addition, HDPs are metabolically unstable and display cytotoxicity and these properties have limited their clinical utility [71]. To overcome these limitations, a series of small-molecule HDP mimetics (smHDPMs) has been developed [71, 72]. These compounds are relatively inexpensive to synthesize and have distinct advantages over HDPs in terms of stability, bioavailability, and low toxicity. Furthermore, these compounds exhibit potent activity against both bacteria and fungi [73]. However, the possibility that smHDPMs harness MCs' immunomodulatory properties via inducing their degranulation has not been tested.

The purpose of this study was to determine if noncytotoxic synthetic smHDPMs that display antifungal and antibacterial activity promote human MC degranulation via MRGPRX2. Although Mrgprb2 was originally identified as the mouse ortholog of human MRGPRX2 in CTMCs [40], a recent study demonstrated that Mrgprb1, Mrgprb10, and Mrgprc11 are also expressed in MCs [74]. Another goal of this study was to determine which of the mouse Mas-related G protein-coupled receptors (GPCRs) contribute to degranulation in response to smHDPMs. Two naturally occurring missense MRPGRX2 variants, G165E and D184H, display loss-of-function phenotype for MC activation by a number of ligands including the HDP, human β-defensin-3 [75]. We also sought to determine the effects of MRGPRX2 missense mutation on MC activation by smHDPMs. The data presented herein suggest that smHDPMs that harness MCs' immunomodulatory properties may serve as novel antifungal and antibacterial agents. However, individuals harboring MRGPRX2 missense mutations G165E and D184H may display susceptibility to infection because of their inability to harness MC-mediated immunity.

Materials and Methods

Mice

C57BL/6 (WT) mice were obtained from the Jackson Laboratory (Bar Harbor, ME). Mrgprb2$^{-/-}$ mice in C57BL/6 background were generated by CRISPR-Cas9 mediated deletion of Mrgprb2 in CRISPR-Cas9 core facility of the University of Pennsylvania. Four pairs of guide RNA (GR1: CaccGCT GCTCCTATTCTGGTCAGG GGG and AaacCCTGACCAGAATAGGAGCAGC; GR2: Cacc GACACTGAGTGTCTATATGG AGG and AaacCCATATAGACACTCAGTGTC; GR3: Cacc GGTTGTAAAAATGGTCCACA CGG and AaacTGTGGACCATTTTTACA ACC; GR4: CaccGAATACTTTTTCTTATCCGTG TGG and AaacCACGGATAAGAA AAAGTATTC) specifically bind to exon2 of Mrgprb2 and were injected into the fertilized eggs to generate Mrgprb2$^{-/-}$ mice. Genomic DNA was isolated from the WT and Mrgprb2$^{-/-}$ mice using the Qiagen DNeasy Blood and Tissue Kit according to the manufacturer's protocol and genotyped using the following primer pair:

Forward ATGAGTGGAGATTTCCTAATCAAGAATCT

Reverse GCTCTGAACAGTTTCCAGTTCTTCAGGGT

The resulted PCR products were run in 1.5% agarose gel and visualized using Kodak 4000MM image station.

Mice were housed in pathogen-free cages on autoclaved hardwood bedding. Seven- to twelve-week-old male and female mice were used in this study. All experiments were approved by the Institutional Animal Care and Use Committee at The University of Pennsylvania.

Materials

All cell culture reagents and DNP-specific mouse IgE (SPE-7) were purchased from Invitrogen (Carlsbad, CA). Recombinant murine interleukin-3 (IL-3), stem cell factor (SCF), and recombinant human SCF were purchased from Peprotech (Rocky Hill, NJ). DNP-BSA and p-nitrophenyl-N-acetyl-β-D-glucosamine (PNAG) were from Sigma-Aldrich (St. Louis, MO), Compound 48/80 was from AnaSpec (Fremont, CA). Amaxa transfection kit (Kit V) was purchased from Lonza (Gaithersburg, MD). PE anti-human MRGPRX2 antibody was purchased from Biolegend (San Diego, CA). Polyclonal MRGPRX2 Ab was purchased from Novus Biologicals (Littleton, CO). HRP-conjugated anti-rabbit IgG was from Cell Signaling Technologies (Danvers, MA). West Pico Chemiluminescent Substrate was from Thermo Scientific (Rockford, IL). DNeasy Blood and Tissue Kit was purchased from Qiagen (Germantown, MD). QuikChange II Site-Directed Mutagenesis Kit was purchased from Agilent Genomics (Santa Clara, CA). Plasmid encoding hemagglutinin (HA)-tagged human MRGPRX2 in pReceiver-MO6 vector was obtained from GeneCopoeia (Rockville, MD). Antimicrobial peptidomimetics (compound 1, compound 2,

compound 3, compound 4, and compound 5) were obtained from Fox Chase Chemical Diversity Center (Doylestown, PA).

Fungus MIC assay

Fungal strains included a clinical isolate of *Candida albicans* (ATCC GDH2346), *Aspergillus fumigatus* (ATCC MYA-3626), and *Aspergillus flavus* (ATCC 204304). Minimum inhibitory concentration (MIC) assays were carried out in 96-well plates using the Clinical and Laboratory Standards Institute (CLSI) method C27-A3 for *C. albicans* and M38-A2 for *Aspergillus* species [32]. smHDPMs, each in stock solutions of 10 mM in DMSO, were diluted in 50 µl RPMI/MOPS pH 7.0 in a 96-well plate and 50 µl of diluted yeast were added to each well. Final DMSO concentrations in the assay did not exceed 1%. The plate was then incubated at 35°C for 48 h. The MIC was determined as the lowest concentration of an antimicrobial agent that substantially inhibits the growth of the organism. All MIC assays were performed in duplicate.

Bacterial MIC assay

smHDPMs were tested for antibacterial activities against three Gram-negative bacteria (*Escherichia coli* [ATCC 25922], *Pseudomonas aeruginosa* [ATCC 10145], and *Klebsiella pneumonia* [ATCC 13883]) and two Gram-positive bacteria (*Staphylococcus aureus* [ATCC 27660] and *Enterococcus faecalis* [ATCC 29212]) using the Hancock modified broth assay [76, 77]. Three milliliters cation-adjusted Mueller–Hinton medium was inoculated with 20 µl of frozen bacterial

stock and incubated at 37 °C on a shaker platform (250 rpm) overnight. The suspension was diluted to approximately 5 × 10^5 cfu/ml and inoculated into a polypropylene (Costar) 96-well, round-bottom plate (90 µl volumes). Compound stock solutions were prepared in DMSO and serial twofold dilutions of compounds were made in 0.01% acetic acid, 0.2% bovine serum albumin directly in the wells of the polypropylene plate at 10 µl/well (final concentrations of 100, 50, 25, 12.5, 6.25, 3.13, 1.56, 0.78, 0.39, 0.19, 0.098, and 0.049 µg/ml). DMSO concentrations did not exceed 1% in the assay. All samples were done in duplicate. One set of control wells included broth-only samples with dilution buffer for testing sterility and providing blank values for the assay readings. Vehicle-control wells containing the bacterial suspension with DMSO (no compound) were also included. Following the overnight incubation (18 hours), the cell growth was assessed by observing the presence of “acceptable growth”, defined by CLSI as a ≥2 mm button or definite turbidity. MIC was defined as the lowest concentration where acceptable growth is not observed.

Cytotoxicity assays

Cytotoxicity (50% effective concentration, CC_{50}) was determined against mouse 3T3 fibroblasts (ATCC CRL-1658) and human transformed liver HepG2 cells (ATCC HB-8065) using an MTS viability assay according to the manufacturer's protocol (Promega CellTiter 96 aqueous nonradioactive cell proliferation assay). Briefly, 3T3 cells were seeded at 2 × 10^4 cells/well in Dulbecco’s modified Eagle’s medium (DMEM) supplemented with 10% bovine calf

serum and HepG2 cells were seeded at 3 × 10^4 cells/well in MEM supplemented with 10% fetal bovine serum. After 24 hours of growth, the culture medium was replaced with medium lacking serum, and eight two-folds dilutions of each of the five compounds were added. Compound stock solutions were prepared in methanol and final methanol concentrations in the assay did not exceed 10%. Following incubation for 1 hour at 37 °C, compound solutions were removed and medium containing serum was replenished. Viability was determined by addition of the tetrazolium compound, MTS, and the electron coupling agent, PMS, and then incubation at 37 ° C for 2 hours (3T3 cells) or 3 hours (HepG2 cells) followed by absorbance measurements at 490 nm [78]. The CC_{50} was calculated using GraphPad Prism software (nonlinear fit).

Mast cell culture

The human mast cell line, LAD2, was maintained in complete StemPro-34 medium supplemented with L-glutamine (2 mM), penicillin (100 IU/ml), streptomycin (100 µg/ml), and 100 ng/ml recombinant human stem cell factor (rhSCF). Hemidepletions were performed weekly with media containing rhSCF (100 ng/ml) [79]. Rat basophilic leukemia (RBL-2H3) cells were maintained as monolayer cultures in DMEM supplemented with 10% FBS, L-glutamine (2 mM), penicillin (100 IU/ml), and streptomycin (100 µg/ml) [80]. Peritoneal mast cells (PMCs) were obtained from 6–8 weeks C57BL/6 and Mrgprb2$^{-/-}$ (C57BL/6 background) mice using i.p. injection of 8 ml MC disassociation medium that was made of HBSS with 3% FCS and 10 mM HEPES. The cells were cultured in

Iscove's Modified Dulbecco's Medium (IMDM) supplemented with 10% FCS, murine IL-3 (10 ng/ml), and murine SCF (30 ng/ml) [81]. After 48 hours, the medium and the suspended cells were removed and replaced with fresh medium containing murine IL-3 (10 ng/ml) and murine SCF (30 ng/ml). The floating cells were then used for the experiment within 2–3 weeks [82]. Bone-marrow-derived mast cells (BMMCs) were harvested by flushing bone marrow cells from the femurs of C57BL/6 mice and culturing the cells for 4–8 weeks in IMDM supplemented with 10% FCS, murine IL-3 (10 ng/ml). The cells were then used within 4–8 weeks.

Lentivirus-mediated knockdown of MRGPRX2 in LAD2 cells

Lentivirus generation was performed in HEK293T cells as per manufacturer's instructions. Transduction of virus particles in LAD2 cells was performed as described previously [67]. Briefly, LAD2 cells (5×10^6) in 3.5 ml of medium were mixed with 1.5 ml viral supernatant at 37 °C for 8 hours. Cells were centrifuged and cultured in the virus-free medium. Antibiotic selection (puromycin 2 µg/ml) was initiated 16 hours after post-treatment. Cells were used for the assay four days after the initiation of antibiotic selection.

Western blotting to determine MRGPRX2 expression

Cell lysates were prepared from scrambled control and MRGPRX2 shRNA transduced LAD2 cells in RIPA buffer and protein was quantified using BCA protein assay kit (Thermo Scientific). Protein was separated in SDS-PAGE (10 %), transferred in PVDF membrane, and incubated overnight with anti-MRGPRX2

antibody (1:500) in blocking buffer (5% skim milk in PBS). This was followed by incubation with HRP conjugated anti-rabbit IgG (1:1000) and development by West Pico Chemiluminescent Substrate.

Transfection of RBL-2H3 cells and flow cytometry

Cells (2 ×10^6) were transfected with plasmids (2 µg/µl) encoding MRGPRX2 or MRGPRX2 missense mutants using the Amaxa kit V using Amaxa Nucleofector device according to the manufacturer's protocol [75]. For stable transfection, cells were cultured in the presence of G-418 (1 mg/ml) and used within one month of transfection. For transient transfection, cells were used within 16–20 h after transfection. To detect MRGPRX2 expression, cells (1 × 10^6) were incubated with the PE-conjugated anti-MRGPRX2 antibody, washed in FACS buffer, fixed, and analyzed on a BD LSR II flow cytometer [75].

Degranulation Assay

RBL-2H3 cells (5 × 104), LAD2 cells (10 × 104), and PMCs (5 ×103), BMMCs (5 × 104), were seeded into 96-well plates in a total volume of 50 µl HEPES buffer containing 0.1% bovine serum albumin (BSA) and exposed to ligands for 30 minuts. Cells without treatment were designated as control. In some experiments, cells were treated with Pertussis toxin (PTx). For total β-hexosaminidase release, unstimulated cells were lysed in 50 µl of 0.1% Triton X-100. Aliquots (20 µl) of supernatants or cell lysates were incubated with 20 µl of 1 mM p-nitrophenyl-N-acetyl-β- D-glucosamine for 1 hour at 37 °C. The reaction was

stopped by adding 250 µl of a 0.1 M Na2CO3/0.1 M NaHCO3 buffer and absorbance was measured at 405 nm.

Statistical analysis

Data shown are mean ± SEM values derived from at least three independent experiments. Statistical significance was determined by nonparametric t-Test and one- or two-way ANOVA. Error bars represent mean ± SEM. Differences were considered statistically significant at a value *p ≥ 0.05, **p ≥ 0.01, and ***p ≥ 0.001 and ****p ≥ 0.001. Data were analyzed by GraphPad Prism version 6.07.

Results

Antifungal and cytotoxic activities of smHDPMs (compounds 1, 2, and 3) against Candida albicans, Aspergillus fumigatus, and Aspergillus flavus

HDPs are a diverse group of agents that are isolated from organisms across the phylogenetic spectrum. Despite this diversity, a hallmark of these peptides is that they display facially amphiphilic (FA) architecture in which the cationic groups and hydrophobic groups segregate into the opposite sides of the molecular backbone. It is thought that positive charges on the HDPs and anionic surface of microbial membrane provide recognition and the subsequent hydrophobic interaction perturbs membrane structure and function leading to microbial death [58]. A series of novel FA synthetic compounds based on a meta-phenylene backbone has been synthesized and tested for antimicrobial activity. Many of these

compounds display antifungal activity *in vitro* and *in vivo* with little cytotoxic activity for mammalian cells [76]. We initially used three FA synthetic smHDPMs, namely compound 1, compound 2, and compound 3, with similar hydrophobic backbones but different cationic residues (Fig. 1A).

Minimal inhibitory concentrations (MICs) against *Candida albicans, Aspergillus fumigatus,* and *Aspergillus flavus* were determined. Compound 2 showed the highest antifungal activity with MIC value of 0.39 μg/ml. Compound 1 exhibited moderate antifungal activity against *Aspergillus fumigatus* with MIC value of 12.5–50 μg/ml but potent activity against *Candida albicans* and *Aspergillus flavus* with MIC values between 0.78 μg/ml and 6.25 μg/ml. By contrast, Compound 3 displayed poor antifungal activity with MIC > 100 μg/ml (Fig. 1B). In order to determine the cytotoxicity of smHDPMs, we used two cell lines HepG2 and 3T3 cells and measured CC_{50} values. Compound 3 displayed cytotoxicity at concentrations similar to those required for antifungal activity. However, at concentrations that are relevant for antifungal activity, Compounds 1 and 2 displayed little to no cytotoxic effects on 3T3 and HepG2 cells (Fig. 1B).

smHDPMs (Compounds 1, 2, and 3) activate human MCs via MRGPRX2

To determine if smHDPMs that display differences in antifungal activity stimulate human MCs, we tested the effects of Compounds 1, 2, and 3 on degranulation in a human MC line, LAD2, by quantitating the release of the enzyme β-hexosaminidase. Surprisingly, we found that while two of the three compounds

had antifungal activity (Fig. 1A), all three compounds induced robust β-hexosaminidase release (Fig. 2A).

To determine if the effects of these compounds are mediated via the activation of Gαi family of G proteins, we incubated cells with pertussis toxin (PTx). As shown in Fig. 2A, degranulation in response to all three compounds was substantially inhibited by PTx, indicating the involvement of G proteins. HDPs induce degranulation in human MCs via MRGPRX2 [62, 65, 69]. To determine if these compounds also activate human MCs via MRGPRX2, we silenced its expression in LAD2 cells with lentiviral shRNA. Compared to the control-shRNA transduction, MRGPRX2-shRNA transduction resulted in a substantial reduction of MRGPRX2 expression as demonstrated by Western blotting (Fig. 2B). Furthermore, degranulation induced by all three compounds was significantly inhibited in MRGPRX2-silenced cells when compared to control shRNA transduced cells (Fig. 2C). RBL-2H3 is a rodent MC line that has been used to study IgE-mediated responses in vitro. Unlike LAD2 cells, it does not express MRGPRX2 and is unresponsive to its ligands. We therefore used RBL-2H3 cells stably expressing MRGPRX2 to confirm the role of this receptor on smHDPM-induced responses in MCs. As shown in Fig. 3A, all compounds (3 μM) induced 40–50% degranulation in MRGPRX2-expressing cells but not in untransfected cells. RBL-2H3 cells expressing MRGPRX2 were used to determine the EC50 value for the smHDPMs. The EC_{50} values were 0.8 μM, 3 μM, and 1.8 μM for Compound 1, 2, and 3, respectively (Fig. 3, B–D).

Effects of Compounds 2, 4, and 5 on antibacterial activity and MC degranulation

We subsequently selected the most potent antifungal compound and its two derivatives for antibacterial screening against an array of bacteria (Fig. 4A). Compound 2 showed potent antibacterial activities against one Gram-negative bacteria, *Escherichia coli*, and Gram-positive bacteria, *Staphylococcus aureus*, with MIC values of 3.1 and 0.1 µg/ml, respectively, which can be correlated with its potent antifungal activity (Fig. 4B). However, this compound showed poor antibacterial activity against *Klebsiella pneumoniae*, *Pseudomonas aeruginosa, and Enterococcus faecalis*.

Two derivatives of Compound 2 (Compound 4 and Compound 5) showed poor antibacterial activity against all the bacterial strains tested (Fig. 4B). Cytotoxicity of these three compounds was tested against two cells lines HepG2 and 3T3 cells. CC_{50} value of Compound 2 was 124 µM and 151 µM in mouse 3T3 and human HepG2 cells, respectively (Fig. 4B). Compound 4 and 5 were 2–10-fold less cytotoxic than Compound 2. These compounds were then tested for their ability to activate MCs by MRGPRX2. We used RBL-2H3 cells stably expressing MRGPRX2 for these studies. As shown in Fig. 5A, Compound 4 and Compound 5 (3 µM) induced 20–25 % degranulation in MRGPRX2-expressing cells but not in untransfected cells. Cells expressing MRGPRX2 were further used to determine

the EC_{50} value for these smHDPMs. The EC_{50} values for Compounds 4 and 5 were 0.4 μM and 0.38 μM, respectively (Fig. 5, B–C).

smHDPMs activate murine MCs via Mrgprb2

Although Mrgprb2 was originally identified as the mouse ortholog of human MRGPRX2 in CTMCs [40], a recent study demonstrated that Mrgprb1, Mrgprb10, and Mrgprc11 are also expressed in these MCs [74]. McNeil et al. [40] utilized zinc finger nuclease-based strategy to generate a mouse line with four-base-pair deletion in Mrgprb2 coding region ($Mrgprb2^{MUT}$). For our studies, we used CRISPR/Cas9 technology to delete *Mrgprb2* in C57BL/6 mice. Deletion of the *Mrgprb2* was confirmed by genotyping (Fig. 6A). Furthermore, as expected, the absence of Mrgprb2 in mouse PMCs had no effect on antigen/IgE-mediated degranulation (Fig. 6B) but almost completely abolished the response to compound 48/80, a polymer known to activate MCs via Mrgprb2 (Fig. 6C). All five smHDPMs induced degranulation in wild-type PMCs but this response was abolished in PMCs derived from $Mrgprb2^{-/-}$ mice. BMMCs, which do not express Mrgprb2 [40], did not respond to compound 48/80 or any of the smHDPMs tested despite their normal responsiveness to antigen/IgE for degranulation (Fig. 6D). These findings demonstrate that all five smHDPMs used in this study induce degranulation in mouse CTMCs via the activation of Mrgprb2.

Naturally occurring missense MRGPRX2 variants D184H, G165E are resistant to activation by smHDPMs

G protein-coupled receptors contain 7-transmembrane bundles that are connected by three extracellular loops (ECL1, ECL2, and ECL3) and three intracellular loops (ICL1, ICL2, and ICL3). The extracellular part also includes the N-terminus (N-term) and the intracellular (IC) part includes the helix VIII and a C-terminal sequence. GPCRs can be divided into modules; the EC and their closest TM regions have the greatest structural diversity and are responsible for the binding of diverse ligands. By contrast, the IC and its closest TM regions are responsible for G protein coupling and downstream signaling[77]. Recently, we screened eight naturally occurring missense variants within MRGPRX2's ECL and TM domains from publicly available databases and found that two variants, D184H and G165E, displayed loss-of-function phenotype for activation by a number of ligands including the HDP, human β-defensin-3 [75]. We therefore sought to determine if these variants display loss-of-function phenotype for MC activation by smHDPMs. For this, RBL-2H3 cells were transfected with cDNAs encoding wild-type, D184H, and G165E variants. Flow cytometry analysis demonstrated that wild-type and mutant receptors are expressed on the cell surface at equivalent levels (Fig. 7A). However, all five smHDPMs induced degranulation in cells expressing wild-type, but not the D184H or G165E variants (Fig. 7B).

Discussion

The recent increase in the incidence of fungal infection has been attributed to the overuse of prophylactic antifungal therapy and increased resistance to these drugs [58-60]. Furthermore, although antibiotics have been used for the treatment of bacterial infections since the early 1900s, the emergence of multidrug-resistant strains of microbes poses a tremendous public health concern globally [61]. Thus, there is an urgent need to develop novel therapy for the treatment of infections caused by drug-resistant microbes. HDPs have important therapeutic potential against bacterial, viral, and fungal infections but their metabolic instability, poor tissue distribution, and cellular cytotoxicity have limited their utility [70, 71]. To overcome these limitations, synthetic smHDPMs have been developed, which display broad-spectrum antimicrobial activity both *in vitro* and *in vivo* with low cytotoxicity [78, 83-86]. Based on these findings, it has been proposed that smHDPMs could be developed as a new class of antifungal agents and antibiotics. The data presented herein raise the interesting possibility that, in addition to their direct antimicrobial activity, the therapeutic potential of smHDPMs reflects their ability to harness the host immune system via the activation of MCs through Mas-related GPCRs.

Fungal skin infections are widespread and very common in humans [46]. Although MCs have been strongly implicated in antifungal host defense, their

mechanisms remain largely unknown [87, 88]. Fungal keratitis (FK), also known as keratomycosis or mycotic keratitis, is an infection caused by opportunistic *Fusarium*, *Aspergillus*, and *Candida albicans,* which are difficult to treat and may eventually require surgery [89, 90]. MCs found in the corneal limbus are of the connective tissue (innate) type and they undergo degranulation in a mouse model of FK, resulting in vasodilation, increased intercellular adhesion molecule-1 (ICAM-1) expression on endothelial cells, and neutrophil infiltration [91]. Interestingly, stabilization of MCs with cromolyn leads to inhibition of MC degranulation, dramatic suppression of vascular dilation/permeability, lower ICAM-1 expression, and markedly reduced neutrophil infiltration, resulting in increased fungal growth and higher corneal perforation [91]. These findings provide strong support for the role of CTMCs (innate) in protecting the cornea against fungal infection through their degranulation and subsequent neutrophil recruitment.

The mechanism via which corneal MCs undergo degranulation in FK is unknown but a role of neuropeptides has been proposed [91]. MRGPRX2 and Mrgprb2 are expressed predominantly in human and murine MCs, respectively, and are not found in any other immune or structural cells [40, 43, 92, 93]. Given that neuropeptides such as SP induce degranulation in MCs via MRGPRX2/Mrgprb2, this raised the interesting possibility that this receptor contributes to the role of MCs in host defense to fungal corneal infection [40, 43, 94]. It is noteworthy that in addition to histamine and proteases, MC granules release HDPs during degranulation, which further induces MC degranulation via MRGPRX2 [8, 67, 92, 95]. These findings are consistent with the notion that

noncytotoxic smHDPMs that display both antifungal activity and harness MCs' immunomodulatory function may serve as a new class of antifungal agents.

Our initial screen utilized three structurally related smHDPMs. We found that Compounds 1 and 2 displayed antifungal activity against *C. albicans, A. fumigitus,* and *A. flavus* with Compound 2 being more potent than Compound 1, but Compound 3 was inactive. At concentrations that are relevant for antifungal activity, Compounds 1 and 2 displayed little to no cytotoxic effects on 3T3 and HepG2 cells. Despite the difference in antifungal activity, we were surprised to find that all three smHDPMs induced strong degranulation in a human MC line, LAD2. The first indication that they induced MC degranulation via a GPCR was the finding that an inhibitor of Gαi family of G proteins completely blocked degranulation in response to all three smHDPMs. Our subsequent studies with shRNA-mediated gene silencing in LAD2 cells and MRGPRX2 transfected RBL-2H3 cells clearly showed that these smHDPMs induce degranulation of human MCs via MRGPRX2. The mouse counterpart of human receptor is Mrgprb2, which is expressed in PMCs but not BMMCs [40]. Our finding that smHDPMs induce degranulation in PMCs but not BMMCs supports our contention that these agents activate CTMCs via Mrgprb2. This contention was confirmed by the demonstration that these compounds did not induce degranulation in PMCs obtained from Mrgprb2$^{-/-}$ mice. These findings suggest that two of the three smHDPMs used in our initial screen display both direct antifungal activity and harness MCs' immunomodulatory property by inducing their degranulation and could serve as novel antifungal agents.

In addition to fungal infection, MCs contribute to host defense against bacterial infection likely via MRGPRX2 and Mrgprb2. Thus, mastoparan, a peptide toxin isolated from wasp venom which has direct antibacterial activity, also induces degranulation in human and murine MCs via MRGPRX2 and Mrgprb2, respectively [40]. Arifuzzaman et al. [50] recently showed that mastoparan induces degranulation in mouse CTMCs to promote neutrophil recruitment, which accelerates bacterial (*S. aureus*) clearance in infected skin. Interestingly, a mastoparan derivative that does not induce MC degranulation but retains its antimicrobial activity against *S. aureus* is ineffective in clearing skin infection. By contrast, a mastoparan derivative devoid of antimicrobial activity against *S. aureus* but that retains its ability to induce MC degranulation effectively clears skin infection. Based on these findings, it has been proposed that the therapeutic effect of mastoparan against *S. aureus* skin infection is attributed to its ability to induce MC degranulation rather than its direct antimicrobial activity [4]. CD301b+ dermal dendritic cells (DCs) promote re-epithelialization of sterile wounds and their numbers are decreased in *S. aureus*-infected skin [50, 96]. However, MCs promote re-epithelialization by restoring the skin CD301b+ DC population. In addition, mastoparan boosts adaptive immunity and controls reinfection through the generation of cytokines from mast cells [50]. These findings suggest that activation of Mrgprb2 in CTMCs by mastoparan not only promotes bacterial clearance by recruiting neutrophils but also facilitates skin regeneration and controls reinfection likely through the production of cytokines and the recruitment of DCs [50].

An interesting finding of the present study was that Compound 2 not only had broad-spectrum antifungal activity, it also effectively killed bacteria such as *E. coli* and *S. aureus*. However, its two structural derivatives with reduced positive charges (Compounds 4 and 5) did not display antibacterial activity. Despite this difference, all three compounds induced degranulation in LAD2 cells via MRGPRX2 and murine PMCs via Mrgprb2. Thus, similar to the case with mastoparan [50], Compounds 4 and 5 may promote *S. aureus* clearance from infected skin, facilitate skin regeneration, and control reinfection. There are, however, a number of important differences between mastoparan and smHDPMs. Thus, while EC_{50} values for human and mouse MC degranulation by mastoparan are between 25 μM and 50 μM [50], these values for smHDPMs are between 0.4 μM and 3 μM. This difference could reflect different affinities of mastoparan and smHDPMs for MRGPRX2/Mrgprb2 or that mastoparan is degraded by proteolytic enzymes released from MC granules, therefore requiring higher concentrations for MC degranulation. These findings have important implications for their effects on bacterial clearance and skin regeneration in vivo. It is likely that smHDPMs will promote these responses at lower concentrations than mastoparan. Brilacidin, a smHDPM structurally similar to the compounds used in the present study, is being developed for the treatment of acute bacterial skin infection [71]. Brilacidin also displays efficacy in a rabbit model of methicillin-resistant *S. aureus* (MRSA)-induced keratitis [97]. Based on the data presented in this study, and the *in vivo* findings with mastoparan and its analogs [50], it is possible that the potential

clinical utility of brilacidin reflects its ability to activate MCs via MRGPRX2 in addition to its direct antimicrobial activities.

One possible complication of using smHDPMs for controlling fungal and bacterial infections is that these agents could induce systemic anaphylaxis. This possibility is unlikely for the following reasons. First, MRGPRX2 and Mrgprb2 are expressed on “innate immune” types of MCs such as those found in the skin but not on “adaptive” types of MCs that are found in the lung and other mucosal tissues [37, 40]. Second, topical application of mastoparan on *S. aureus*-infected mouse skin promotes both bacterial clearance and skin regeneration without any noticeable side effects at the application site or systemically [50]. Third, two peptide antibiotics approved by the US Food and Drug Administration, polymyxin B and colistin, activate MCs but do not induce anaphylaxis in patients [50, 98]. One important finding of the present study was that MCs expressing missense MRGPRX2 variants G165E (rs141744602) and D184H (rs372988289) were resistant to degranulation in response to all smHDPMs tested [75]. Thus, if the potential clinical utility of smHDPMs reflects their ability to activate MCs via MRGPRX2, individuals harboring these mutations may be resistant to this type of therapy.

In conclusion, we found that five smHDPMs with low cytotoxicity induced degranulation in human MCs via MRGPRX2 and murine MCs via Mrgprb2. These compounds displayed differences in their ability to kill bacteria and fungi. It is possible that these novel synthetic peptide mimetic MRGPRX2/Mrgprb2 agonists

could form the basis of developing novel therapeutic agents for the treatment of drug-resistant fungal and bacterial infection via the harnessing of MCs' immunomodulatory properties.

Figures

(A)

Compound 1

Compound 2

Compound 3

(B)

Compound (Cpd)	MIC (µg/ml)			Cytotoxicity (CC_{50}, µM)	
	C. albicans	*A. fumigatus*	*A. flavus*	3T3	HepG2
Cpd 1	0.78 - 1.56	12.5 - 50	6.25	209	257
Cpd 2	0.39	0.39	0.39	124	151
Cpd 3	>100	>100	>100	60	111

MICs are reported as range over 2 independent assays. CC_{50} is mean +/- SD from 2 independent assays.

Fig. 1: Structure and antifungal activity of three smHDPMs compounds (Cpd).

(A), Structure of Cpd 1, Cpd 2, and Cpd 3. **(B),** Minimum inhibitory concentration (MIC) values (µg/ml) of smHDPMs against *C. albicans, A. fumigatus,* and *A. flavus.* Cytotoxicity of smHDPMs on 3T3 and HepG2 cell lines. $CC_{50;}$ concentration of drug that reduces 50% cell viability.

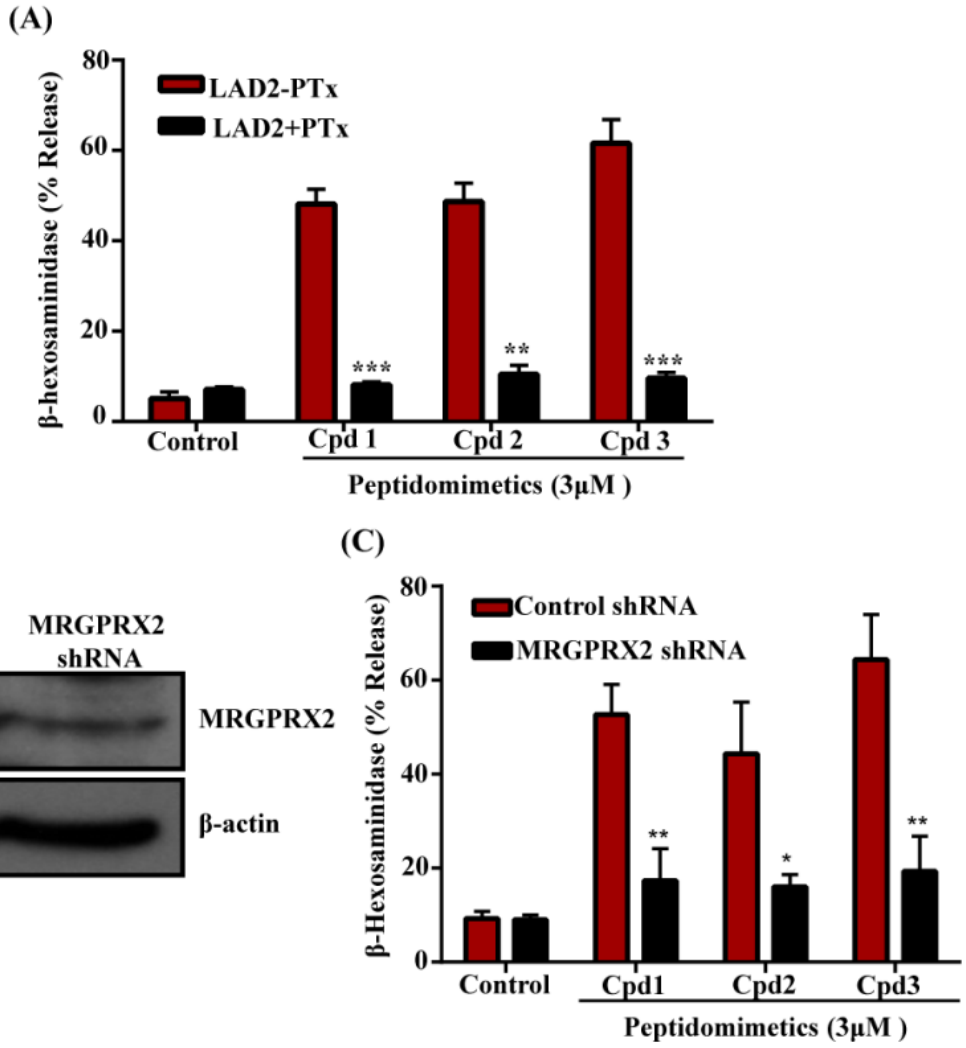
(A)
β-hexosaminidase (% Release)
80
60
40
20
0
LAD2-PTx
LAD2+PTx
***
**
***
Control
Cpd 1
Cpd 2
Cpd 3
Peptidomimetics (3μM)
(B)
Control shRNA
MRGPRX2 shRNA
MRGPRX2
β-actin
(C)
β-Hexosaminidase (% Release)
80
60
40
20
0
Control shRNA
MRGPRX2 shRNA
**
*
**
Control
Cpd1
Cpd2
Cpd3
Peptidomimetics (3μM)

Fig. 2: smHDPMs activate human mast cells via MRGPRX2.

(A), LAD2 cells pretreated with or without pertussis toxin (PTx, 100 ng/ml, 16h) were exposed to vehicle (Control) or smHDPMs compounds (Cpd) 1, 2, and 3 (3 μM each) for 30 min and percentage of β-hexosaminidase release was measured. **(B),** Western blotting was performed to determine the expression level of MRGPRX2 in Control and MRGPRX2 knockdown LAD2 cells. **(C),** Control and knockdown cells were stimulated with smHDPMs Cpd 1, 2, and 3 (3 μM each) and percentage of β-hexosaminidase release was determined. All the points are expressed as a mean ± SEM of three experiments in triplicate. Statistical significance was determined by two-tailed unpaired t-Test. *** indicates P value <0.001,** indicates P value <0.01 and * indicates P value <0.05.

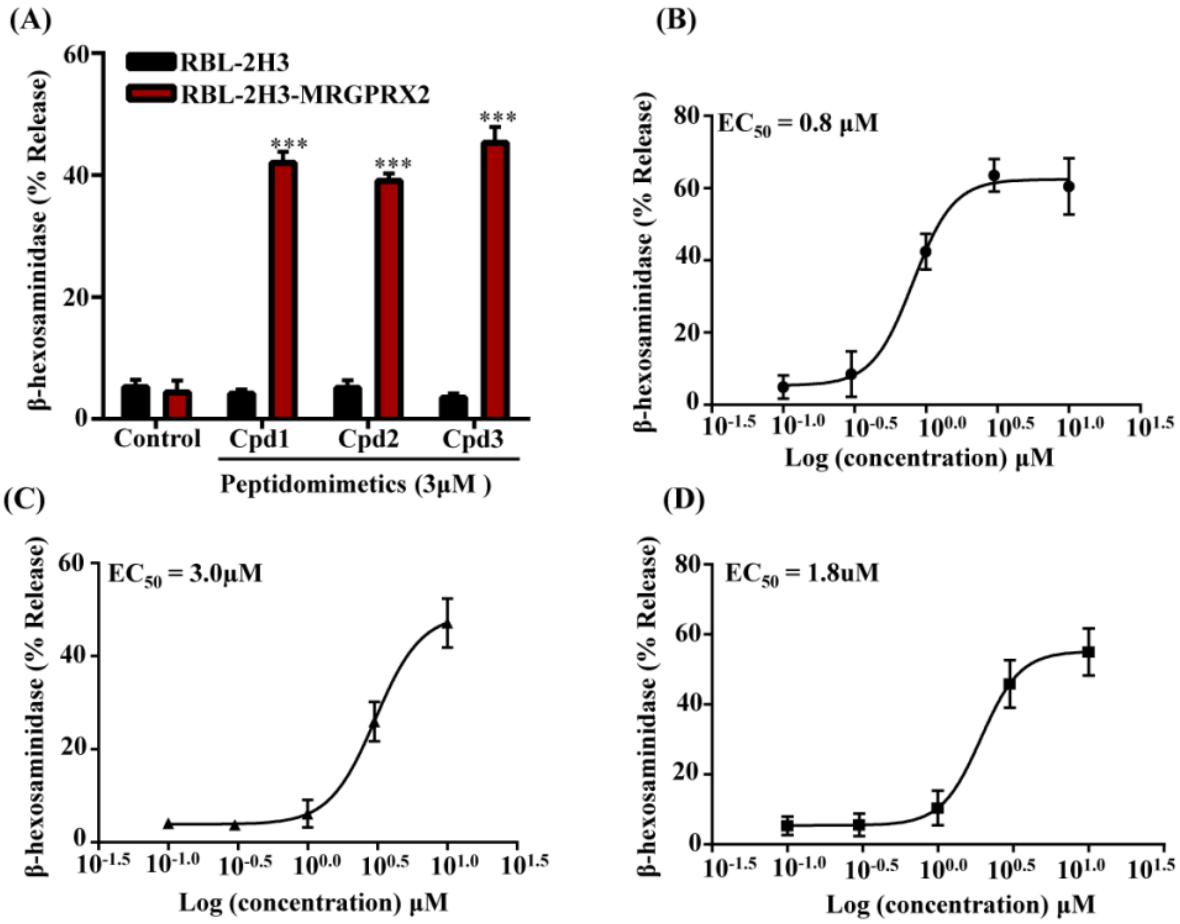
(A)
RBL-2H3
RBL-2H3-MRGPRX2
β-hexosaminidase (% Release)
***
***
***
Control
Cpd1
Cpd2
Cpd3
Peptidomimetics (3μM)
(B)
EC50 = 0.8 μM
β-hexosaminidase (% Release)
Log (concentration) μM
(C)
EC50 = 3.0μM
β-hexosaminidase (% Release)
Log (concentration) μM
(D)
EC50 = 1.8uM
β-hexosaminidase (% Release)
Log (concentration) μM

Fig. 3: smHDPMs induce degranulation in RBL-2H3 cells expressing MRGPRX2.

(A), Untransfected RBL-2H3 cells (RBL-2H3) and cells stably expressing MRGPRX2 (RBL-2H3-MRGPRX2) were exposed to vehicle (Control) or smHDPMs, (Cpd 1, 2, and 3, 3 μM) for 30 min and percentage of β-hexosaminidase release was determined. Concentration–response curves for **(B),** Cpd 1, **(C),** Cpd 2, and **(D),** Cpd 3 were determined using RBL-2H3-MRGPRX2 cells. Data are presented as a mean ± SEM and are representative of three independent experiments in triplicate. Statistical significance was determined by two-tailed unpaired t-Test. *** indicates P value <0.001.

(A)

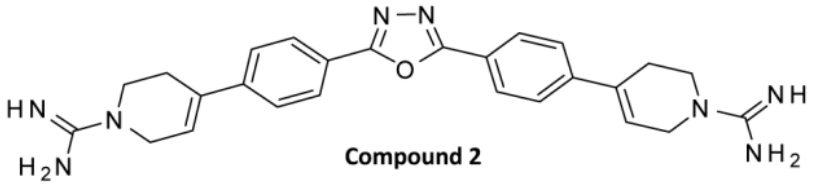

Compound 2

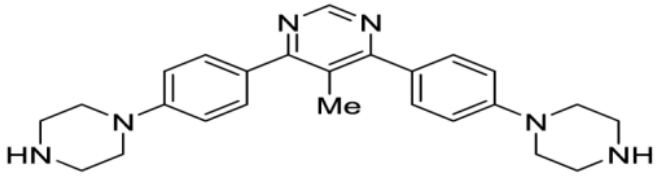

Compound 4

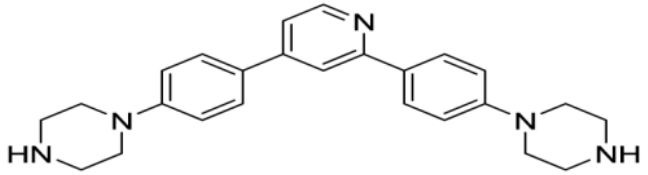

Compound 5

(B)

Compound (Cpd)	Bacterial MIC (µg/ml)					Fungal MIC (µg/ml)			Cytotoxicity (µM)	
	Escherichia coli	*Klebsiella pneumoniae*	*Pseudomonas aeruginosa*	*Staphylococcus aureus*	*Enterococcus faecalis*	*Candida albicans*	*Aspergillus flavus*	*Aspergillus fumigatus*	Mouse 3T3	Human HepG2
Cpd 2	3.1	>100	>100	0.1	>100	0.39	0.39	0.39	124	151
Cpd 4	>100	>100	>100	>100	>100	>100	>100	>100	883	>1555
Cpd 5	>100	>100	>100	>100	>100	>100	>100	>100	200	447

Fig. 4. Structure and antibacterial activity of three smHDPMs compounds.

(A), Structure of compound (Cpd) 2 and two of its derivatives, Cpd 4 and Cpd 5. **(B),** Minimum inhibitory concentration (MIC) values (μg/ml) of smHDPMs against three Gram-negative bacteria (*Escherichia coli, Pseudomonas aeruginosa, Klebsiella pneumonia*) and two Gram-positive bacteria (*Staphylococcus aureus and Enterococcus faecalis*). Cytotoxicity of smHDPMs on 3T3 and HepG2 cell lines. CC_{50} concentration of drug that reduces 50% cell growth.

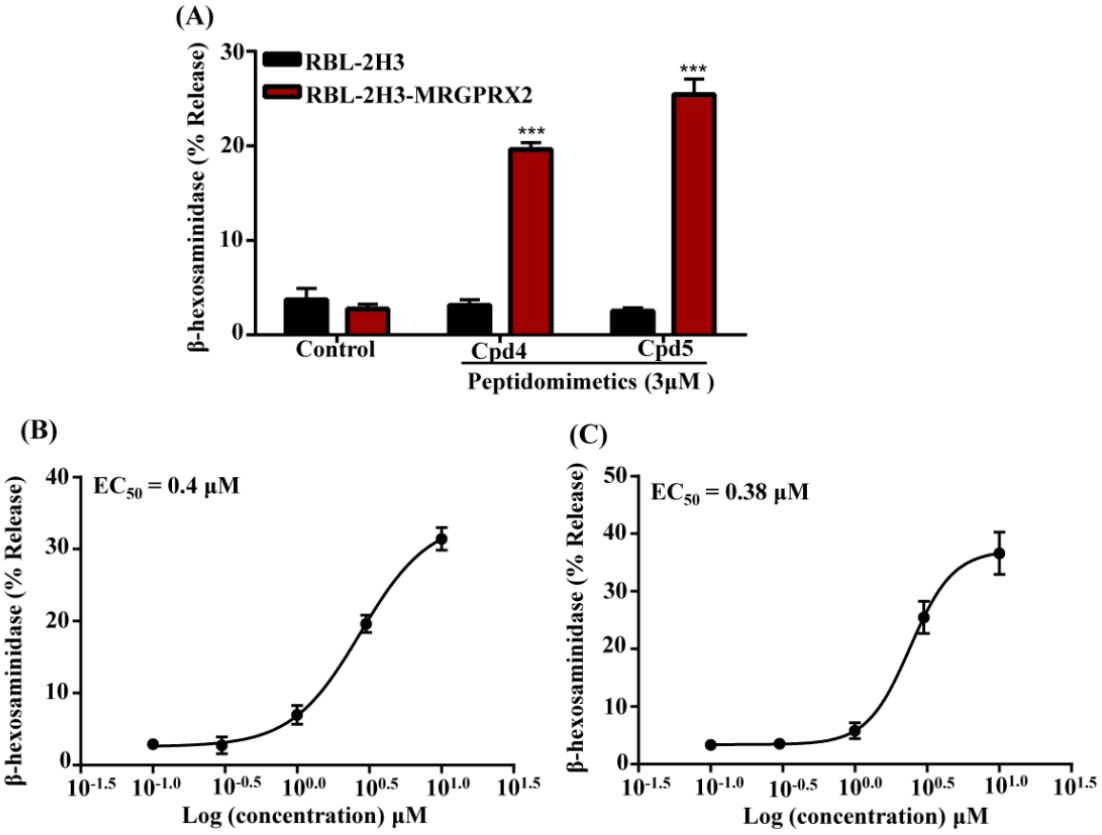
(A)
RBL-2H3
RBL-2H3-MRGPRX2
β-hexosaminidase (% Release)
30
20
10
0
***
***
Control
Cpd4
Cpd5
Peptidomimetics (3μM)
(B)
EC50 = 0.4 μM
β-hexosaminidase (% Release)
40
30
20
10
0
10-1.5 10-1.0 10-0.5 100.0 100.5 101.0 101.5
Log (concentration) μM
(C)
EC50 = 0.38 μM
β-hexosaminidase (% Release)
50
40
30
20
10
0
10-1.5 10-1.0 10-0.5 100.0 100.5 101.0 101.5
Log (concentration) μM

Fig. 5: Compound 4 and Compound 5 induce degranulation in RBL-2H3 cells expressing MRGPRX2.

(A), Untransfected RBL-2H3 cells (RBL-2H3) and cells stably expressing MRGPRX2 (RBL-2H3-MRGPRX2) were exposed to vehicle (Control), smHDPMs compound (Cpd) 4, and Cpd 5 (3 μM each) for 30 minutes and percentage of β-hexosaminidase release was determined. Concentration–response curves for **(B),** Cpd 4 and **(C),** Cpd 5 were performed using RBL-2H3-MRGPRX2 cells. Data are presented as mean ± SEM and are representative of three independent experiments in triplicate. Statistical significance was determined by two-tailed unpaired t-Test. *** indicates P value <0.001.

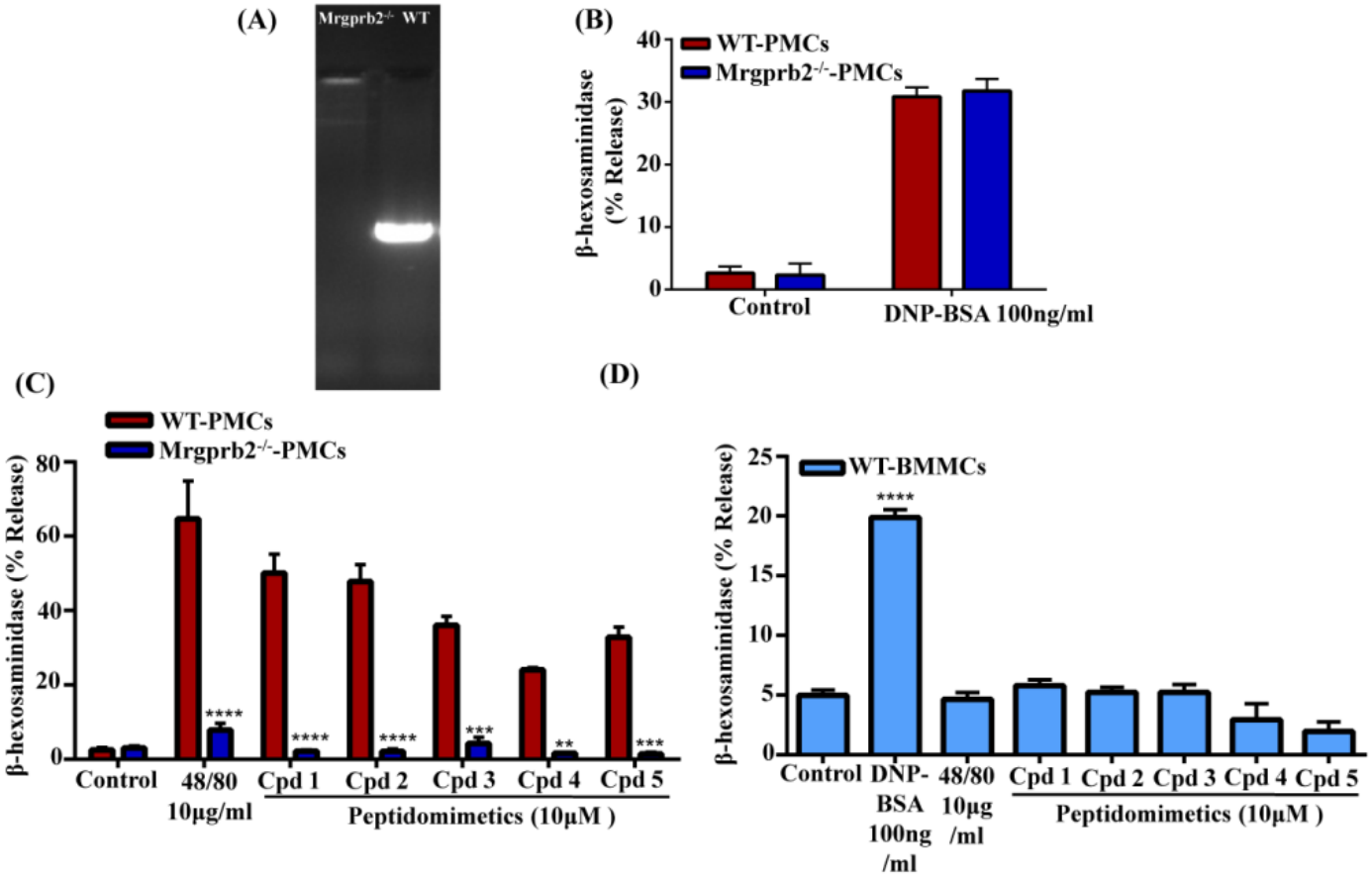
(A)
Mrgprb2-/-
WT
(B)
WT-PMCs
Mrgprb2-/--PMCs
β-hexosaminidase (% Release)
Control
DNP-BSA 100ng/ml
(C)
WT-PMCs
Mrgprb2-/--PMCs
β-hexosaminidase (% Release)
Control
48/80 10µg/ml
Cpd 1
Cpd 2
Cpd 3
Cpd 4
Cpd 5
Peptidomimetics (10µM)
(D)
WT-BMMCs
β-hexosaminidase (% Release)
Control
DNP-BSA 100ng /ml
48/80 10µg /ml
Cpd 1
Cpd 2
Cpd 3
Cpd 4
Cpd 5
Peptidomimetics (10µM)

Fig. 6: smHDPMs induce degranulation in PMCs via Mrgprb2.

(A), Genotyping of wild-type (WT) and Mrgprb2$^{-/-}$ by PCR using Mrgprb2-specific primers. **(B),** PMCs isolated from WT and Mrgprb2$^{-/-}$ mice were exposed to IgE (1 µg/ml, 16 houres) and then stimulated with antigen (DNP-BSA, 100 ng/ml, 30 minutes) and β-hexosaminidase release was determined. **(C)** PMCs were stimulated with compound 48/80 (10 µg/ml) or smHDPMs (Cps 1–5, 10 µM) for 30 minutes and β-hexosaminidase release was determined. **(D),** BMMCs were exposed to IgE (1 µg/ml, 16 hours) and stimulated with antigen (DNP-BSA, 100 ng/ml), 48/80 (10 µg/ml), smHDPMs (10 µM) for 30 minutes and β-hexosaminidase release was determined. All the points expressed as a mean ± SEM of three experiments in triplicate. Statistical significance was determined by two-way and one-way ANOVA. **** indicates P value <0.0001, *** indicates P value <0.001 and ** indicates P value <0.01.

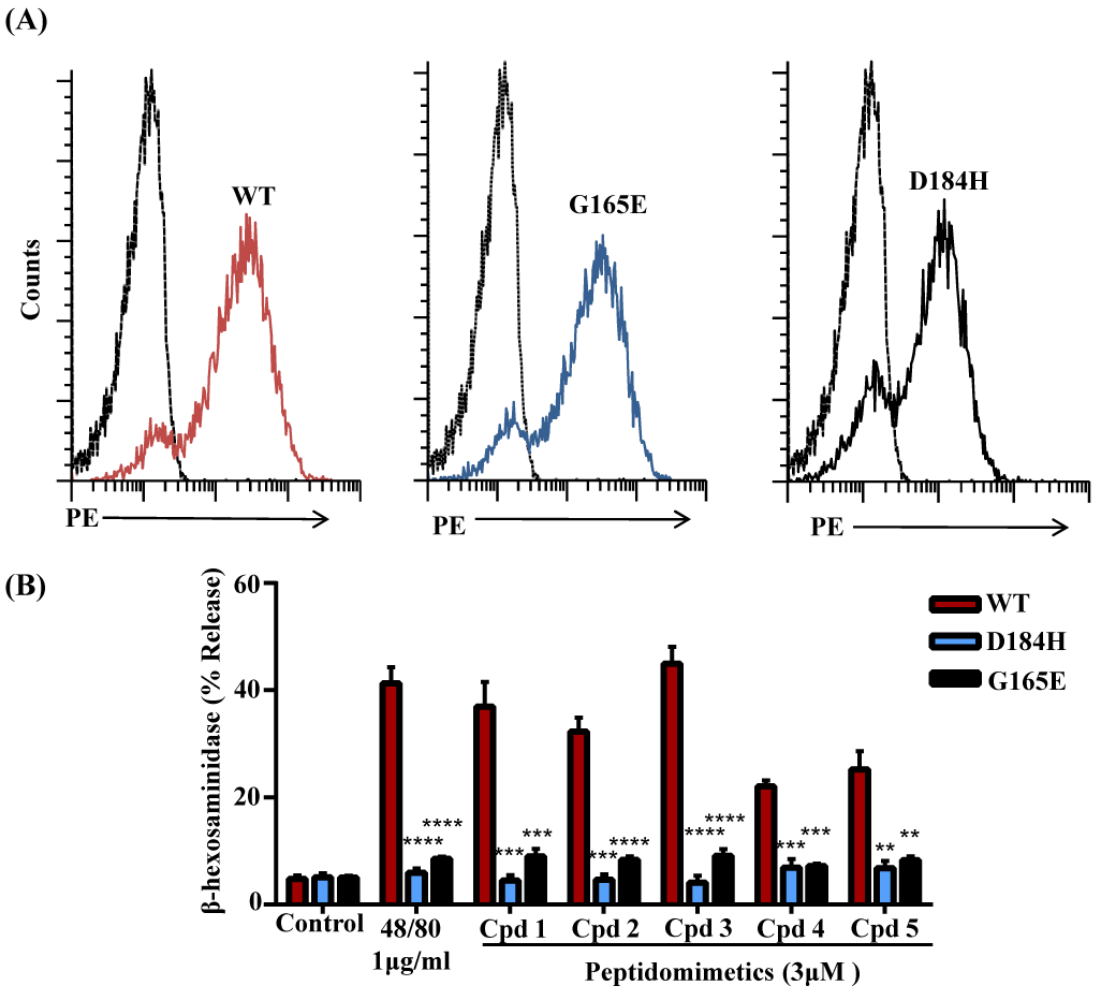
(A)
Counts
WT
G165E
D184H
PE
PE
PE
(B)
β-hexosaminidase (% Release)
60
40
20
0
WT
D184H
G165E
****
****
***
***
***
****
****
***
***
**
**
Control
48/80
1µg/ml
Cpd 1
Cpd 2
Cpd 3
Cpd 4
Cpd 5
Peptidomimetics (3µM)

Fig. 7: Missense MRGPRX2 variants do not respond to smHDPMs for degranulation.

(A), RBL-2H3 cells were transiently transfected with cDNA encoding MRGPRX2 or its missense variants D184H and G165E. Receptor expression was determined by flow cytometry using anti-MRGPRX2-PE antibody. **(B),** RBL-2H3 expressing MRGPRX2 variants (D184H and G165E) were stimulated with smHDPMs (Cpds 1–5, 3.0 μM) for 30 min and β-hexosaminidase release was determined. All the points are expressed as a mean ± SEM of three experiments in triplicate. Statistical significance was determined by one-way ANOVA. **** indicates P value <0.0001,*** indicates P value <0.001 and ** indicates P value <0.01.

Chapter 3: Mas-Related G Protein Coupled Receptors mediate skin inflammation in rosacea and Orai1 contributes to mast cell activation by LL-37 and substance P

Ibrahim Alkanfari[1], Anirban Ganguly[1], and Hydar Ali[1]

[1]Department of Pathology, University of Pennsylvania, School of Dental Medicine, Philadelphia, Pennsylvania, USA

Abstract

Mast cells (MCs) play a central role in the pathogenesis of rosacea likely via the activation of Mas-related G protein coupled receptor X2 (MRGPRX2) by the cathelicidin LL-37 and the neuropeptide substance P (SP). Here we found the skin samples obtained from individuals with rosacea display higher frequencies of MRGPRX2-expressing MCs when compared to normal skin. Mrgprb2 is regarded as the ortholog of human MRPGRX2, and therefore, we utilized Mrgprb2$^{-/-}$ and MC-deficient W^{sh}/W^{sh} mice in a murine model of rosacea. We found that intradermal injection of LL-37 resulted in the development of erythema in WT mice, which was significantly but not fully reduced in Mrgprb2$^{-/-}$ mice. LL-37 induced erythema was completely inhibited in W^{sh}/W^{sh} mice, indicating MC dependency in rosacea. LL-37 and SP caused increased expression of inflammatory molecules matrix metalloproteinases-9 (MMP-9) and CXCL-2 mRNA in WT mice, but these responses were substantially reduced Mrgprb2$^{-/-}$ and abolished in W^{sh}/W^{sh} mice. This reduction was associated with decreases in LL-37-induced inflammatory cell infiltration in Mrgprb2$^{-/-}$ and W^{sh}/W^{sh} mice when compared to WT mice. Ca^{2+} mobilization is prerequisite for MC activation and thus calcium channel plays a crucial role in MC-induced pathogenesis. We used freshly isolated skin MCs to identify the role of Orai Ca^{2+} channel in MRGPRX2-mediated MC activation. We found that Orai channel inhibitors caused significant decrease in LL-37 and SP-induced degranulation in human skin MCs as well as human MC line (LAD2). Furthermore, shRNA mediated knockdown of Orai1 and its upstream molecule STIM1 led to significant reduction in LL-37 and SP-induced Ca^{2+} influx and

degranulation in LAD2 cells. These findings suggest that Mrgprb2 partially contributes to the development rosacea and that STIM1/Orai1 and could serve as a new target for its treatment.

Introduction

Rosacea is a common chronic inflammatory disorder with multiple subtypes that mainly affects the facial skin. The pathophysiology of rosacea is not fully understood but it is likely associated with dysregulation of the immune, vascular, and nervous systems [99]. Expression of the cathelicidin LL-37 is significantly increased in all subtypes of rosacea [100]. Also, there is an increased expression of the epidermal trypsin-like serine protease enzyme, kallikerin 5 (KLK5) in rosacea skin. This enzyme is responsible for cleaving the inactive precursor protein (hCAP18) to the biologically active LL-37 [101]. Besides its direct antimicrobial activity, LL-37 also has proinflammatory and angiogenic properties which exacerbate rosacea [102]. Skin is highly innervated with nerve fibers that have the ability to release many neuronal proinflammatory mediators upon central or peripheral stimulation [103]. Cevikbas et al. [104], showed that neuropeptides such as substance P (SP) released by the stimulation of nerve endings cause the development of skin lesions that resemble clinical and histologic features of rosacea. These findings suggest that LL-37 and SP play important roles in the pathogenesis of rosacea.

Recent studies have strongly implicated MCs in rosacea [100, 105-109]. Thus, the number of MCs in rosacea skin is increased compared to normal skin [105]. Furthermore, Muto et al. [108], showed that unlike wild-type (WT) mice, MC-deficient mice do not develop rosacea characteristics following intradermal injection of LL-37. Also, the production of MMP-9 and tryptase are significantly

increased in experimental WT mice compared to control and MC-deficient mice, further indicating the pivotal role of MCs in the pathogenesis of rosacea. Mas-related G protein-coupled receptor (GPCR) X2 (MRGPRX2) is a seven transmembrane domain receptor that has predominantly expressed in a subtype of MCs found in the skin [43]. Subramanian et al. [67], provided the first demonstration that LL-37 activates human MCs via MRGPRX2. Although SP induces its biological responses via the activation of neurokinin receptors in a variety of cell types, it activates human MCs via MRGPRX2 [43, 45, 93, 110]. These findings suggest that the effects of MCs on rosacea are mediated via MRGPRX2. Unlike humans, there are 22 Mas-related GPCR coding genes in mice and mouse MCs highly express Mrgprb1 and Mrgprb2 [40, 111, 112]. McNeil et al., [40] demonstrated that SP activates murine MCs via Mrgprb2. However, the possibility that LL-37 also activates murine MCs via Mrgprb2 and the role of this receptor on the well-established mouse model of rosacea have not been determined.

Ca^{2+} mobilization is an essential requirement for the MRGPRX2-dependent degranulation and the release of cytokines from MCs. Non-neuronal transient receptor potential-4 (TRPV4) ion channel is upregulated in rosacea skin MC and by LL-37 in human cord-derived MCs. However, a TRPV4 inhibitor and silencing of TRPV4 in MCs partially inhibits MRGPRX2-meidated degranulation in human MCs [113-115]. These findings suggest that while TRPV4 may contribute to MC activation via MRGPRX2 in rosacea additional mechanisms for Ca^{2+} are also likely to be involved. MCs express Orai1 -a calcium release activated calcium (CRAC)

channel- which is responsible for store operated calcium entry (SOCE). Orai1 has been shown to be essential for IgE mediated Ca^{2+} influx and degranulation [116, 117]. Activation of CRAC requires a sensor protein known as Stromal Interaction Molecule 1 (STIM1) that conveys the calcium level of the endoplasmic reticulum (ER) to CRAC at the plasma membrane. However, the possibility that Orai1/STIM1 contribute to LL-37 and SP-induced MRGPRX2-mediated MC Ca^{2+} influx and degranulation have not been tested.

The goals of the present study were (a) to determine if Mrgprb2 contributes to rosacea pathogenesis *in vivo* and (b) to assess the roles of STIM1/Orai1 on LL-37 and SP-induced Ca^{2+} influx and degranulation in human MCs. The data presented herein demonstrate that Mrgprb2, at least in part, contributes to rosacea and that STIM1/Orai could be targeted for its modulation.

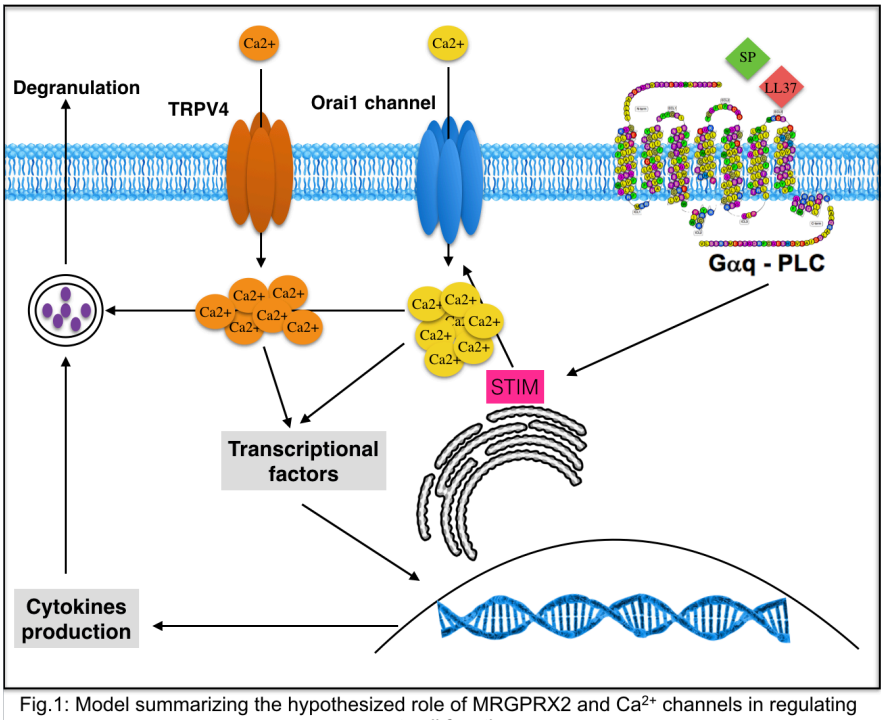

Fig.1: Model summarizing the hypothesized role of MRGPRX2 and Ca^{2+} channels in regulating mast cell function

Materials and Methods

Materials

All cell culture reagents and DNP-specific mouse IgE (SPE-7) were purchased from Invitrogen (Carlsbad, CA) except X-VIVO medium which was purchased from Lonza (Walkersville, MD). Recombinant murine interleukin-3 (IL-3), recombinant murine stem cell factor (SCF), and recombinant human SCF were purchased from Peprotech (Rocky Hill, NJ). DNP-BSA and p-nitrophenyl-N-acetyl-β-D-glucosamine (PNAG) were acquired from Sigma-Aldrich (St. Louis, MO), Compound 48/80, LL-37, and SP were purchased from AnaSpec (Fremont, CA). Orai inhibitors Synta-66 and GSK-7975A were obtained from MedChem Express (Monmouth Junction, NJ). Fura-2 was purchased from Abcam (Cambridge, UK).

Polyclonal MRGPRX2 Ab was purchased from Novus Biologicals (Littleton, CO). PE anti-human MRGPRX2 Ab was purchased from Biolegend (San Diego, CA). Polyclonal Orai1 Ab was purchased from alomone (Jerusalem, Israel). STIM1 and HRP-conjugated anti-rabbit IgG was from Cell Signaling Technologies (Danvers, MA). West Pico and femto Chemiluminescent Substrate were acquired from Thermo Scientific (Rockford, IL). DNeasy Blood and Tissue Kit was purchased from Qiagen (Germantown, MD). Collagenase Type 2 was purchased from Worthington Biochemical Corporation (Lakewood,NJ). DNase I was from Roche Diagnostics (Mannheim, Germany). Hyaluronidase was bought from Sigma

Aldrich (St. Louis, MO). Mouse *GAPDH*, *MMP-9,* and *CXCL-2* Primers were purchased from Thermo Fisher Scientific (Waltham, MA).

Staining

Immunohistochemistry

Immunohistochemistry (IHC) experiments were performed using normal and rosacea skin samples obtained from 5 patients in order to evaluate the relative presence and the abundance of MCs. Tryptase was used as a MC marker for this experiment. The slides are archival slides from Skin Biology and Diseases Resource-Based Center (SBDRC). The slides were heated to 55 ^{o}C overnight, deparaffinized in Histoclear and, hydrated in a series of graded ethanol incubations. Afterward, antigen retrieval was performed by heat treatment using 1X antigen retrieval solution in a water bath at 95 ^{o}C for 1 hour. Then the slides were left to cool down at room temperature for about 30 minutes. The tissue was then surrounded with a ring made by hydrophobic pen. The slides were then placed in a humidified chamber and peroxidase quenching was performed using 0.3% H_2O_2 blocking solution for 10 minutes at room temperature. This was followed by 2 washes in PBS. The slides were incubated for 1 hour at room temperature with blocking serum using normal horse serum followed by monoclonal mouse anti-human tryptase Ab at a dilution of 1:500 overnight at 4 ^{o}C in a humidified chamber. For negative control, serum blocking reagent was used instead of the primary Ab on the top section of all slides.

In the next day, the sections were then washed 3 times with PBS/0.1% Tween and incubated with diluted secondary antibody, biotinylated horse anti mouse IgG for one hour at room temperature. Following secondary Ab incubation, the slides were washed 3 times in PBS/0.1% Tween and incubated for 30 minutes with Vectastain ABC reagent. Subsequently, they were washed 3 times in PBS/0.1% Tween and incubated in NovaRed peroxidase substrate solution from a DAB peroxidase substrate kit until desired color intensity was observed. The slides were rinsed under running tap water until solution was clear (approximately for 5 minutes), counterstained in Mayer's hematoxylin solution for around 2 seconds and repeated it as necessary; then rinsed again in running tap water until excess solution was removed. Rehydration of the tissue was done using increasing graded alcohol series. Then the slides were cleaned manually histoclear on a cotton tip to remove the hydrophobic ring and moisture. The slides were then mounted with Permount mounting medium. Images were captured on a Nikon Eclipse N*i* microscope using 20X and 40X magnification.

Immunofluorescence

Immunofluorescence (IF) experiments were performed using the same samples used in IHC experiment which include normal and rosacea skin samples that were obtained from 3 patients in order to evaluate the presence of any MRGPRX2^{+} MCs. Tryptase was used again as a MC marker. The slides were blocked with 5% donkey serum and incubated with monoclonal mouse anti-human tryptase (1:500) and polyclonal rabbit anti-MRGPRX2 (1:500) primary antibodies.

AlexaFlour 448-conjugated donkey anti-mouse (1:400) in conjunction with DAPI (1:1000) and AlexaFluor568-conjugated donkey (1:400) (Molecular Probes), were used as secondary antibodies. We mounted sections in ProLong Gold Anti-Fade reagent (Molecular Probes). Images were captured on a Nikon Eclipse Ni microscope with an Olympus digital microscope camera using 20X and 60X magnifications.

Alcian Blue/Safranin Staining

Same protocol mentioned in chapter 2 was followed. PMCs (5×10^4) were cytocentrifuged, air-dried, incubated for 20 minutes with 0.5% Alcian blue in 0.3% acetic acid, rinsed in water, and then incubated for 20 min with 0.1% safranin in 1% acetic acid. The cells were inspected using a Nikon Eclipse N*i* microscope.

Mouse Experiments

All animal experiments were approved by the Institutional Animal Care and Use Committee (IACUC) of the University of Pennsylvania. Wild-type mice (C57BL/6), MC-deficient mice (W^{sh}/W^{sh}), and MRGPRB2$^{-/-}$ mice were used for these experiments. MRGPRB2$^{-/-}$ mice were generated via CRISPR/Cas9 (see chapter2 for more details). The mice were shaved 24 hours before intradermal injection with 50 µl LL-37 (320 uM) or filtered PBS for experimental and control groups respectively, twice a day for 2 days. Dorsal skin was evaluated for the degree of inflammation and then excised after 72 hours. The excised tissue was

either immersed immediately into 10% formalin for histology (Hemoxlyne/Eosin, Toluidine blue) or RNA stabilization reagent for qPCR (RNAlater; QIAGEN science, Germantown, MD). For the neuropeptide experiments, 100 μM SP or PBS was injected into WT mice and MRGPRB2$^{-/-}$ mice intradermally. Skin biopsies were taken 6 hours after injection and analyzed by RT-PCR.

Mast Cells Culture

PMCs and LAD2 were cultured following detailed protocol mentioned earlier in chapter 2. Human skin MCs were cultured in X-VIVO medium with rhSCF (100 ng/ml), penicillin (100 IU/ml), streptomycin (100 μg/ml) and Amphotericin B (2.5 μg/ml). The human skin MCs were used for experiments on the following day.

Human Skin MCs Isolation

Skin tissue was obtained from patients undergoing cosmetic breast reduction surgery. Wash buffer was prepared by adding the following components into 1 L of sterile water: 100 ml of 10X HBSS solution, 7 ml of 7.5 % $NaHCO_3$ solution, 10 ml of heat inactivated FCS, 10 ml of 1 M HEPES solution, 10 ml of 100X solution Amphotericin B, 10 ml of 100X Antibiotic/Antimycotic (Sigma A5955) solution. Digestion buffer was prepared in 100 ml of the washing buffer by adding Collagenase Type 2 (1.5 mg/ml), Hyaluronidase Type I-S (0.70 mg/ml), DNase I Type IV (0.1 mg/ml), and CaCl2 (1 mM).

The fat tissue was removed from the skin using sharp scissor. Then the skin tissue was finely minced as possible and digested with the digestion buffer at 37˚C while shaking for 1 hour. The digestion step was repeated three times. After each digestion the supernatant was collected, filtered, centrifuged and washed with the washing buffer. The mixed cells population was then purified using positive selection with magnetic sorting using CD117 Ab and magnetic beads. The cells were then culture as mentioned in the previous section.

Calcium Assay

LAD2 cells (0.3 x 10^6) were loaded with 1 μM Fura-2 AM for 30 minutes at 37 ˚C. Cells were then washed and resuspended in 1.5 ml of calcium free HEPES-buffered saline. The cells were then stimulated with LL-37 3 μM and SP 1 μM at 100 seconds and intracellular calcium mobilization was determined in the absence of extracellular calcium; then 1 mM Ca^{2+} was added at 400 seconds and Ca^{2+} influx was determined using a Hitachi F-2700 spectrophotometer with an excitation wavelength of 340 nm and an emission wavelength of 380 nm. Some experiments used Orai (Synta-66 and GSK7975A 10 μM) inhibitors were used.

Degranulation Assay

PMCs (5 x 10^3), LAD2 (10x 10^3), and human skin MCs (5 x 10^3) were seeded into 96-well plates in a total volume of 50 μl HEPES buffer containing 0.1% bovine serum albumin (BSA) and exposed to LL-37 and SP for 30 minutes. Cells without treatment were designated as controls. For some experiments, calcium

channels inhibitors were used as the following: LAD2 and skin MCs were seeded into 96-well plates and divided into two groups – the control group (no inhibitors), and a group that was pre-treated with 10 μM Orai inhibitors (Synta-66 and GSK-7975A). For total β-hexosaminidase release, unstimulated cells were lysed in 50 μl of 0.1% Triton X-100. Aliquots (20 μl) of supernatants or cell lysates were incubated with 20 μl of 1 mM p-nitrophenyl-N-acetyl-β- D-glucosamine for 1 hour at 37°C. The reaction was stopped by adding 250 μl of a 0.1 M Na_2CO_3/0.1 M $NaHCO_3$ buffer and absorbance was measured at 405 nm.

Lentivirus-Mediated Knockdown of STIM1 and Orai1 in LAD2

STIM1 and Orai1 targeted mission shRNA lentiviral plasmids were purchased from Sigma Aldrich (St. Louis, MO). A scrambled control nontarget vector (SHC002), which does not bind to any known human mRNAs, was also purchased from Sigma Aldrich. Lentivirus generation was performed according to the manufacturer's manual. Cell transduction was conducted by mixing 1.5 ml of viral supernatant with 3.5 ml of LAD2 (10×10^6 cells). Twenty-four hours post-infection, the medium was changed to virus-free complete medium, and antibiotic selection was initiated after 48 hours of transduction with (puromycin, 2 μg/ml, Sigma). The cells were analyzed for STIM1 and Orai1 knockdown and used for subsequent assays 6 days following initiation of puromycin selection.

Quantitative Real-Time PCR

Samples were homogenized, and total RNA was extracted and purified by RNeasy Fibrous Tissue Kit (QIAGEN science) to assess the mRNA expression of *MMP-9* and *CXCL-2* by qRT-PCR. 0.5 to 1 µg of RNA was used to synthesize cDNA using the High-Capacity RNA-to-cDNA™ Kit (Applied biosystem, Foster City, CA) according to the manufacturer's protocol. Using TaqMan Gene Expression Assays, the mRNA expression of mouse *MMP-9* and mouse *CXCL-2* and human *Orai1* was analyzed following the manufacturer's instructions. The analysis was performed in triplicate and *GAPDH* was used as an internal control to validate RNA for each sample. mRNA expression was calculated as the relative expression to *GAPDH* mRNA. All data are presented as fold change of each control.

Western Blotting

Cell lysates were prepared from scrambled control and STIM1, and Orai1 shRNA transduced LAD2 cells in RIPA buffer and protein was quantified using BCA Protein Assay Kit (Thermo Scientific). Protein was separated in SDS-PAGE (10 %), transferred to PVDF membrane, and incubated overnight with anti-STIM1, Orai1, and β-actin antibodies (1:1000) in blocking buffer (5% skim milk in TBST 0.1%). This was followed by incubation with HRP conjugated anti-rabbit IgG (1:1000) and development using West Femto or Pico Chemiluminescent Substrate.

Results

MRGPRX2-Tryptase double positive MCs are present in normal skin and their numbers are increased in rosacea.

We have initially used skin sample slides obtained from normal and rosacea patient to study the role of MRGPRX2 receptor in this disease. Using anti-tryptase antibody, we confirmed that MC numbers are significantly elevated in rosacea skin when compared to normal skin (Fig. 1a and b). MRGPRX2 is expressed in MCs and dorsal ganglia but not in other immune or structural cells [43, 45, 118]. To compare MRGPRX2 expression in normal and rosacea skin, we performed immunofluorescence staining with anti-tryptase and anti-MRGPRX2 antibodies. We found that MRGPRX2 is expressed in normal skin tissue and the number of cells expressing this receptor is increased in rosacea (Fig. 1, C and D; red cells). Overlay of panels 1Cand 1D showed that MCs express MRGPRX2 in both normal and rosacea skin (arrows). Several MRGPRX2-expressing cells did not stain with anti-tryptase antibody were also detected (Fig. 1 C and D). Fujisawa et al., [43] recently showed that in the skin of patients with chronic urticaria most $MRGPRX2^{+}$ cells are MCs.

LL-37-induced MC degranulation is partially dependent on Mrgprb2

Mrgprb2 has been identified as the mouse orthologue of human MRGPRX2. Mrgrb2 is predominantly expressed in connective tissue-type of MCs, including those in the skin and the peritoneal cavity (PMCs) [108]. Compound 48/80 and SP

activate mouse PMCs via Mrgprb2. We therefore utilized Mrgprb2$^{-/-}$ mice for our *in vitro* an and *in vivo* experiments (Fig. 2 A). Alcian/Safranin staining of cultured PMCs revealed rich heparin content, indicating high maturity of the cell population (Fig. 2 B). Antigen (DNP-BSA, 10 ng/ml) stimulation of both WT and Mrgprb2$^{-/-}$ PMCs shows comparable amounts of β-hexosaminidase release (Fig. 2 C). However, β-hexosaminidase release after stimulation with compound 48/80 (10 ng/ml) and SP (100 μM) were abolished in Mrgprb2$^{-/-}$ PMCs compared to WT-PMCs (Fig. 2 D). By contrast, LL-37 (10 μM)-induced degranulation was reduced by ~50% Mrgprb2$^{-/-}$ PMCs (Fig. 2 D). This suggests that LL-37 utilizes both Mrgprb2-depedent and independent pathways for degranulation in mouse MCs.

Mrgprb2 partially contributes to LL-37-induced MC-dependent rosacea.

Subcutaneous injection of LL-37 induces rosacea-like inflammation manifesting as a local erythema at the injection site [119]. We therefore used this model to study rosacea *in vivo*. We generated Mrgprb2 global knockout mice (Mrgprb2$^{-/-}$) to determine the role of Mrgprb2 in LL-37 and SP MCs activation *in vivo*. Because MC-deficient W^{sh}/W^{sh} mice were previously used to demonstrate an essential role of MCs in experimental rosacea, we used these mice as a control. LL-37 induced substantial increase in surface area of erythema in WT mice, which was absent in W^{sh}/W^{sh} mice, confirming the role of MCs in this process. However LL-37 induced surface erythema was significantly decreased in Mrgprb2$^{-/-}$ mice, but this reduction was less than that observed with W^{sh}/W^{sh} mice (Fig. 3 A and B). The LL-37-induced rosacea model used in this study is associated with the

recruitment of inflammatory cells. In correlation with the erythema size, histological study showed reduction in inflammatory cells in Mrgprb2$^{-/-}$ mice tissue and almost abolished in W^{sh}/W^{sh} mice (Fig. 4 A and B).

MCs possess granules that occupy the majority of the cytoplasm. The release of granules filled with a wide variety of mediators, including chemokines and proteases, contributes to attracting inflammatory cells and rosacea development. MCs produce chemotactic factors such as *CXCL-2* which can attract more neutrophils to the tissue and thereby aggravate the inflammatory reaction. Moreover, *MMP-9* can result in KLK-5 activation which in turn leads to further activation of LL-37 and rosacea exacerbation [120]. Thus, we evaluated the expression level of *MMP-9* and *CXCL-2* in this experiment. There was a significant reduction in mRNA transcripts level of *MMP-9* and *CXCL-2* in skin excised from Mrgprb2$^{-/-}$, and W^{sh}/W^{sh} mice compared to WT (Fig. 5 A and B). These findings in total suggest while LL-37-induced rosacea in mice is entirely dependent on the presence of MCs, and Mrgprb2 contributes partially to this response.

Substance P induced *MMP-9* and *CXCL-2* expression in WT mice but reduced in Mrgprb2 $^{-/-}$ mice

Neuronal dysregulation and the release of several neuropeptides such as SP has been implicated in the pathogenesis and rosacea flare-up. The location of the MCs in close proximity to nerves helps in direct interaction with the sensory nerves [121]. MC-deficient mice demonstrated considerable reduction in *MMP-9* and *CXCL-2* expression upon stimulation with SP [108]. Therefore, we investigated

the role of the Mrgprb2 receptor in mediating *MMP-9* and *CXCL-2* expression in WT and Mrgprb2$^{-/-}$ mice skin when injected intradermally with 100 uM of SP. After 6 hours of SP injection, the skin was excised, processed, and total RNA was isolated. The expression level of *MMP-9* and *CXCL-2* was determined by qRT-PCR. *MMP-9* and *CXCL-2* expression level was observed to be markedly reduced in Mrgprb2$^{-/-}$ mice compare to the WT mice (Fig. 6 A and B).

Substance P and LL-37-induced degranulation is inhibited by Orai Ca^{2+} channel inhibitors in human skin MCs and LAD2 cells.

Ca^{2+} influx is an essential phenomenon for MRGPRX2-mediated MC activation. Ca^{2+} influx is mediated by different calcium channels present in the cell membrane. Synta-66 and GSK-7975A are both Orai inhibitors that have shown to attenuate IgE-dependent Ca^{2+} influx and mediators release [117]. However, the role of Orai calcium channels in LL-37 and SP induced MRGPRX2-MC activation remains unknown. We used Orai inhibitors to investigate the role of Orai Ca^{2+} channels on MRGPRX2-mediated Ca^{2+} influx and degranulation. Initially we used MCs freshly isolated from healthy human skin, which is particularly useful to understand the role of Orai Ca^{2+} channels in rosacea. Isolated cells were stained with IF staining (DAPI Blue, FcεRI Green, MRGPRX2 Red) for characterization (Fig. 7 A). Staining showed expression of both FcεRI and MRGPRX2 in the skin MCs. We found that Orai channel inhibitors significantly reduced MRGPRX2-mediated degranulation in human skin MCs when stimulated with LL-37 and SP

(Fig. 7 B). Similarly, Orai channel inhibitors substantially reduced Ca^{2+} influx (Fig. 6 C), and degranulation (Fig. 6 D) in LAD2 human MCs line.

Knockdown of STIM1 attenuates MRGPRX2 mediated Ca^{2+} influx and mediators release in LAD2 cells.

Due to lower yield and difficulties in performing the knockdown experiment in skin MCs and the fact that LAD2 cells have demonstrated inhibitory effect similar to the one observed in skin MCs when pretreated with Orai inhibitors, we therefore used human MC line LAD2 for the subsequent studies.

STIM1 is a key regulator of SOCE which get activated after Ca^{2+} depletion from endoplasmic reticulum (ER) stores. Upon activation of STIM1, it undergoes certain conformational changes that result in its oligomerization and activation of Orai1 channel [122]. MCs lacking STIM1 demonstrated substantial inhibition in FcεRI-mediated Ca^{2+} influx and degranulation [123]. Therefore, we utilized lentiviral shRNA to knockdown STIM1 and determine its role in MRGPRX2-mediated Ca^{2+} influx and degranulation in LAD2 cells. Multiple clones of MISSION STIM1 shRNA were screened (data not shown). We found that clone 2 exhibited a significant reduction in STIM1 protein expression (Fig. 8 A). So, we used this clone for the subsequent experiments. We found that Ca^{2+} influx and degranulation were significantly reduced in the group stimulated with 3 μM LL-37 (Fig. 8 B and D) compared to control shRNA transduced cells. Similarly, SP-mediated MRGPRX2 Ca^{2+} influx and degranulation were substantially reduced in STIM1 knockdown LAD2 cells (Fig. 8 C and D).

Orai1 knockdown LAD2 cells demonstrated marked decrease in MRGPRX2 mediated Ca^{2+} influx and degranulation with LL-37 and SP compared to control group

We used lentiviral shRNA targeting Orai1 in order to understand its role in mediating MRGPRX2 Ca^{2+} influx and degranulation. We used scramble shRNA as a control. The efficiency of the knockdown was tested with western blot. Western blot demonstrated about 75% efficiency in Orai1 knockdown (Fig. 9 A). When compared to control; calcium influx was substantially reduced following stimulation with both 3 μM LL-37 and 1 μM SP (Fig. 9 B and C) in Orai1 knockdown cells. At the functional level, the knockdown of Orai1 resulted in a significant reduction in degranulation when stimulated with 1 μM LL-37 and 0.5 μM SP (Fig. 9 D).

Discussion

Previous research has established that MCs are a key element in rosacea development. A unique feature of rosacea is that it is characterized by dysregulation of the host defense mechanisms and overexpression of the host defense antimicrobial peptide LL-37. Moreover, NPs such as SP play a key role in rosacea exacerbation and flare-up [20]. LL-37 and SP are known ligands that activate MCs through a cell surface receptor known as MRGPRX2 [40, 41, 108]. MRGPRX2 and its murine ortholog of the human receptor are predominantly expressed in human MCs and murine MCs respectively which raises the interesting possibility that it could play a role in rosacea. Moreover, the involvement of the STIM1/Orai1 Ca^{2+} channels in mediating calcium influx in rosacea is still not fully clear. The findings presented in this study suggest that MRGPRX2/Mrgprb2 partially contributes LL-37 induced rosacea in mice. Another important finding this chapter shows is that the Orai1 channel and its sensor protein STIM1 are essential for MRGPRX2 mediated Ca^{2+} influx when MCs were stimulated with LL-37 and SP.

Choi et al. [124] recently showed a significant reduction in LL-37-induced skin erythema, MC degranulation, and mRNA expression of proteases in a rosacea mouse model when Onabotulineium toxin (BoNT) was used as an inhibitor for MCs. The explanation this study provided was that BoNT is involved in the blockage of MC degranulation by preventing granules fusion and release. Muto et al. [108] showed that MC-deficient mice failed to demonstrate erythema *in vivo*

when injected with LL-37 intradermally. In agreement to previous studies [108, 124], our results demonstrate that MC-deficient mice failed to display erythema presentation as compared to the WT group, indicating the central role of MC in rosacea. This was correlated with the histological finding which indicated absence of infiltrated cells in the skin. Moreover, our IHC and IF data of the human skin samples indicate that rosacea skin exhibited higher number of MRGPRX2-expressing MCs compared to the control. We therefore sought to use Mrgprb2$^{-/-}$ mice to assess the receptor role in rosacea pathogenesis.

Another important finding that in contrast to SP, PMCs activation with LL-37 showed to be partially dependent on Mrgprb2 *in vitro.* Mrgprb2$^{-/-}$ mice exhibited less erythema presentation and less inflammatory cell infiltration histologically following intradermal injection with LL-37. This reduction in inflammatory cell infiltrations was not due to differences in MC numbers as there was no significant differences between WT and Mrgprb2$^{-/-}$ knockout experimental groups (data not shown). A recent study demonstrated that Mrgprb1, Mrgprb10, and Mrgprc11 are also expressed in murine CTMCs [74]. It is possible, therefore, that other Mrgprs also participate in LL-37 mediated MC activation and rosacea inflammation. Our data also shows that mRNA expression of *MMP-9* and *CXCl-2* were significantly less in Mrgprb2$^{-/-}$ mice compared to the WT.

Neuropeptides such as SP have been associated with rosacea exacerbation and flare-up [125]. Vasodilatation can be directly induced by neuronal stimulation and the release of neuropeptides but can also result from inflammatory

mediators released during the early phase of rosacea by inflammatory cells [126]. MCs are located perivascularly in close proximity to skin nerve fibers and it is now generally accepted that MC activation by NPs contributes to neurogenic inflammation, pain, and itch [20]. Proteases released by MCs directly signal to neurons through proteinase-activated receptor 2 (PAR-2) to stimulate the release of SP, which mediates inflammatory edema [23]. The activation of CTMCs through MRGPRX2/Mrgprb2 results in the release of inflammatory mediators via degranulation *in vitro* [23]. Our study confirmed this result with *in vitro* and *in vivo* experiments. Utilizing CTMCs isolated from the peritoneal cavity from both WT and Mrgprb2$^{-/-}$ mice, degranulation with SP was significantly reduced in Mrgprb2$^{-/-}$-PMCs. Similarly, mRNA expression level of *MMP-9* and *CXCl-2* were significantly less in Mrgprb2$^{-/-}$ mice compared to the WT when mice were injected intradermally with SP indicating that they are MRGPRX2/Mrgprb2 dependent. Recently, in accordance to our findings Green et al. [127] used a similar Mrgprb2$^{-/-}$ mouse model and demonstrated less inflammatory cell infiltration, protease and chemokine production after SP was injected into mice hindpaws compared to WT. In another recent study Meixiong et al.[128] showed that Mrgprb2$^{-/-}$ mice were protected from allergic contact dermatitis-associated itch with lower CD45^{+} cells infiltration compared to WT. Thus, our findings as well as those of other studies suggest that the interaction between MRGPRX2/Mrgprb2 expressing MCs and nerve endings in the skin possibly form a bidirectional positive feedback loop that induces both protease and neuropeptide secretion which synergistically result in the exacerbation and development of rosacea symptoms.

Another objective of this study was to understand the role Ca^{2+} channels in LL-37 and SP mediated Ca^{2+} influx in MCs. Human skin obtained from rosacea patients showed an upregulation of TRPV4 in MCs [113]. Moreover, Mascarenhas et al. [115] demonstrated that human $CD34^{+}$ derived MCs displayed upregulation of TRPV4 following stimulation with LL-37 for 24 hours and this upregulation was MRGPRX2-dependent. Unlike other GPCRs, MRGPRX2 is resistance to LL-37-induced receptor phosphorylation, desensitization, and internalization [67]. Therefore, absence of MRGPRX2 desensitization result in continues activation of MCs and possibly increase the expression of TRPV4. The fact that TRPV4 inhibitors and TRPV4 deficient-MCs showed only partial reduction of MRGPRX2 mediated MCs degranulation raises the interesting possibility other calcium channels are involved. Ashmol et al. [116, 117], studied the role of Orai channels in IgE mediated MC activation and demonstrated that Orai inhibitors significantly blocked calcium influx and degranulation. Furthermore, Orai1 shRNA transduced HLMCs resulted in significant reduction in IgE dependent MCs activation. Activation of Orai1 channel require STIM1 sensor protein. These findings present in the literature raised the interesting possibility that STIM1/Orai1 channel may also be involved in the Ca^{2+} influx upon MRGPRX2/Mrgprb2 mediated-MC activation. Also, that the upregulation of TRPV4 channels upon long-term stimulation of MCs by LL-37 in rosacea may be critical for augmenting more Ca^{2+} influx and inducing sustain MC degranulation in chronic inflammation. Therefore, another goal of this study was to understand the role of STIM1/Orai1 Ca^{2+} channels in LL-37 and SP mediated Ca^{2+} influx in MCs. We conducted *in vitro* experiments using two types

of cells: MCs freshly isolated from human skin and the LAD2 MCs line. We believe that both models were particularly useful to further our understanding in this aim as the skin MCs are primary cells that will give a true representation of the Ca^{2+} channels function in skin and LAD2 cell line has been shown to express the Ca^{2+} channels in a similar pattern to primary human lung MCs [129]. We found that Orai inhibitors showed significant reduction in MRGPRX2 mediated MCs degranulation when skin MCs were stimulated with LL-37 and SP.

One of the drawbacks of using human skin MCs is the limited MC number isolated from the skin. We therefore proceeded with LAD2 cells to conduct the remaining experiments. Likewise, MRGPRX2 mediated Ca^{2+} mobilization and degranulation assays demonstrated significant reduction with Orai inhibitors in LAD2. Also, silencing of STIM1 and Orai1 had a significant effect on IgE independent MRGPRX2 mediated degranulation and Ca^{2+} influx when MCs were stimulated with LL-37 and SP. Moreover, qPCR showed slight reduction in transcript level of Orai1 at 24 hours (data not shown) when LAD2 cells were continually stimulated with LL-37. Although this reduction was not statistically significant, but it suggests that changes in expression between TRPV4 and Orai1 is to possibly fine-tune the Ca^{2+} influx according to the MC needs. Taken together, these results show that there is significant therapeutics potential to target STIM1/Orai1 for the treatment of rosacea.

In conclusion, a higher frequency of $MRGPRX2^{+}$-MCs was observed in patients with rosacea than from normal subjects. MRGPRX2/Mrgprb2 is a major

effector in mediating MC degranulation and promoting immune cell recruitment in rosacea. One of the most significant findings to emerge from this study is that STIM1/Orai1 play an important role in Ca^{2+} influx in MRGPRX2 mediated MC activation. Strategies to target MRGPRX2 and STIM1/Orai1 might offer a novel approach for the treatment of rosacea.

Figures

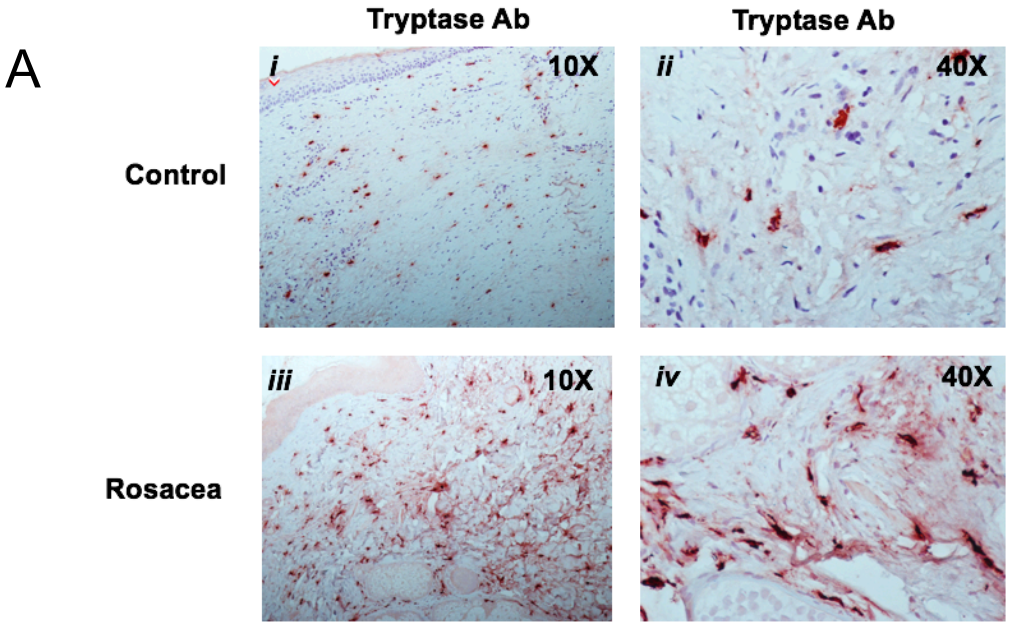
A
Tryptase Ab
Tryptase Ab
i
10X
ii
40X
Control
iii
10X
iv
40X
Rosacea

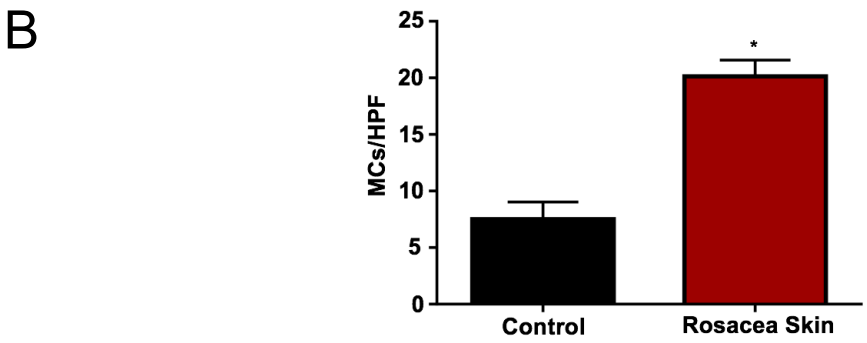
B
25
20
15
10
5
0
MCs/HPF
*
Control
Rosacea Skin

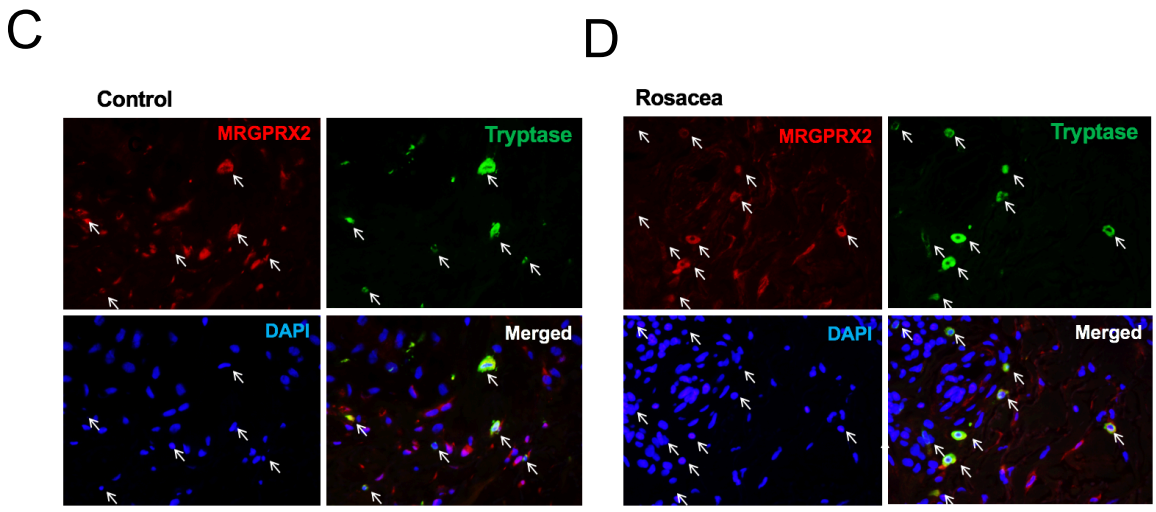
C
D
Control
MRGPRX2
Tryptase
DAPI
Merged
Rosacea
MRGPRX2
Tryptase
DAPI
Merged

Fig. 1: Rosacea samples displayed mast cells expressing MRGPRX2.

(A) Images obtained from the skin tissue of normal (*i* and *ii*) and rosacea (*iii and iv*) *subjects*. **(B)** Quantitative analysis of MCs number was done by counting MCs in a total of 15 high power images. Data presented are mean ± SEM of MCs counts obtained from 5 donors. Statistical significance was determined by unpaired t-test * indicates $P<0.05$. Immunochemical staining of skin specimens from control **(C)** and rosacea **(D)** subjects with anti-tryptase mAb (green), anti-MRGPRX2 antibody (red), and 4′-6-diamidino-2-phenylindole dihydrochloride (*DAPI*; blue).

A

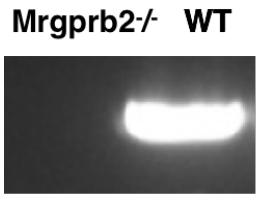

B

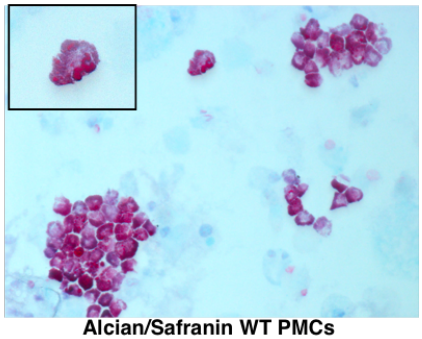
Alcian/Safranin WT PMCs

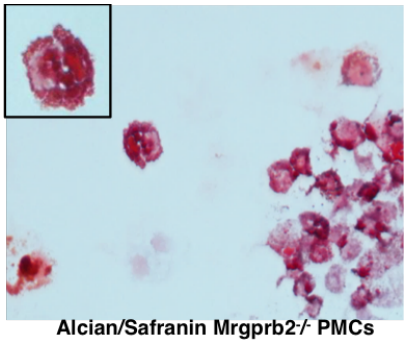
Alcian/Safranin Mrgprb2-/- PMCs

C

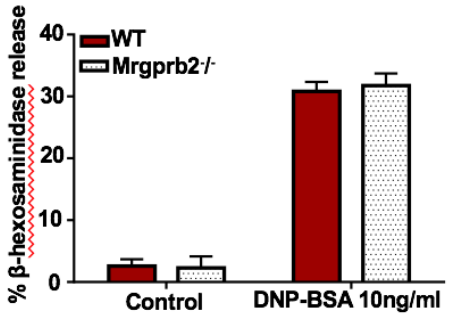

D

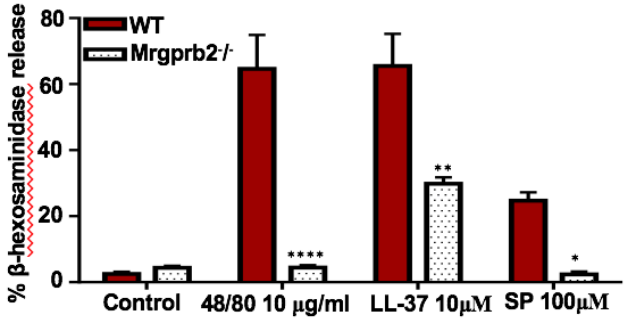

Fig. 2: Peritoneal mast cells isolated from Mrgprb2$^{-/-}$ mice exhibited partial reduction degranulation following LL-37 stimulation compared to WT peritoneal mast cells.

(A) Agarose gel electrophoresis shows success in generating Mrgprb2$^{-/-}$ mice using CRISPR/Cas9 technology. **(B)** PMCs were cytocentrifuged and stained with Alcian blue/Safranin red. **(C)** PMCs were stimulated with DNP-BSA (100 ng/ml). **(D)** PMCs were stimulated with 48/80 (10 ng/ml), LL-37 (10 μM) and SP (100 μM) for 30 minutes, and β-hexosaminidase release was measured. Statistical significance was determined by two-way ANOVA * indicates $P<.05$, ** indicates $P<.01$ and **** indicates $P<.0001$.

A

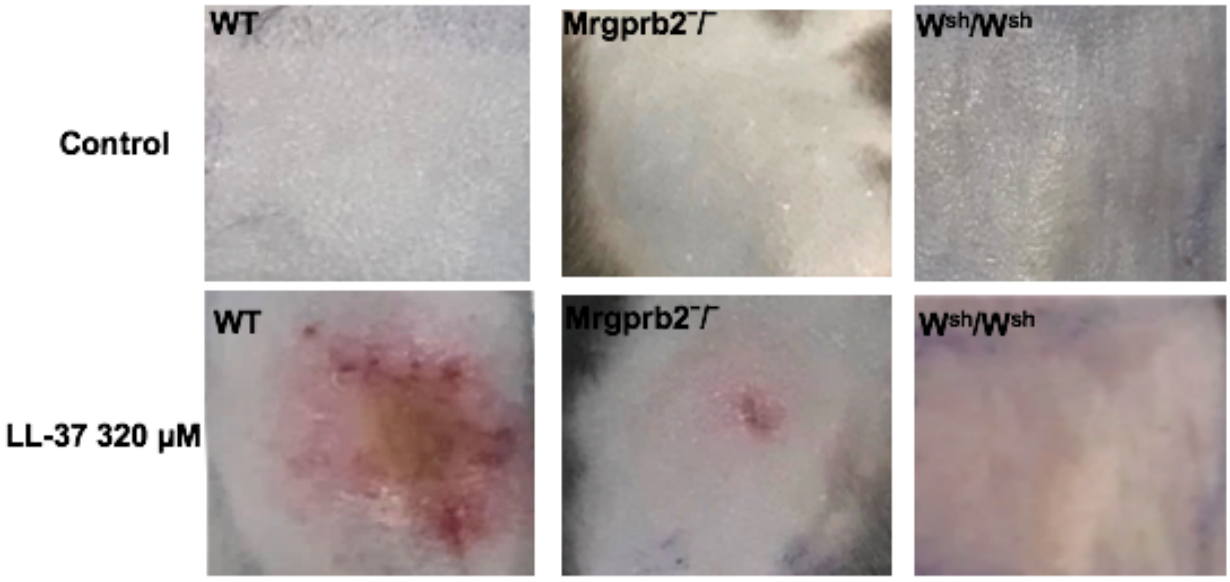
WT
Mrgprb2-/-
Wsh/Wsh
Control
WT
Mrgprb2-/-
Wsh/Wsh
LL-37 320 µM

B

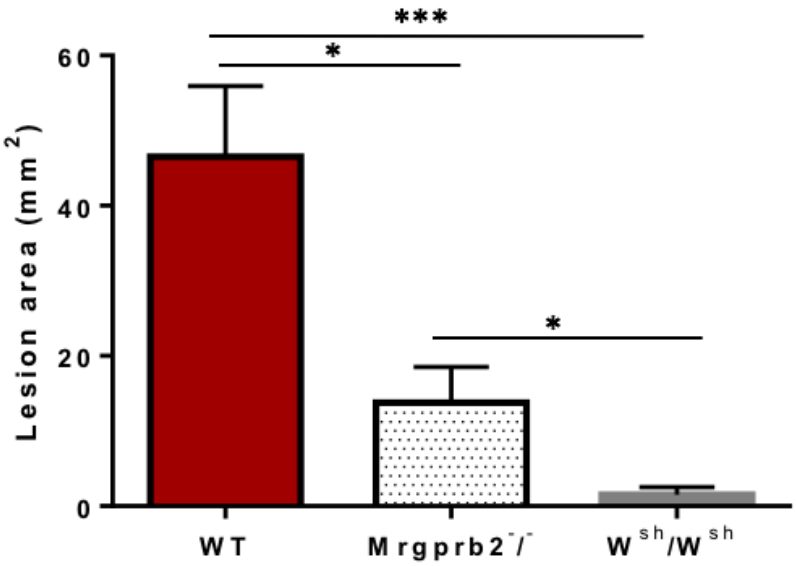
***
*
*
60
40
20
0
Lesion area (mm2)
WT
Mrgprb2-/-
Wsh/Wsh

Fig. 3: Mrgprb2$^{-/-}$ mice displayed significantly less erythema.

(A) WT, Mrgprb2$^{-/-}$, and MC deficient mice (W^{sh}/W^{sh}) were intradermally injected with filtered PBS (control) or LL-37 (320 μM) in the dorsum skin. **(B)** A comparison of the size of erythema measured (mm^2) 72 hours after the initial injection. Statistical significance was determined by two-tailed unpaired t-test. * indicates *P*<.05. and *** indicates *P*< .001. All the points expressed as a mean ± SEM of fives experiments.

A

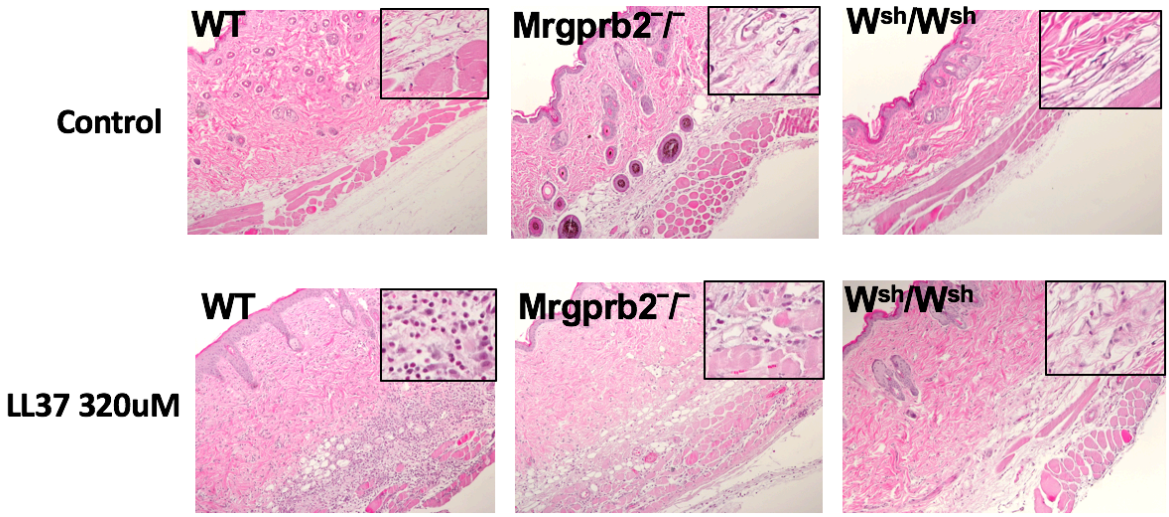
WT
Mrgprb2-/-
Wsh/Wsh
Control
WT
Mrgprb2-/-
Wsh/Wsh
LL37 320uM

B

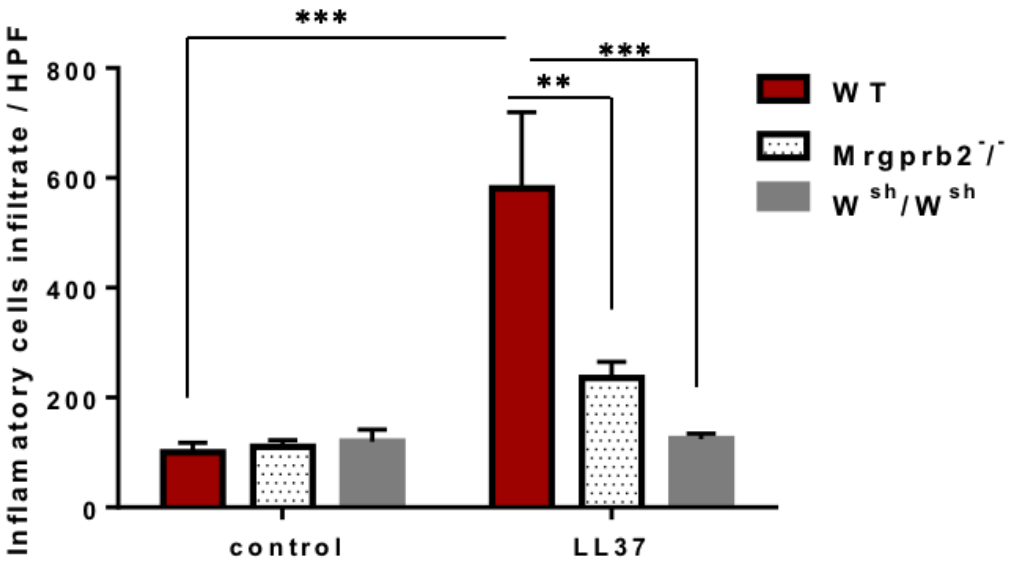
***
***
**
Inflamatory cells infiltrate / HPF
800
600
400
200
0
control
LL37
WT
Mrgprb2-/-
Wsh/Wsh

Fig. 4: Robust inflammatory cells infiltration in WT experimental mice compared to Mrgprb2$^{-/-}$ and MC-deficient mice.

(A) WT, Mrgprb2$^{-/-}$, and W^{sh}/W^{sh} were intradermally injected with filtered PBS (control) or LL-37 (320 μM) and then were stained via hematoxylin/eosin. **(B)** The mean ± S.E.M of inflammatory cells infiltration per HPF was plotted. Statistical significance was determined by two-way ANOVA. ** indicates $P<0.01$ and *** indicates $P<0.001$.

A

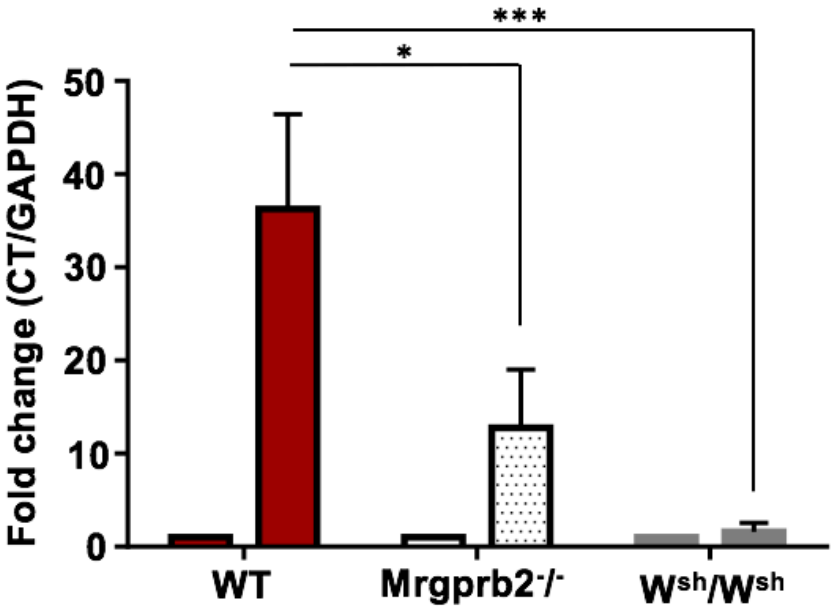
CXCL-2
***
*
Fold change (CT/GAPDH)
50
40
30
20
10
0
WT
Mrgprb2-/-
Wsh/Wsh

B

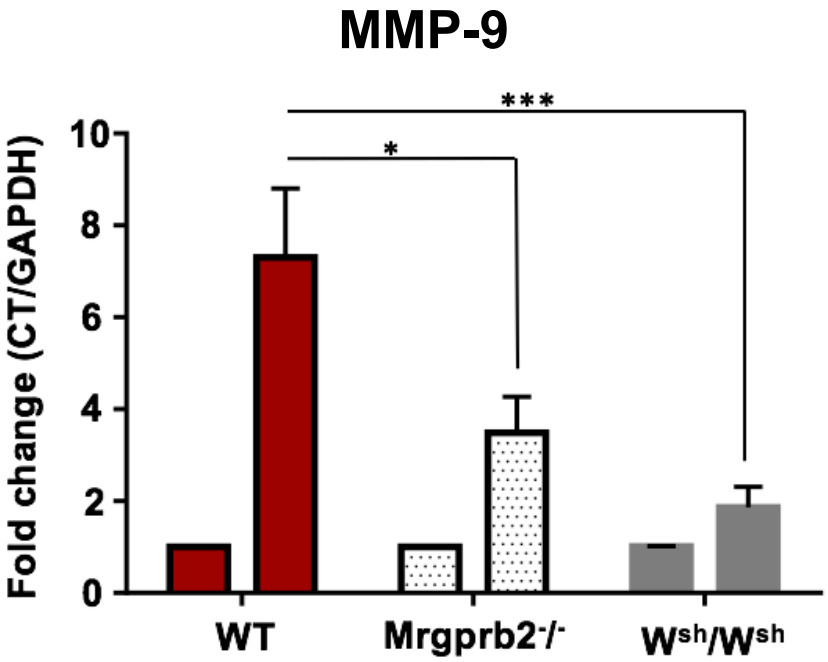
MMP-9
***
*
Fold change (CT/GAPDH)
10
8
6
4
2
0
WT
Mrgprb2-/-
Wsh/Wsh

Fig. 5: *CXCL-2* and *MMP9* are overexpressed in WT experimental group but reduced in Mrgprb2$^{-/-}$ and W^{sh}/W^{sh} following intradermal injection with LL37.

Skin was excised from mice intradermally injected with LL-37 (320 μM), and mRNA transcripts level of **(A),** *CXCL-2* and **(B),** *MMP-9* was determined with qPCR. Statistical significance was determined by two-way ANOVA. * indicates $P<0.05$ and *** indicates $P<0.001$.

A

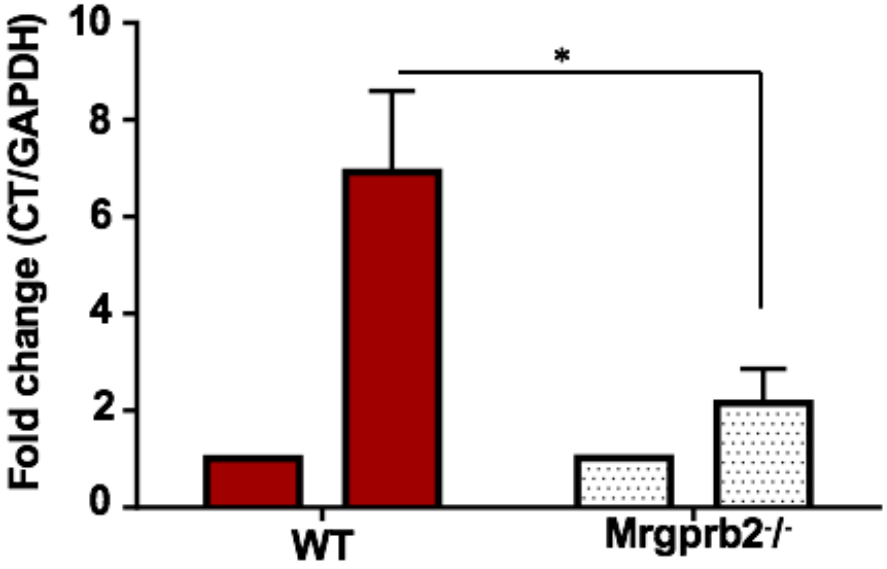
CXCL-2
Fold change (CT/GAPDH)
10
8
6
4
2
0
*
WT
Mrgprb2-/-

B

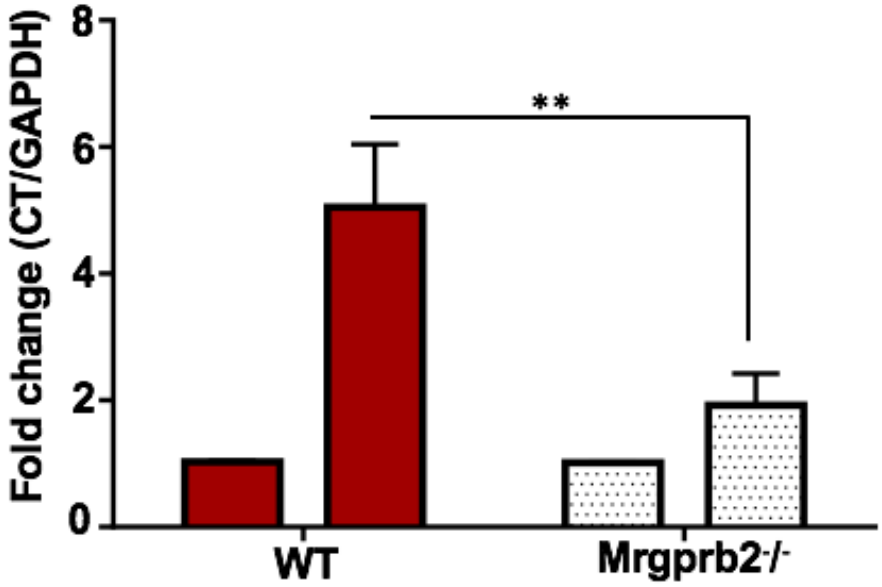
MMP-9
Fold change (CT/GAPDH)
8
6
4
2
0
**
WT
Mrgprb2-/-

Fig. 6: Mrgprb2 mediates SP induced MC CXCL-2 and MMP-9 release.

Skin was excised from mice intradermally injected with SP (100 μM), and mRNA transcripts level of **(A),** *CXCL-2* and **(B),** *MMP-9* was determined with qPCR. Statistical significance was determined by two-way ANOVA. * indicates $P < .05$ and ** indicates $P < .001$.

A

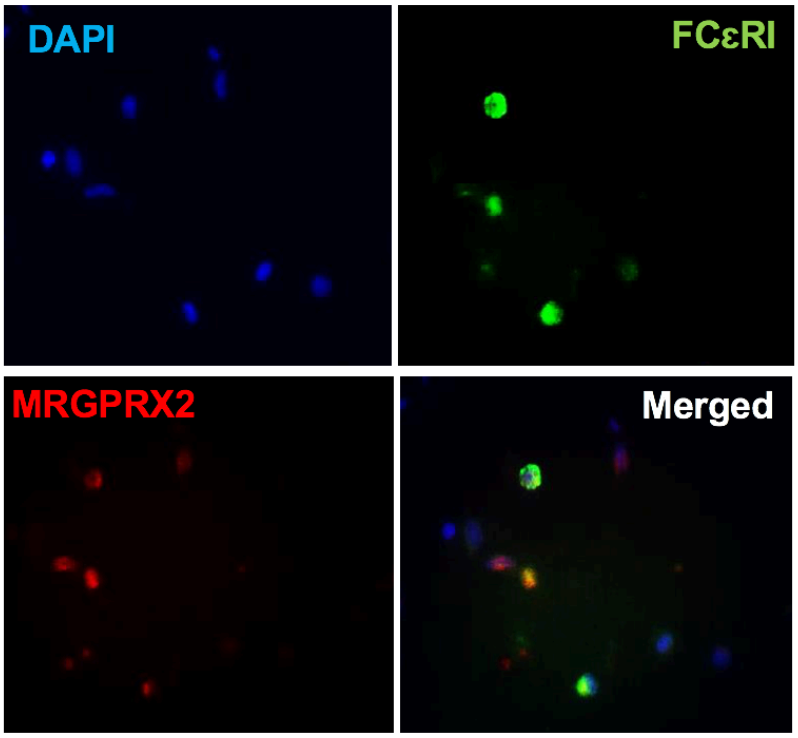
DAPI
FCεRI
MRGPRX2
Merged

B

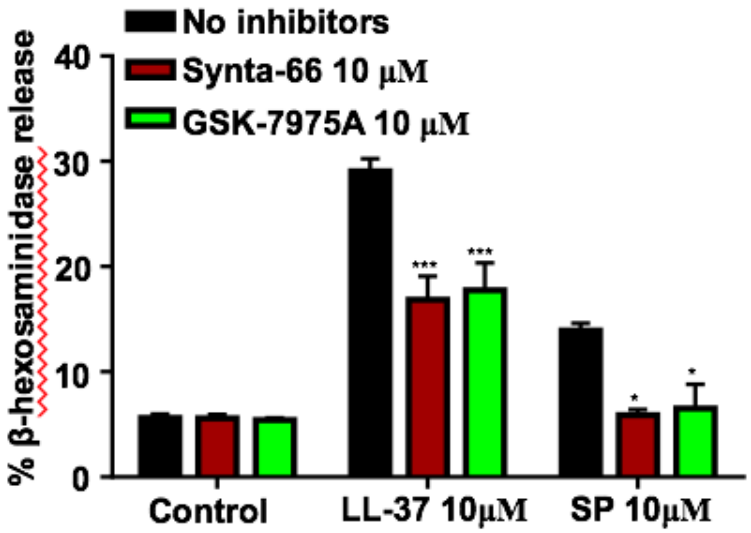
No inhibitors
Synta-66 10 μM
GSK-7975A 10 μM
% β-hexosaminidase release
40
30
20
10
0
***
***
*
*
Control
LL-37 10μM
SP 10μM

C

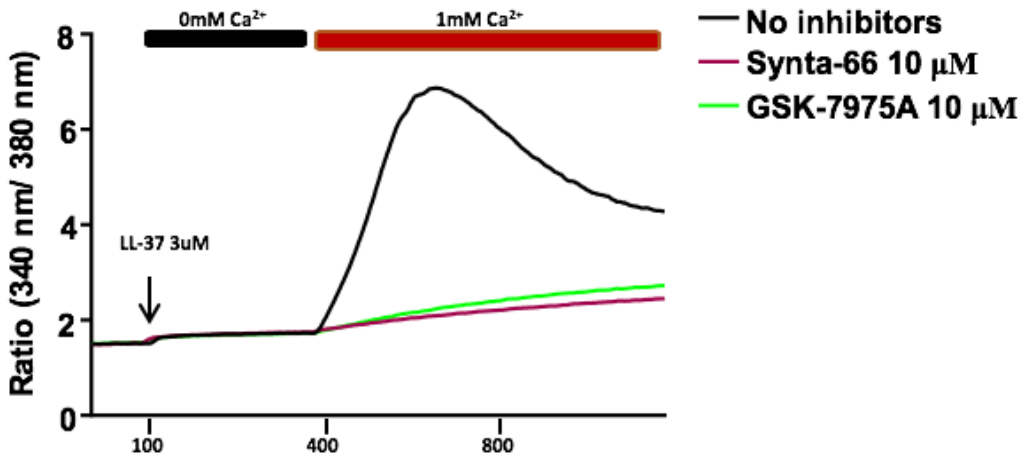
0mM Ca2+
1mM Ca2+
No inhibitors
Synta-66 10 µM
GSK-7975A 10 µM
Ratio (340 nm/ 380 nm)
LL-37 3uM
0
2
4
6
8
100
400
800

D

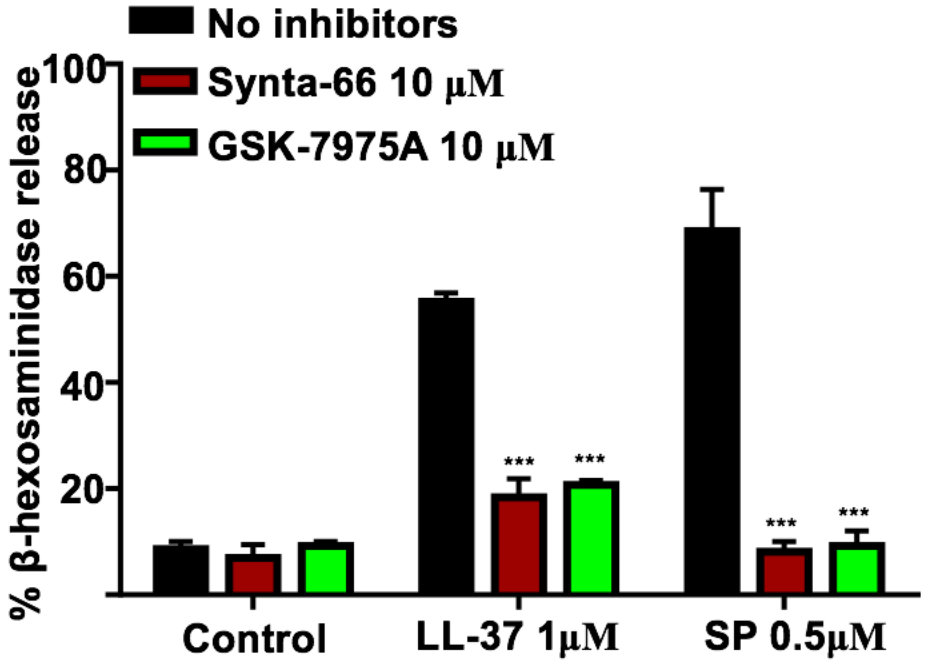
No inhibitors
Synta-66 10 µM
GSK-7975A 10 µM
% β-hexosaminidase release
0
20
40
60
80
100
***
***
***
***
Control
LL-37 1µM
SP 0.5µM

Fig. 7: Mast cells isolated from the skin of human subjects and LAD2 cells displayed a significant reduction in degranulation with Orai inhibitors.

Human skin MCs were isolated, cytocentrifuged, and stained for **(A)** Immunofluorescence staining with DAPI (Blue), FCεR (Green), and MRGPRX2 (Red). **(B)** Degranulation in non-treated (no inhibitors) and pre-treated (with inhibitors) human skin MCs with Orai inhibitors (10 μM of Synta-66 or GSK-7975A) and stimulated with LL-37 (10 μM) and SP (10 μM). **(C)** LAD2 cells were pre-treated with 10 μM Orai inhibitors (Synta-66 or GSK-7579A) and stimulated with 3 μM LL-37 subsequent Ca^{2+} influx was determined. **(D)** LAD2 cells were pre-treated with Orai inhibitors (10 μM Synta-66 or GSK-7579A) and stimulated with 1 μM LL-37 and 0.5 μM SP and percent of degranulation was determined. Statistical significance was determined by two-way ANOVA. * indicates P value <.05 and *** indicates P value <.001

A

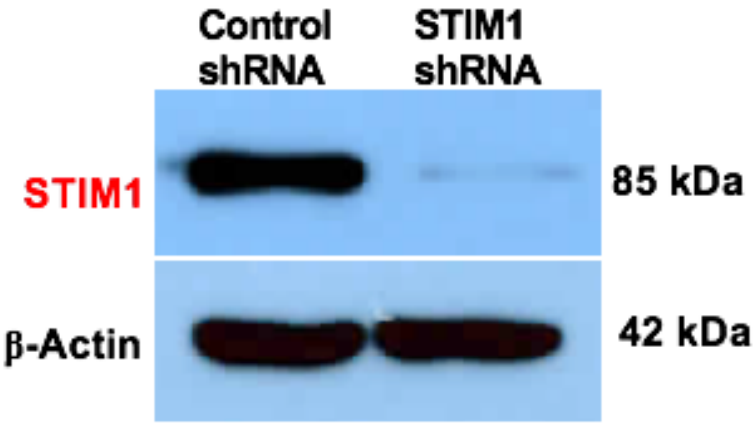
Control shRNA
STIM1 shRNA
STIM1
85 kDa
β-Actin
42 kDa

B

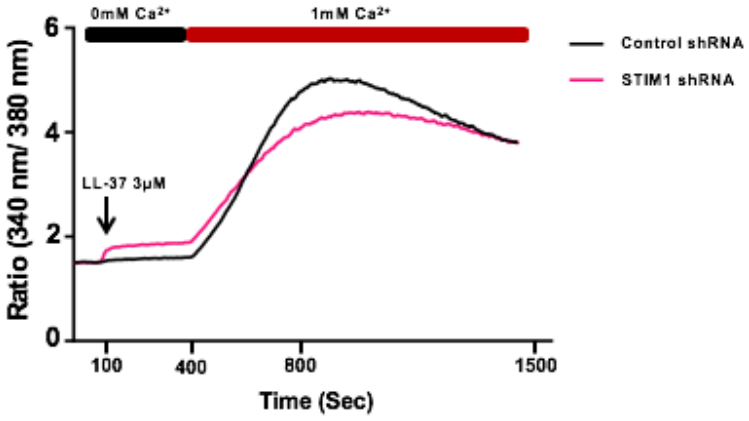
0mM Ca2+
1mM Ca2+
Control shRNA
STIM1 shRNA
LL-37 3μM
Ratio (340 nm/ 380 nm)
0
2
4
6
100
400
800
1500
Time (Sec)

C

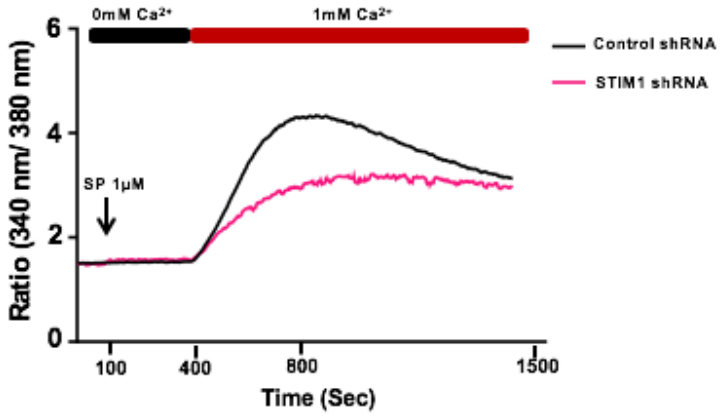
0mM Ca2+
1mM Ca2+
Control shRNA
STIM1 shRNA
SP 1μM
Ratio (340 nm/ 380 nm)
0
2
4
6
100
400
800
1500
Time (Sec)

D

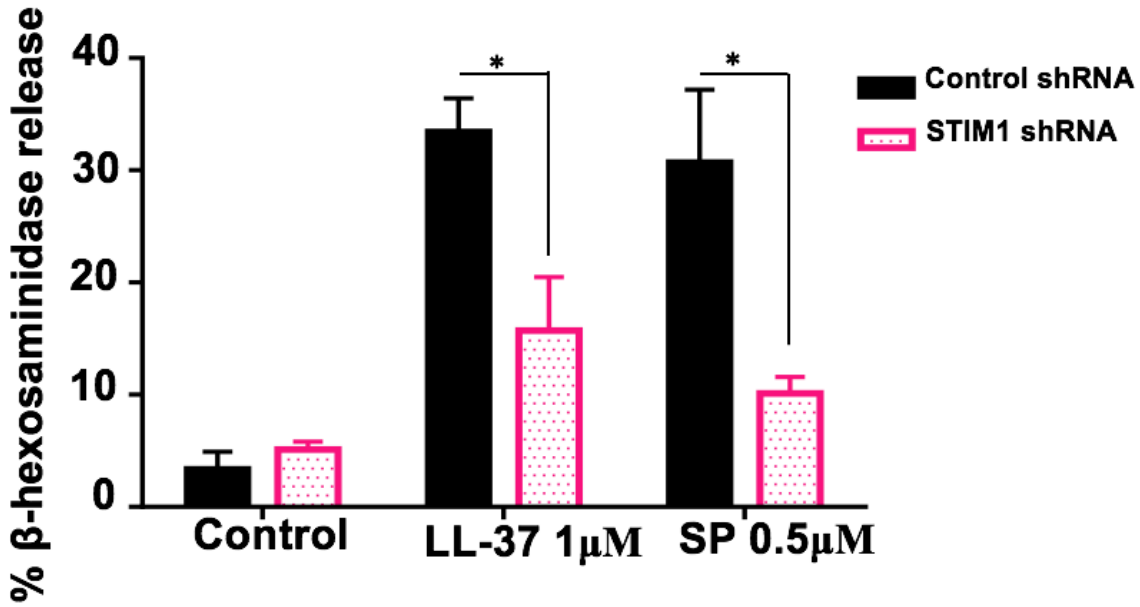
% β-hexosaminidase release
40
30
20
10
0
*
*
Control
LL-37 1μM
SP 0.5μM
Control shRNA
STIM1 shRNA

Fig. 8: Knockdown of STIM1 significantly reduced LL-37 and SP induced calcium mobilization and degranulation.

LAD2 cells were transduced with scrambled shRNA control lentivirus or shRNA lentivirus targeted against STIM1. (**A**), representative immunoblot of the transduced LAD2 is shown. Transduced cells were stimulated were incubated with Fura-2, washed and resuspended in Ca^{2+} free buffer, and stimulated with **(B)**, 3 μM LL-37 or **(*C*)**, 1 μM SP at 100 seconds and Calcium mobilization was determined in the absence of extracellular calcium. At 400 seconds, 1 mM of Ca^{2+} was added and Ca^{2+} influx was determined. **(D),** Control shRNA, and STIM1 shRNA transduced cells were stimulated with 3 μM of LL-37 and 0.5 μM of SP, and percent degranulation was determined. Statistical significance was determined by two-way ANOVA. * indicates P value <.05.

A


Control shRNA
Orai1 shRNA
Orai1
33 kDa
β-Actin
42 kDa

B

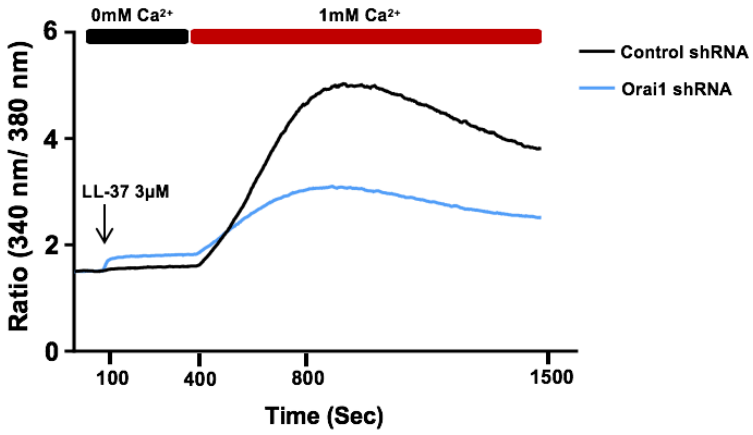
0mM Ca2+
1mM Ca2+
Control shRNA
Orai1 shRNA
LL-37 3μM
Ratio (340 nm/ 380 nm)
0
2
4
6
100
400
800
1500
Time (Sec)

C

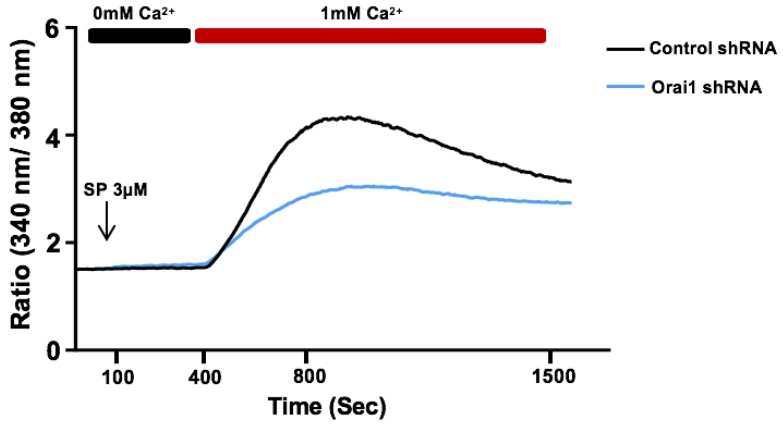
0mM Ca2+
1mM Ca2+
Control shRNA
Orai1 shRNA
SP 3μM
Ratio (340 nm/ 380 nm)
0
2
4
6
100
400
800
1500
Time (Sec)

D

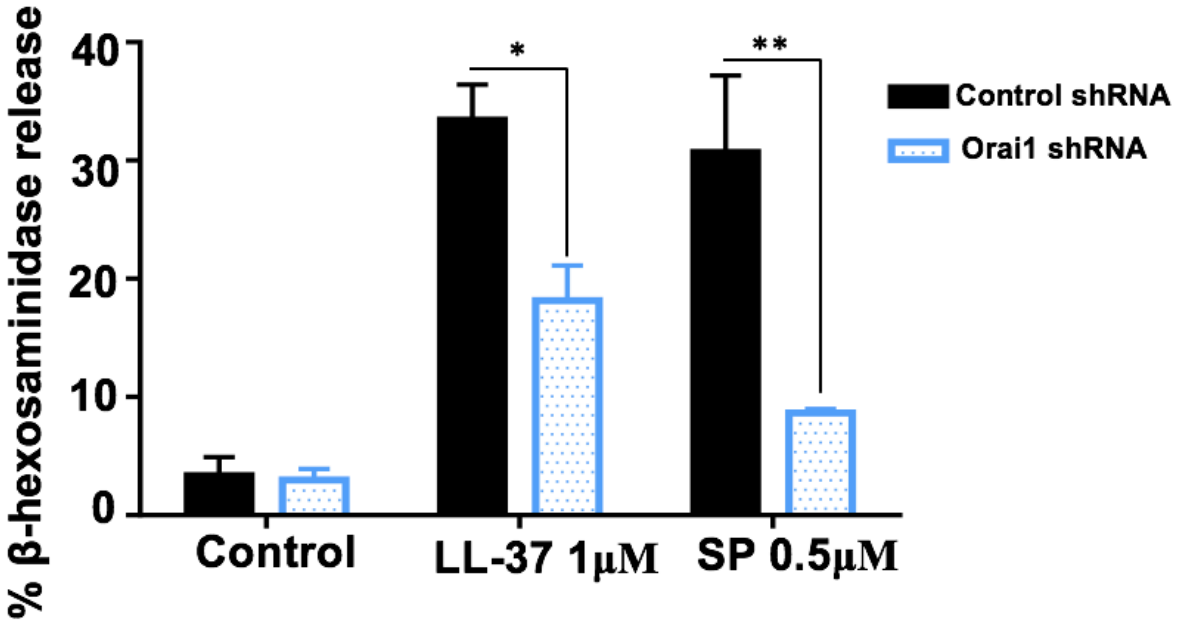
% β-hexosaminidase release
40
30
20
10
0
*
**
Control
LL-37 1μM
SP 0.5μM
Control shRNA
Orai1 shRNA

Fig. 9: Knockdown of Orai1 significantly reduced LL-37 and SP induced calcium mobilization and degranulation.

LAD2 cells were transduced with scrambled shRNA control lentivirus or shRNA lentivirus targeted against Orai1. (**A**), A representative immunoblot of the transduced LAD2 is shown. Transduced cells were incubated with Fura-2, washed and resuspended in Ca2+ free buffer and stimulated with **(B),** 3 μM LL-37, or **(*C*)**, 1μM SP at 100 seconds and Calcium mobilization was determined in the absence of extracellular calcium. At 400 seconds, 1 mM of Ca^{2+} was added and Ca^{2+} influx was determined. **(D),** Control shRNA and Orai1 were stimulated with1 μM of LL-37 and 0.5 μM of SP, and percent degranulation was determined. Statistical significance was determined by two-way ANOVA. * indicates P value <.05 and ** indicates P value <.01.

Chapter 4: Naturally occurring Missense MRGPRX2 variants display Loss of Function Phenotype for Mast Cell Degranulation in response to Substance P, Hemokinin-1, Human β-defensin 3 and Icatibant

Ibrahim Alkanfari, Kshitij Gupta, Tahsin Jahan and Hydar Ali‡

Department of Pathology, University of Pennsylvania, School of Dental Medicine, Philadelphia, Pennsylvania 19104

This chapter was published in the Journal of Immunology

Abstract

Human mast cells (MCs) express a novel G protein-coupled receptor (GPCR), known as Mas-related G protein coupled receptor X2 (MRGPRX2). Activation of this GPCR by a diverse group of cationic ligands such as neuropeptides (NPs), host defense peptides (HDPs) and Food and Drug Approved drugs contributes to chronic inflammatory diseases and pseudo-allergic drug reactions. For most GPCRs, the extracellular domains and their associated transmembrane domains display the greatest structural diversity and are responsible for binding different ligands. The goal of the present study was to determine if naturally occurring missense variants within MRGPRX2's extracellular/transmembrane domains contribute to gain or loss of function phenotype for MC degranulation in response to NPs (substance P; SP and hemokinin-1, HK-1), an HDP (human β-defensin-3, hBD3) and an FDA-approved cationic drug (bradykinin B2 receptor antagonist, icatibant). We have identified eight missense variants within MRGPRX2's extracellular/transmembrane domains from publically available exome-sequencing databases. We investigated the ability of MRGPRX2 ligands to induce degranulation in RBL-2H3 cells individually expressing these naturally occurring MRGPRX2 missense variants. Using stable and transient transfections, we found that all variants express in RBL cells. However, four natural MRGPRX2 variants, G165E (rs141744602), D184H (rs372988289), W243R (rs150365137) and H259Y (rs140862085) failed to respond to any of the ligands tested. Thus, diverse MRGPRX2 ligands utilize common sites on the receptor to induce MC degranulation. These findings have

important clinical implications for MRGPRX2 and MC-mediated pseudo-allergy and chronic inflammatory diseases.

Introduction

In addition to FcεRI, mast cells (MCs) express a novel seven transmembrane (7TM) domain receptor known as MAS-related G protein-coupled receptor X2 (MRGPRX2) [45, 130]. Emerging evidence suggests that MRGPRX2 contributes to the pathogenesis of a number of chronic inflammatory diseases and is responsible for injection site reactions to opioids and other FDA-approved cationic drugs [43, 92, 110, 131-134]. For example, expression of MRGPRX2 is upregulated in skin MCs of patients with chronic urticaria when compared to MCs of normal subjects [43]. Furthermore, MRGPRX2-mediated MC activation by the neuropeptide, SP contributes to the pathogenesis of chronic urticaria. Hemokinin-1 (HK-1) is a novel neuropeptide, which is released from antigen/IgE activated MCs and human bronchial cells and causes contraction of human bronchi *ex vivo* [135, 136]. We recently reported that MRGPRX2 is expressed at low level in non-asthmatic lung MCs but its expression is significantly upregulated in asthmatic lung MCs and demonstrated that HK-1 causes MC degranulation via this receptor [93].

Human β-defensin-3 (hBD3) and MRGPRX2-expressing MCs are present in healthy gingiva and their levels are elevated in patients with chronic periodontitis [92, 137]. Furthermore, hBD3 causes MC degranulation via MRPGRX2 [42]. Icatibant, a bradykinin B_2 receptor antagonist used for the treatment of hereditary angioedema, promotes MC degranulation via MRPGRX2 and causes injection-site erythema and swelling in nearly every patient [40, 138]. These findings suggest that activation of MRGPRX2 by a diverse group of ligands such as SP, HK-1, hBD3

and icatibant contribute to the pathogenesis of chronic urticaria, asthma, periodontitis and pseudo-allergic reactions. Modeling and mutagenesis studies with SP and various opioid ligands led to the suggestion that different agonists interact with different amino acid residues in MRGPRX2's predicted ligand-binding pocket to induce MC degranulation [139, 140]. However, the sites of interaction of HK-1, hBD3 and icatibant on MRGPRX2 for MC degranulation have not been determined.

Recent crystallography data obtained for a number of GPCRs and comparison of sequence homology have provided prediction regarding the regions of GPCRs that are involved in ligand binding and G protein coupling. The 7TM bundles are connected by three extracellular loops (ECL1, ECL2 and ECL3) and three intracellular loops (ICL1, ICL-2 and ICL-3). The extracellular part also includes the N-terminus (N-term) and the intracellular (IC) part includes the helix VIII and a C-terminal sequence. GPCRs can be divided into modules. The EC and their closest TM regions (see Fig. 1A) have the greatest structural diversity and are responsible for the binding of diverse ligands. By contrast, the IC and its closest TM regions are responsible for G protein coupling and downstream signaling [46].

We have identified eight naturally occurring missense variants within MRGPRX2's extracellular and transmembrane domains from three publically available databases; Exome Sequencing Project (NHLBI-GO-ESP), 1000 Genomes project and Exome Aggregation Consortium (ExAC). The goal of the present study was to determine if any of these variants display gain or loss of

function phenotype for MC degranulation in response to NPs (substance P; SP and hemokinin-1, HK-1), an HDP (hBD3) and a cationic drug (bradykinin B2 receptor antagonist, icatibant). The data presented herein provide novel insights on the impact of single naturally occurring mutation on MRGPRX2 activation by a diverse group of cationic ligands and have important implications for MC-mediated health and disease.

Materials and Methods

Materials

All cell culture reagents and Indo-1 were purchased from Invitrogen (Gaithersburg, MD). Substance P, Fluorescent-labeled substance P (FAM-SP), hBD3 and icatibant were purchased from Anaspec (Fremont, CA). Human hemokinin-1 was purchased from Alpha Diagnostic (San Antonio, TX). MRGPRX2 plasmid encoding hemagglutinin (HA)-tagged human MRGPRX2 in pReceiver-MO6 vector was obtained from GeneCopoeia (Rockville, MD). Amaxa transfection kit (Kit V) was purchased from Lonza (Gaithersburg, MD). PE-Anti human MRGPRX2 was obtained from Biolegend (San Diego, CA). QuikChange II Site-Directed Mutagenesis kit was purchased from Agilent Genomics (Santa Clara, CA).

Cell culture

Rat basophilic leukemia (RBL-2H3) cells were maintained as monolayer cultures in Dulbecco's modified Eagle's medium (DMEM) supplemented with 10% FBS, L-glutamine (2 mM), penicillin (100 IU/ml) and streptomycin (100 µg/ml) [80].

Site-directed mutagenesis

Quick II change site-directed mutagenesis kit (Agilent) was used to generate MRGPRX2 variants. DNA sequencing was performed to confirm the

nucleotide sequences for each construct. The forward and reverse primers were used for each variant are listed below.

N16H: Forward: 5'-GGGCTTGGTCATTTCCATGCACTGTTGTACTTTCTGT-3' Reverse: 5'-ACAGAAAGTACAACAGTGCATGGAAATGACCAAGCCC-3' **L31V:** Forward: 5'-GAAGACCGGGATCACGGTCTCCTTGCCAC-3' Reverse: 5'-GTGGCAAGGAGACCGTGATCCCGGTCTTC-3' **V43I**: Forward: 5'-TTTCCTACCAGCCCGATCAGGGCAATGAAAAGG-3' Reverse: 5'-CCTTTTCATTGCCCTGATCGGGCTGGTAGGAAA-3' **F78L:** Forward: 5'-GGAAGCAGAGTAAGAGGAAGTCGGCCCCG-3' Reverse: 5'-CGGGGCCGACTTCCTCTTACTCTGCTTCC-3' **G165E:** Forward: 5'-GCTGAGCATCTTGGAAGAGAAGTTCTGTGGCTTCT-3' Reverse: 5'-AGAAGCCACAGAACTTCTCTTCCAAGATGCTCAGC-3' **D184H:** Forward: 5'-CTCTGGTTGGTGTCAGACATTTCATTTCATCACTGC-3' Reverse: 5'-GCAGTGATGAAATGAAATGTCTGACACCAACCAGAG-3' **W243R:** Forward: 5'-CTGCCCTTTGGCATTCAGCGGTTCCTAATATTATGGAT-3' Reverse: 5'-ATCCATAATATTAGGAACCGCTGAATGCCAAAGGGCAG-3' **H259Y:** Forward: 5'-AAGGATTCTGATGTCTTATTTTGTTATATTCATCCAGTTTCAGTTGTC-3' Reverse: 5'GACAACTGAAACTGGATGAATATAACAAAATAAGACATCAGAATC CTT-3'

Transfection of RBL cells and Flow cytometry

Cells (1. 5 x10^6) were transfected with plasmids (1.5 μg) encoding MRGPRX2 or its missense variants using the Amaxa Nucleofector device and Amaxa kit V according to the manufacturer's protocol. For stable transfection, cells were cultured in the presence of G-418 (1 mg/ml) and used within one month of transfection [41]. For transient transfection, cells were used within 16-20 hours after transfection. To detect MRGPRX2 expression, cells (0.5 x 10^6) were incubated with PE-conjugated anti-MRGPRX2 antibody, washed in FACS buffer, fixed and analyzed on a BD LSR II flow cytometer. For FAM-SP binding RBL-2H3 cells stably overexpressing MRGPRX2 (RBL-MRGPRX2) were used [93]. Untransfected RBL cells and RBL-MRGPRX2 cells (0.5 x 10^6) were incubated for with FAM-SP (1 μM, 60 min, 4°C). The cells were washed twice with FACS buffer and analyzed by flow cytometry.

Calcium Mobilization

Ca^{2+} mobilization was determined as described previously [41]. Briefly, cells (2 x 10^6) were loaded with 1 μM indo-1 AM for 30 minutes at room temperature. Cells were then washed and resuspended in 1.5 ml of HEPES-buffered saline. The cells were then stimulated with SP and Ca^{2+} mobilization was determined using a Hitachi F-2700 spectrophotometer with an excitation wavelength of 355 nm and an emission wavelength of 410 nm.

Degranulation

Cells (5 x 10^4) were seeded into 96-well plates in a total volume of 50 µl HEPES buffer containing 0.1% bovine serum albumin (BSA) and exposed to ligands for 30 minutes. Cells without treatment were designated as controls. For total β-hexosaminidase release, unstimulated cells were lysed in 50 µl of 0.1% Triton X-100. Aliquots (20 µl) of supernatants or cell lysates were incubated with 20 µl of 1 mM p-nitrophenyl-N-acetyl-β-D-glucosamine for 1 hour at 37 °C. The reaction was stopped by adding 250 µl of a 0.1 M Na_2CO_3/0.1 M $NaHCO_3$ buffer and absorbance was measured at 405 nm [41].

Results

Identification of D184H and G165E as loss of function MRGPRX2 variants for SP, hemokinin-1, hBD3 and Icatibant in stably transfected RBL-2H3 cells

To identify naturally occurring missense variants in the extracellular and transmembrane domains of MRGPRX2, we searched publically available databases, NHLBI-GO-ESP, 1000 Genomes and ExAC. We found eight targets in the MRGPRX2 gene with missense mutations (Fig. 1A). Amino acid change for each mutation is shown in Fig. 1B. Data from a computational protein prediction program, Polymorphism Phenotyping v2 (PolyPhen-2), under the HumDiv model on a scale of 0 (benign) to 1 (damaging) are shown in are shown in Fig. 1B [141]. The G165E and D184H variants have the lowest minor allele frequency (average MAF, <0.01%) whereas the N16H variant has the highest MAF (8.95%). Combined annotation-dependent depletion (CADD) is an in silico tool used for scoring the deleteriousness of single nucleotide variants as well as insertion/deletion variants in the human genome [142]. A CADD score of >10 indicates that a variant may be deleterious. As shown in Fig. 1B, all eight MRGPRX2 variants targeted for the present study have CADD scores of <10. Thus, the combined in silico analyses suggest that although some of the MRGPRX2 variants may be damaging (Polyphen2 score >0.5), these mutations are rare (MAF <1%) and may not be associated with pathogenicity (CADD <10) (Fig. 1).

Studies on the effects of missense or other mutations on GPCR functions are routinely conducted with transiently transfected HEK293 cells [139, 140, 143-

145]. However, our previous studies on the regulation of MRGPRX2 have been performed with stably transfected rodent mast cell line (RBL-2H3 cell) that does not endogenously express the receptor [92, 93]. To determine if any of the MRGPRX2 variants shown in Fig. 1 display gain or loss of function for MC activation, we first generated stable transfectants in RBL cells. The stable transfection procedure involves cDNA nucleofection followed by culturing cells in the presence of selection marker G418. We were quite surprised to find cells expressing three mutants (N16H, W243R or H259Y) did not survive the G418 selection procedure. We found that 5 days after the start of G418 selection, cells expressing the wild-type (WT) receptor were almost fully covering the surface of the tissue culture dish but only few cells could be detected in N16H, W243R or H259Y transfectants. We used Triton X to lyse the cells and measured total β-hexosaminidase content as an assay to quantitate cell number. As shown in Fig. 2A, unlike the situation with cells expressing the WT receptor, we could not detect any β-hexosaminidase in transfectants with cDNA encoding N16H, W243R or H259Y (Fig. 2A). We therefore focused our initial studies on variants L31V, V43I, F78L, G165E and D184H, which stably express on the cell surface similar to the WT receptor (Fig 2B). Although MRGPRX2 is activated by multiple ligands, SP is probably the most well characterized [40, 43, 45, 130, 132, 140]. We therefore tested the effects of SP on Ca^{2+} mobilization and degranulation in cells expressing these variants. We found that the variants L31V, V43I and F78L responded normally to SP for Ca^{2+} mobilization and degranulation (Fig. 2C and D). By contrast, when compared to the WT receptor, Ca^{2+} mobilization and degranulation

to SP were substantially inhibited in cells expressing G165E and D184H variants (Fig. 2C and 2D), despite normal cell surface expression (Fig. 2B). These findings are consistent with higher polyPhen2 score for G165E and D184H when compared to L31A, V43I and F78L variants (Fig. 1B).

Reddy et al., [139] recently showed that a point mutant of MRGPRX2 (E164R) was resistant to SP for Ca^{2+} mobilization but responded normally to a host defense peptide, LL-37. Based on this finding, it was proposed that different amino acid residues on MRGPRX2 are responsible for binding to different ligands. We therefore tested the effects of naturally occurring missense mutations (L31A, V43I, F78L, G165E and D184H) on degranulation in response to HK-1, hBD3 and icatibant. As shown in Fig. 3, A-C, cells expressing L31V, V43I or F78L variant responded to all ligands tested for degranulation similar in extent to the WT receptor. By contrast, cells expressing G165E or D184H variant were resistant to HK-1, hBD3 and icatibant for degranulation. These findings suggest that SP, HK-1, hBD3 and icatibant all interact with the same amino acids on MRGPRX2's 4^{th} and 5^{th} TM domains (Fig. 1) to induce MC degranulation.

Our next goal was to perform binding studies to determine if reduced MC activation in missense variants correlates with correspondingly reduced ligand binding to MRGPRX2. Of the agonists used in this study, only SP is available as a fluorescent-labeled conjugate (FAM-SP). Our initial goal was to perform flow cytometry analysis to determine if FAM-SP binds to RBL cells stably expressing MRGPRX2 and to test if this binding could be blocked by unlabeled HK-1, hBD3

or Icatibant. For these studies, we used RBL cells stably overexpressing MRGPRX2 (RBL-MRGPRX2). We confirmed cell surface MRGPRX2 expression by flow cytometry using PE-conjugated anti-MRGPRX2 antibody (Fig. 4A). To validate the functional activity of FAM-SP for MRGPRX2, we compared its ability to induce degranulation in untransfected RBL and RBL-MRGPRX2 cells. As shown in Fig. 4B, both unlabeled SP and FAM-SP induced degranulation in RBL-MRGPRX2 cells but not in untransfected cells, validating the specificity of FAM-SP for the receptor. However, flow cytometry experiment demonstrated that FAM-SP interact equally well with untransfected RBL and RBL-MRGPRX2 cells (Fig. 4C). These findings suggest that the amphipathic nature of SP facilitates a strong interaction with the plasma membrane even in the absence of MRGPRX2, thus making it difficult to perform the proposed binding studies.

Identification of W243R and H259Y as loss of function MRGPRX2 variants for SP, HK-1, hBD3 and Icatibant in transiently transfected RBL cells

The low PolyPhen-2 score for the MRGPRX2 variant H259Y (Fig. 1B) indicates that this mutation is benign. Thus, our inability to generate a stable transfectant expressing this variant in RBL cells was surprising. We therefore, generated transient transfectant in RBL cells expressing H259Y. We also performed similar studies with two other variants with high PolyPhen2 score (N16H; 0.937 and W243R; 0.760) that did not survive the stable transfection procedure (Fig. 1A). We found that all three variants expressed on the surface of

RBL cells (Fig. 5A). The N16H variant responded to SP for Ca^{2+} mobilization and degranulation similar to the WT receptor (Fig. 5B and C). However, W243R and H259Y variants were resistant to SP-induced Ca^{2+} mobilization and degranulation (Fig. 5B and C). HK-1, hBD3 and icatibant induced normal degranulation in cells transiently expressing N16H but they failed to activate this response in cells expressing W243R or H259Y variant (Fig. 6).

Discussion

The unique features of MRGPRX2 that distinguish it from other GPCRs are its predominant expression on human MCs and its activation by a diverse group of cationic ligands [40, 43, 92, 93]. Emerging evidence suggests that MRGPRX2 contributes to pseudo-allergic drug reactions and a number of chronic inflammatory diseases [40, 146, 147]. Although activation of MRGPRX2 or FcεRI on MCs elicits intracellular Ca^{2+} mobilization and comparable MC degranulation, MRGPRX2 stimulation triggers little to no cytokine or prostaglandin E_2 generation [40, 148, 149]. Thus, the effects on MRGPRX2 on MC-mediated disorders likely reflects Ca^{2+} mobilization and degranulation. In the present study, we have utilized eight naturally occurring missense MRGPRX2 variants and identified rare mutations that display loss of function phenotype for MC degranulation in response to ligands that participate in pseudo-allergy (icatibant) [40], itch/chronic urticaria (SP) [43, 132], asthma (HK-1) [93, 135, 136] and periodontitis (hBD3) [92].

Molecular modeling and docking approaches have recently been used to identify Glu^{164} (E164) and Asp^{184} (D184) in MRPGRX2's 4^{th} and 5^{th} TM domains as the negatively charged residues that make ionic contact with cationic opioid ligands [140]. Accordingly, E164Q or D184N substitution that retains the steric property of the wild-type residue but removes the negative charge resulted in loss of receptor activation by dextromethorphan, morphine and related opioids ligands. These findings suggest that both Glu^{164} and Asp^{184} are important for the binding of opioids to MRGPRX2 and that removal of one negatively charged residue results

in loss of ligand-receptor interaction. However, MRGPRX2 activation by a metabolite of an endogenous opioid peptide, dynorphin A (1–13), is lost in the D184N but not the E164Q mutation [140]. Modeling studies predict that Arg^{7} and Phe^{4} of dynorphin interact with Asp^{184} but not Glu^{164}. These findings suggest that one or both anionic Glu^{164} and Asp^{184} participate in the binding of cationic opioids and endogenous opioid peptide metabolites. Using publically available web portals, Reddy et al., [139] also predicted that SP-binding pocket in MRGPRX2 consists of a number of structurally conserved hydrophilic residues along with a buried glutamic acid residue ($Glu^{164,}$ E164). Accordingly, replacement of Glu^{164} with a positively charged Arg (E164R) results in loss MRGPRX2 activation by SP. However, this mutant respond normally to the host defense peptide, LL-37 [139]. These findings suggest that different ligands interact with different amino acid residues on MRGPRX2's predicted ligand binding pocket to induce MC degranulation [139, 140].

The goal of the present study was to use publically available databases to identify naturally occurring missense MRGPRX2 variants that display gain or loss of function phenotype for MC degranulation by a diverse group of cationic ligands. There are a number of interesting features regarding the rare MRGPRX2 variant G165E (MAF; <0.01%) that warrant discussion. First, it is present within the predicted binding pocket for opioids and SP, as determined from modeling studies [139, 140]. Second, although we were unsuccessful in demonstrating specific binding of FAM-SP to RBL cells stably overexpressing MRGPRX2 due to high background binding, it is likely that this mutation interferes with SP's binding to

MRGPRX2. This contention was supported by the finding that cells expressing G165E variant did not respond to SP for Ca^{2+} mobilization despite normal cell surface expression. Third, and most importantly, none of the other MRGPRX2 ligands tested caused degranulation in cells expressing this variant. It is noteworthy that G165E mutation results in the replacement of an aliphatic side chain with a positively charged residue next to a negatively charged amino ($Glu^{164,}$ E164) required for ionic interaction with SP and opioids [139, 140]. It is therefore likely that the presence two adjacent negatively charged side chains (E164, E165) in the variant G165E interferes with the integrity of the binding pocket and thus preventing MC activation by SP and all other cationic ligands used in this study.

Studies by Reddy et al., [139] did not consider Asp^{184} as a possible site for SP interaction with MRGPRX2 despite the fact this amino acid is critical for receptor activation of by all opioid ligands tested, including dynorphin A [140]. It is interesting to note that the naturally occurring D184H variant results in the switching of a negatively charged side chain to a positively charged one. An important finding of the present study was that none of the MRGPRX2 agonists tested stimulated degranulation in RBL cells stably expressing either G165E or D184H variant. These results suggest that SP and opioid binding pocket identified within MRGPRX2's 4^{th} and 5^{th} TM domains [139, 140] is shared by all MRGPRX2 agonists that induce MC degranulation and that G165E or D184H mutation disrupts the integrity of the binding pocket preventing receptor activation.

We found that two additional mutations, W243R and H259Y, in the 6th and 7th TM domains outside MRGPRX2's predicted ligand binding pocket also rendered the receptor unresponsive to all ligands tested. The mechanism by which these mutations lead to loss of degranulation is unknown. Interestingly, we found that while cells expressing these variants do not survive the stable transfection procedure they express normally in transiently transfected cells. It is therefore possible that replacement of the bulky Trp with a positively charged Arg in variant W243R and His with Tyr in variant H269Y influences both the receptor's expression status and its ability to interact with diverse ligands. In future studies, it will be interesting to determine the MC status of individuals harboring these mutations and their responsiveness to MGRPRX2 ligands.

In summary, we have shown that naturally occurring rare MRGPRX2 variants with single amino acid substitution in the receptor's predicted ligand binding pocket (G165E and D184H) renders it unresponsive to SP, HK-1, hBD3 and icatibant for MC degranulation. Although the naturally occurring variants W243R and H259Y in the receptor's 6th and 7th TM domain also rendered the receptor unresponsive to all ligands tested for degranulation, the mechanisms of their actions are unknown and remain to be determined. An important clinical implication of the present study is that individuals harboring any of the missense MRGPRX2 mutation (G165E, D184H, W243R or H259Y) may be protected from MC-mediated drug-induced pseudo-allergy and chronic inflammatory diseases such as itch, chronic urticaria, asthma and periodontitis. A goal of our future studies is to determine the responsiveness of MCs isolated from these individuals to

MRGPRX2 ligands and to test whether these individuals develop skin reactions to pseudo-allergic drugs.

Figures

(A)

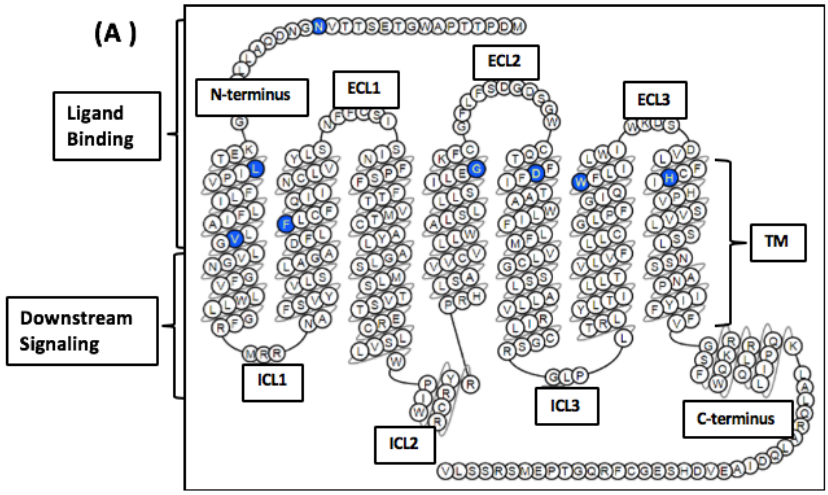

(B)

rs ID	Protein change	PolyPhen2 (Class:score)	MAF (%) NHLBI-GO-EXOME	1000 Genome	ExAc	Average	CADD
rs11024970	N16H	Possibly damaging:0.937	8.70	11.30	6.85	8.95	1,1
rs145992601	L31V	Benign:0.001	0.20	0.20	0.20	0.20	0.001
rs11823569	V43I	Possibly damaging:0.502	0.91	0.66	0.24	0.60	6.35
rs79763999	F78L	Benign:0.129	0.35	0.32	0.10	0.25	6.01
rs141744602	G165E	Possibly damaging:0.567	< 0.01	not available	< 0.01	< 0.01	4.32
rs372988289	D184H	Possibly damaging:0.736	< 0.01	not available	< 0.01	< 0.01	4.03
rs150365137	W243R	Possibly damaging:0.760	0.43	0.14	0.33	0.30	2.15
rs140862085	H259Y	Benign:0.009	0.03	0.04	0.01	0.02	0.001

Fig. 1: Naturally occurrence MRGPRX2 variants identified from the NHLBI GO ESP database

(A), Serpentine diagram of the secondary structure of human MRGPRX2. Each circle represents amino acid residue with one letter code. Solid background denotes the eight naturally occurring missense variants used in the present study. Extracellular (ECL), intracellular (ILC) and transmembrane (TM) domains are shown. **(B),** Amino acid change for each MRGPRX2 variant, PolyPhen-2 score, Minor allele frequency (MAF) and CADD score are shown.

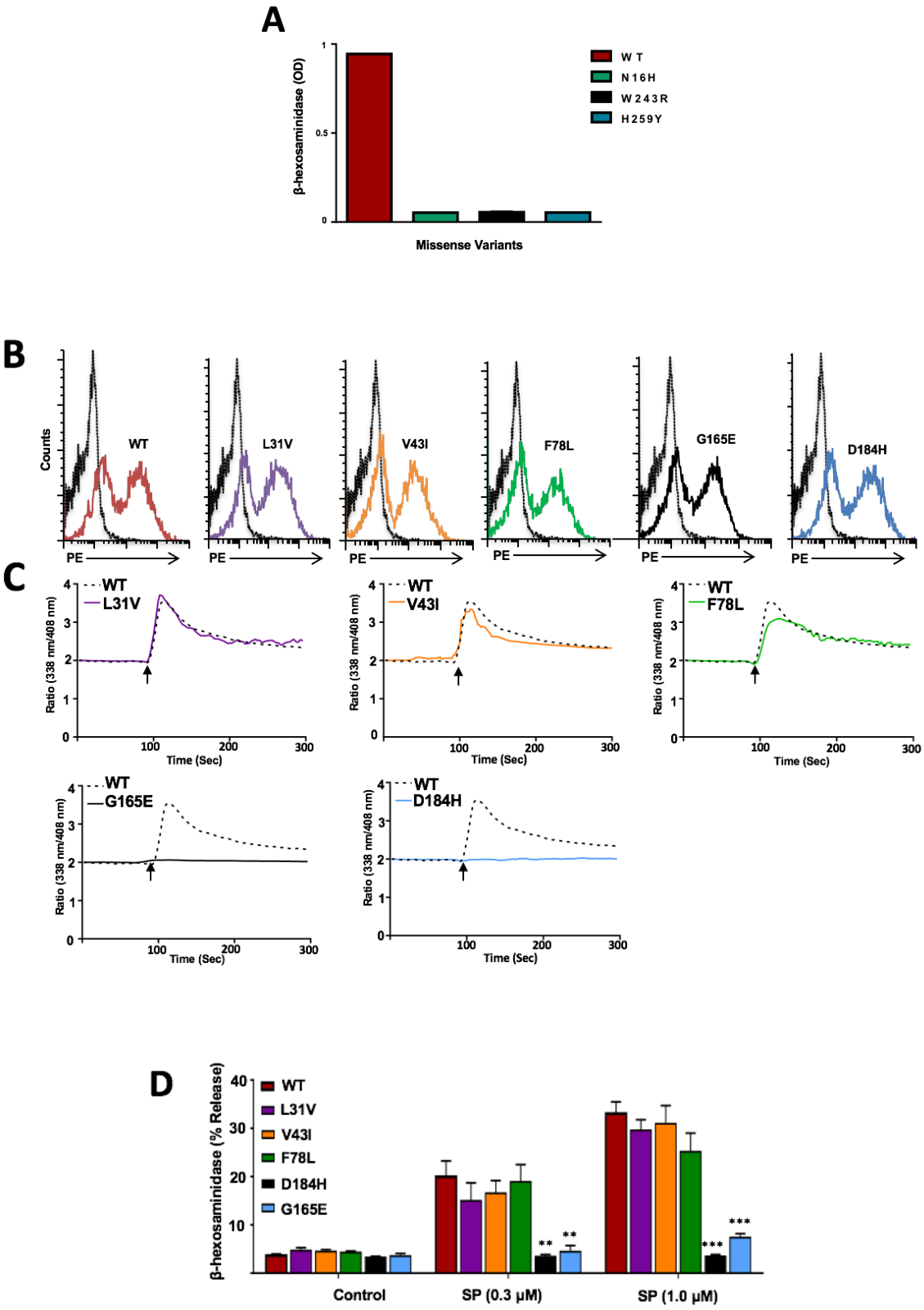
A
β-hexosaminidase (OD)
1
0.5
0
W T
N16H
W243R
H259Y
Missense Variants
B
Counts
WT
L31V
V43I
F78L
G165E
D184H
PE
C
WT
L31V
V43I
F78L
G165E
D184H
Ratio (338 nm/408 nm)
Time (Sec)
100
200
300
D
β-hexosaminidase (% Release)
40
30
20
10
WT
L31V
V43I
F78L
D184H
G165E
**
***
Control
SP (0.3 μM)
SP (1.0 μM)

Fig. 2: Effects of naturally occurring MRGPRX2 mutations (L31I, V43I, F78L, G165E and D184H) on cell surface expression, SP-induced Ca^{2+} mobilization and degranulation in stably transfected RBL cells.

(A), Cells were transfected with cDNA encoding wild-type (WT), N16H, W243R, or H253Y variant, transferred to 24 well plate and G418 was added to the culture medium 16 hours after transfection. After 5 days, non-adherent cells were removed, adherent cells were lysed and total β-hexosaminidase content was determined. **(B),** Flow cytometry was performed with PE-anti-MRGPRX2 antibody to determine cell surface expression of WT and variants in stably transfected RBL cells. Representative histograms for WT/Variant (*black*) and control untransfected cells (colored line) are shown. **(C),** Cells expressing WT and MRGPRX2 variants were loaded with Indo-1 and intracellular Ca^{2+} mobilization in response to SP (1 μM) was determined. Data shown are representative of three independent experiments. **(D),** Cells were exposed to buffer (control) or SP (0. 3μM and 1 μM) for 30 minutes and β-hexosaminidase release was determined. All data points are expressed as mean ± SEM of three experiments performed in triplicate. Statistical significance was determined by two-tailed unpaired t-Test. *** indicates P value<.001, and ** indicates P value <.01.

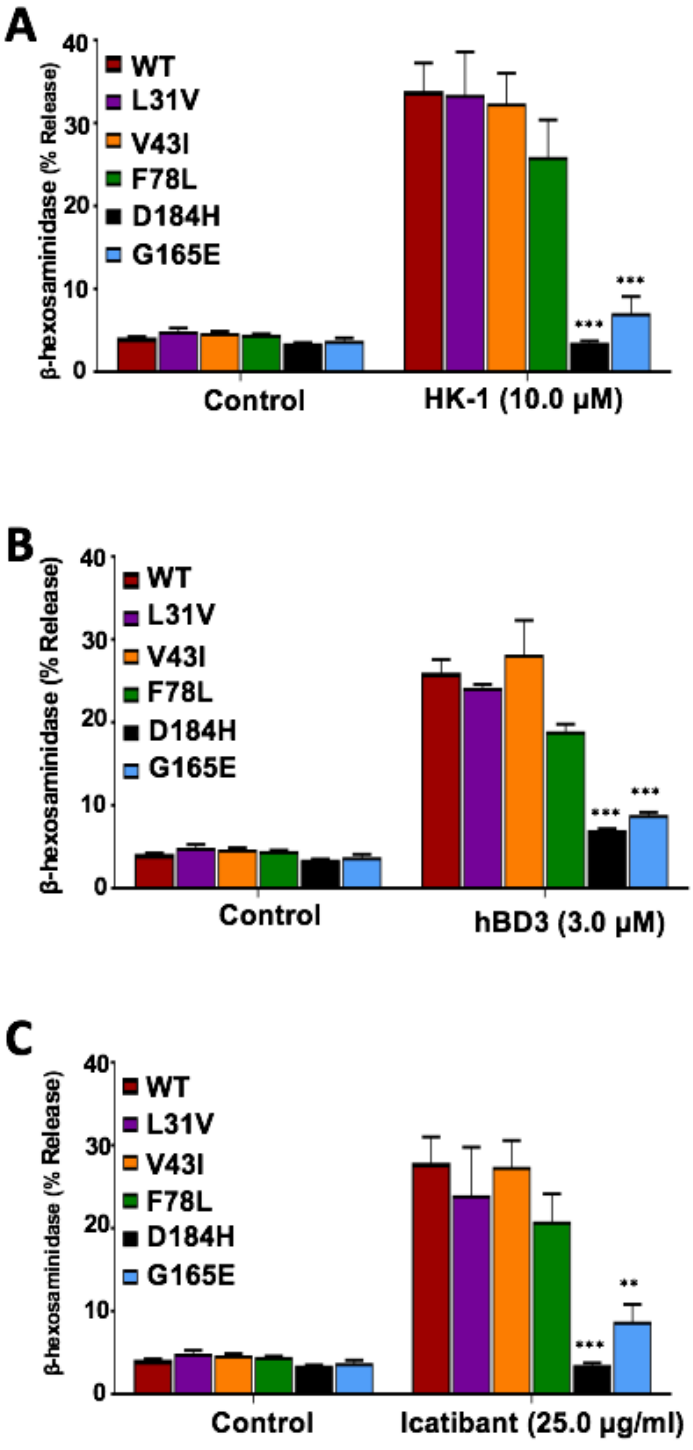
A
β-hexosaminidase (% Release)
40
30
20
10
0
WT
L31V
V43I
F78L
D184H
G165E
***
***
Control
HK-1 (10.0 μM)
B
β-hexosaminidase (% Release)
40
30
20
10
0
WT
L31V
V43I
F78L
D184H
G165E
***
***
Control
hBD3 (3.0 μM)
C
β-hexosaminidase (% Release)
40
30
20
10
0
WT
L31V
V43I
F78L
D184H
G165E
**
***
Control
Icatibant (25.0 μg/ml)

Fig. 3: Effects of naturally occurring MRGPRX2 mutations (L31I, V43I, F78L, G165E and D184H) on HK-1, hBD3 and icatibant-induced degranulation in stably transfected RBL cells.

Cells stably expressing WT and MRGPRX2 variants were exposed to buffer (control) or stimulated with **(A),** hemokinin-1 (HK-1, 10 μM), **(B),** hBD3 (3 μM) or **(C),** icatibant (25 μg/ml) for 30 minutes and β-hexosaminidase release was determined. Statistical significance was determined by two tailed unpaired t-Test. *** indicates P value<.001, ** indicates P value <.01.

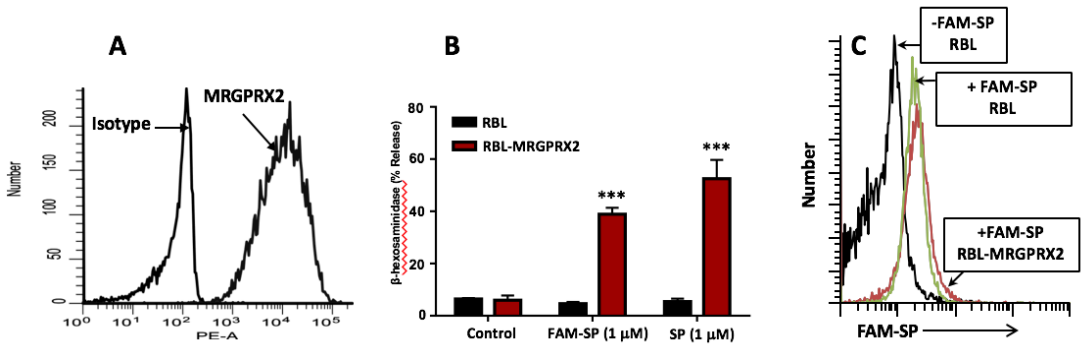

Fig. 4: FAM-SP-induced degranulation and binding in RBL cells overexpressing MRGPRX2.

(A), RBL cells stably overexpressing MRGPRX2 (RBL-MRGPRX2) were exposed to PE-conjugated anti-MRGPRX2 or PE-conjugated isotype matched antibody and cell surface receptor expression was determined by flow cytometry. **(B),** RBL and RBL-MRGPRX2 cells were exposed to buffer (control), SP or FAM-SP for 30 minutes and β-hexosaminidase release was determined. **(C),** RBL or RBL-MRGPRX2 cells were exposed to FAM-SP (1 μM, 60 minutes, 4°C), washed and fluorescence was determined by flow cytometry. Statistical significance was determined by two tailed unpaired t-Test. *** indicates P value<.001.

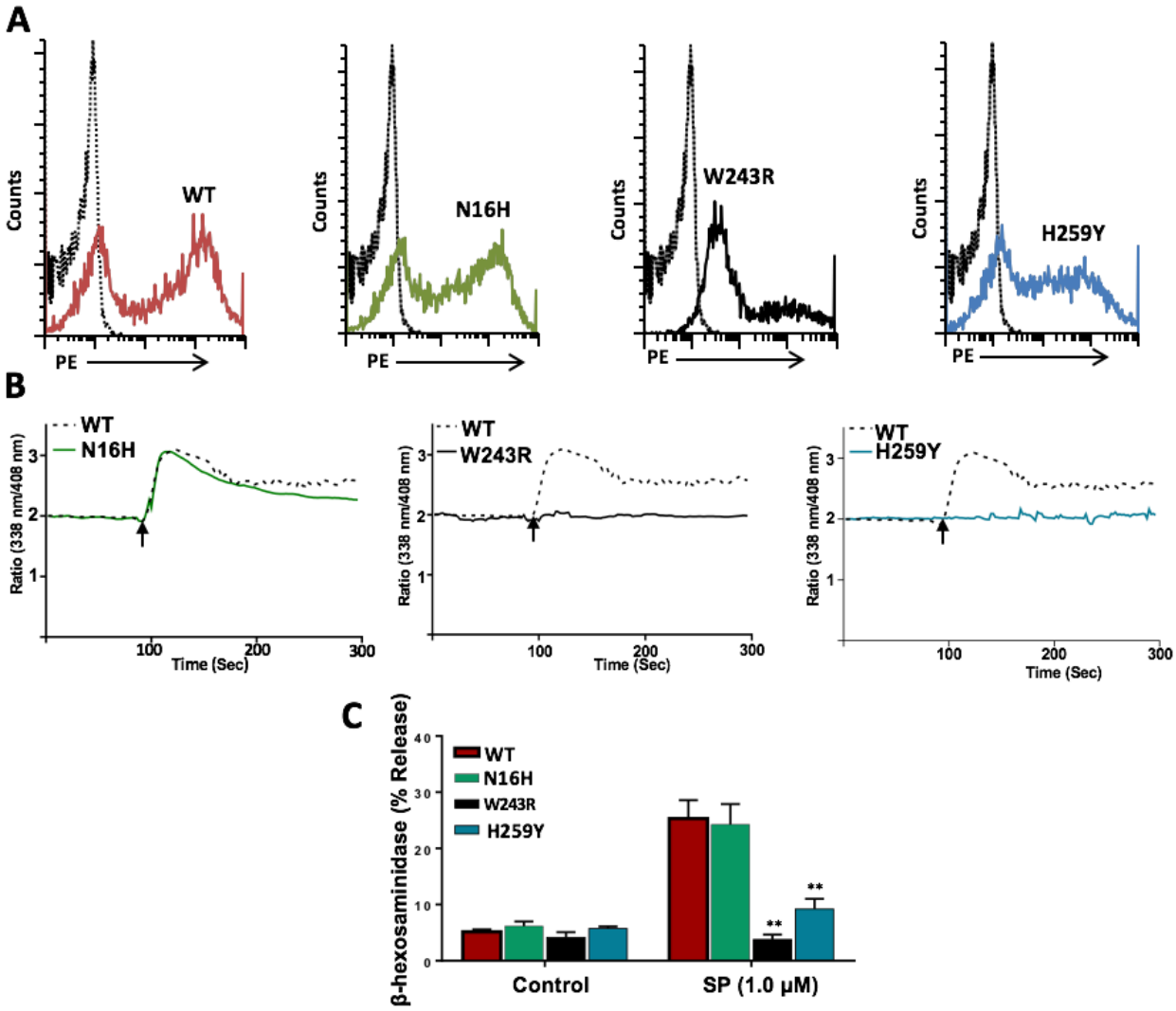
A
Counts
WT
PE
Counts
N16H
PE
Counts
W243R
PE
Counts
H259Y
PE
B
WT
N16H
Ratio (338 nm/408 nm)
Time (Sec)
WT
W243R
Ratio (338 nm/408 nm)
Time (Sec)
WT
H259Y
Ratio (338 nm/408 nm)
Time (Sec)
C
β-hexosaminidase (% Release)
WT
N16H
W243R
H259Y
**
**
Control
SP (1.0 μM)

Fig. 5: Effects of naturally occurring MRGPRX2 mutations (N16H, W243R and H259Y) on cell surface expression, Ca^{2+} mobilization and SP-induced degranulation in transiently transfected RBL cells.

(A), Flow cytometry was performed using PE-anti-MRGPRX2 antibody to determine cell surface expression of wild-type (WT) and variants in transiently transfected in RBL cells. Representative histograms for WT/Variant (*black intermittent*) and control untransfected cells (colored) are shown. **(B),** Cells expressing WT and MRGPRX2 variants were loaded with Indo-1 and intracellular calcium mobilization in response to SP (1 μM) was determined. Data shown are representative of three independent experiments. **(C),** Cells were exposed to buffer (control) or SP (1 μM) for 30 minutes and β-hexosaminidase release was determined. Statistical significance was determined by two tailed unpaired t-Test. ** indicates P value <.01.

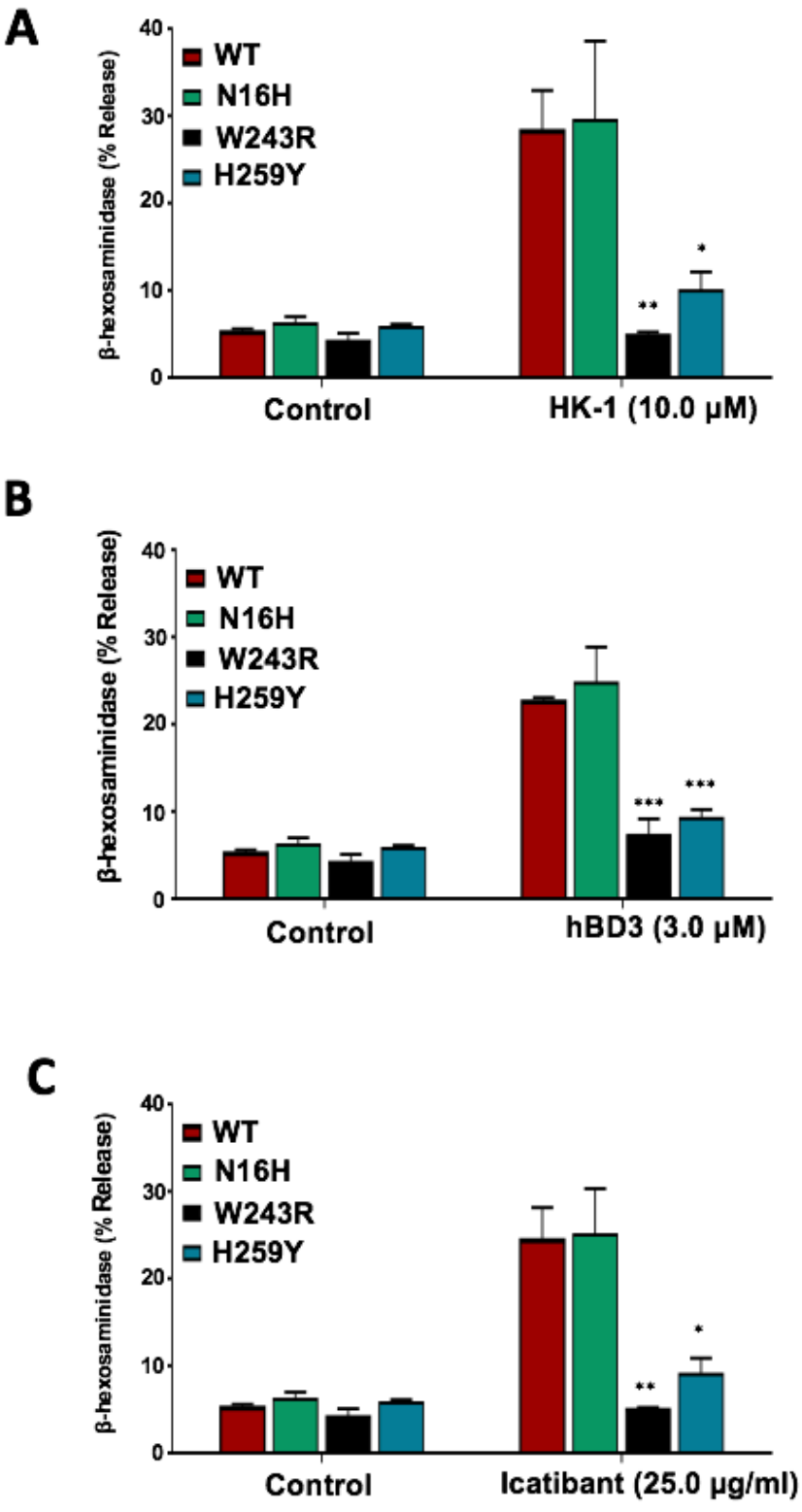
A
β-hexosaminidase (% Release)
WT
N16H
W243R
H259Y
Control
HK-1 (10.0 μM)
B
β-hexosaminidase (% Release)
WT
N16H
W243R
H259Y
Control
hBD3 (3.0 μM)
C
β-hexosaminidase (% Release)
WT
N16H
W243R
H259Y
Control
Icatibant (25.0 μg/ml)

Fig. 6: Effects of MRGPRX2 mutations (N16H, W243R and H259Y) on degranulation in response to HK-1, hBD3 and icatibant.

RBL cells transiently expressing WT, N16H, W243R and H259Y variants were stimulated with **(A),** HK-1 (10 μM) **(B),** hBD3 (3 μM) and **(C),** icatibant (25 μg/ml) and β-hexosaminidase release was determined. Statistical significance was determined by two tailed unpaired t-Test. *** indicates P value<.001, ** indicates P value <.01 and * indicates P value <.05.

Conclusion and Future Directions

MCs are pleiotropic cells that can be activated through various receptors when they are exposed to the corresponding ligands. Activated MCs release several mediators which can have proinflammatory, anti-inflammatory, or immunoregulatory functions. In this thesis I discussed the possible role of GPCR MRGPRX2/Mrgprb2 that known to be expressed predominantly in MCs among all other immune cells, in health and disease. Although Mrgprb2 was originally identified as the mouse ortholog of human MRGPRX2 in CTMCs, a recent study demonstrated that Mrgprb1, Mrgprb10, and Mrgprc11 are also expressed in these MCs [74]. The positive role of MRGPRX2/Mrgprb2 in mediating MC activation and protection against pathogens was discussed in the second chapter. We demonstrated the ability of the novel compounds named small molecule Host Defense Peptidomimetics (smHDPMs) in inducing MCs degranulation via this receptor and its possible significant impact when treating multidrug resistant microbes not only by its direct antimicrobial activity but by harnessing MCs activity as well.

The other side of the coin is the negative role of MRGPRX2/Mrgprb2 in mediating MCs activation when the innate host defense is dysregulated. This was discussed in the third chapter in the contest of rosacea. In addition to C57BL/6 and MC-deficient (W^{sh}/W^{sh}) mouse models, we used a Mrgprb2 $^{-/-}$ mouse model to delineate the MC and receptor role in rosacea pathogenesis. We showed that MRGPRX2/Mrgprb2 is a major effector in mediating MC activation and immune

cells recruitments in rosacea *in vitro* and *in vivo*. It is important to consider the possible differences between the human and mouse receptor that we discussed earlier in chapter one in regard to the differences in the ligand concentration required to stimulate MRGPRX2 (human) or Mrgprb2 (mouse) [40]. This renders the mouse receptor unsuitable to screen drugs to be used in humans.

Growing evidence indicating TRPV4 is significantly involved in rosacea development [113, 115]. However, TRPV4 inhibitor and TRPV4-knockdown $CD34^{+}$ derived MCs only resulted to in partial reduction in MRGPRX2 mediated MCs activation [115]. Therefore, chapter three also studied possible contribution STIM1/Orai1 calcium channel in mediating Ca^{+2} influx in MCs when stimulated with the key ligands in rosacea: LL-37 and SP. In addition to the LAD2 human MC line, we also used MCs isolated from patients' skin. This allowed deeper insight into the role of Orai Ca^{2+} channels in skin MCs and rosacea. One drawback in using skin MCs was the limitation in obtaining high numbers from each sample. We therefore used skin MCs at the initial phase of the experiments, then we utilized LAD2 cell line to overcome this limitation and to conduct more experiments using pharmacological and genetic approaches. Thus, we believe chapter three adds to the growing body of research that indicates the pivotal role of MCs and Ca^{2+} channels in rosacea. Future researches can focus on delineating the role of other members of the Orai Ca^{2+} channels, Orai2 and Orai3 and to possibly enhance the yield of skin MCs isolation to conduct more experiments that will give true representation of what happen in the skin.

The final part of this thesis took a closer look at studying the structure of MRGPRX2 itself. MRGPRX2 consists of amino acids which form seven transmembrane (TM) bundles that are connected by three extracellular loops and three intracellular loops. We selected eight missense mutants that located in extracellular (EC) and EC-TM regions according to crystallography data and comparison of sequence homology. These regions are known to be involved in ligand binding [150]. We have shown that the replacement of neutral or negatively charged amino acid residues in the ligand binding pocket of MRGPRX2 with positively charged residues in the naturally occurring MRGPRX2 variants (G194E and D184H) renders the receptor unresponsive to ligands that induce pseudo-allergic drug reactions and chronic inflammatory diseases.

Moreover, although the naturally occurring variants W243R and H259Y in the receptor's 6^{th} and 7^{th} TM domain also rendered the receptor unresponsive to all ligands tested for Ca^{2+} mobilization and degranulation, the exact mechanism of their actions are unknown and remain to be determined. Nevertheless, an important clinical implication for this chapter is that individuals harboring any of the single loss of function missense mutation (G165E, D184H, W243R and, H259Y) may be protected from MRGPRX2-mediated pseudo-allergy and chronic inflammatory diseases. The presence of these mutations may thus serve as biomarkers to predict individuals who may be resistant to developing injection site reactions to commonly used drugs and MC-mediated chronic inflammatory diseases.

List of Publications

1. **Small-Molecule Host-Defense Peptide Mimetic antibacterial and antifungal agents activate human and mouse mast cells via Mas-Related GPCRs. *Cells, 2019*.**

2. **Naturally occurring Missense MRGPRX2 variants display Loss of Function Phenotype for Mast Cell Degranulation in response to Substance P, Hemokinin-1, Human β-defensin 3 and Icatibant. *Journal of Immunology, 2018.***

References

1. Reber, L.L., et al., *Potential effector and immunoregulatory functions of mast cells in mucosal immunity.* Mucosal Immunol, 2015. **8**(3): p. 444-63.
2. Gilfillan, A.M., S.J. Austin, and D.D. Metcalfe, *Mast cell biology: introduction and overview.* Adv Exp Med Biol, 2011. **716**: p. 2-12.
3. Hallgren, J. and M.F. Gurish, *Mast cell progenitor trafficking and maturation.* Adv Exp Med Biol, 2011. **716**: p. 14-28.
4. Metz, M., F. Siebenhaar, and M. Maurer, *Mast cell functions in the innate skin immune system.* Immunobiology, 2008. **213**(3-4): p. 251-60.
5. Boesiger, J., et al., *Mast cells can secrete vascular permeability factor/ vascular endothelial cell growth factor and exhibit enhanced release after immunoglobulin E-dependent upregulation of fc epsilon receptor I expression.* J Exp Med, 1998. **188**(6): p. 1135-45.
6. Echtenacher, B., D.N. Mannel, and L. Hultner, *Critical protective role of mast cells in a model of acute septic peritonitis.* Nature, 1996. **381**(6577): p. 75-7.
7. Supajatura, V., et al., *Protective roles of mast cells against enterobacterial infection are mediated by Toll-like receptor 4.* J Immunol, 2001. **167**(4): p. 2250-6.
8. Di Nardo, A., A. Vitiello, and R.L. Gallo, *Cutting edge: mast cell antimicrobial activity is mediated by expression of cathelicidin antimicrobial peptide.* J Immunol, 2003. **170**(5): p. 2274-8.
9. Metz, M., et al., *Mast cells can enhance resistance to snake and honeybee venoms.* Science, 2006. **313**(5786): p. 526-30.
10. Jawdat, D.M., G. Rowden, and J.S. Marshall, *Mast cells have a pivotal role in TNF-independent lymph node hypertrophy and the mobilization of Langerhans cells in response to bacterial peptidoglycan.* J Immunol, 2006. **177**(3): p. 1755-62.
11. Bryce, P.J., et al., *Immune sensitization in the skin is enhanced by antigen-independent effects of IgE.* Immunity, 2004. **20**(4): p. 381-92.
12. Galli, S.J., S. Nakae, and M. Tsai, *Mast cells in the development of adaptive immune responses.* Nat Immunol, 2005. **6**(2): p. 135-42.
13. Stelekati, E., et al., *Mast cell-mediated antigen presentation regulates CD8+ T cell effector functions.* Immunity, 2009. **31**(4): p. 665-76.
14. Lagdive, S.S., et al., *Correlation of mast cells in periodontal diseases.* J Indian Soc Periodontol, 2013. **17**(1): p. 63-7.
15. Huang, S., et al., *Mast cell degranulation in human periodontitis.* J Periodontol, 2013. **84**(2): p. 248-55.
16. Malcolm, J., et al., *Mast Cells Contribute to Porphyromonas gingivalis-induced Bone Loss.* J Dent Res, 2016. **95**(6): p. 704-10.

17. Mihm, M.C., Jr., et al., *The structure of normal skin and the morphology of atopic eczema.* J Invest Dermatol, 1976. **67**(3): p. 305-12.
18. Nankervis, H., et al., in *Scoping systematic review of treatments for eczema*. 2016: Southampton (UK).
19. Sokol, K.C., et al., *Ketotifen in the management of chronic urticaria: resurrection of an old drug.* Ann Allergy Asthma Immunol, 2013. **111**(6): p. 433-6.
20. Steinhoff, M., et al., *Modern aspects of cutaneous neurogenic inflammation.* Arch Dermatol, 2003. **139**(11): p. 1479-88.
21. Janiszewski, J., J. Bienenstock, and M.G. Blennerhassett, *Picomolar doses of substance P trigger electrical responses in mast cells without degranulation.* Am J Physiol, 1994. **267**(1 Pt 1): p. C138-45.
22. Forsythe, P. and J. Bienenstock, *The mast cell-nerve functional unit: a key component of physiologic and pathophysiologic responses.* Chem Immunol Allergy, 2012. **98**: p. 196-221.
23. Steinhoff, M., et al., *Agonists of proteinase-activated receptor 2 induce inflammation by a neurogenic mechanism.* Nat Med, 2000. **6**(2): p. 151-8.
24. Taylor-Clark, T.E., C. Nassenstein, and B.J. Undem, *Leukotriene D4 increases the excitability of capsaicin-sensitive nasal sensory nerves to electrical and chemical stimuli.* Br J Pharmacol, 2008. **154**(6): p. 1359-68.
25. Vena, G.A., et al., *Focus on the role of substance P in chronic urticaria.* Clin Mol Allergy, 2018. **16**: p. 24.
26. Spergel, J.M., et al., *Roles of TH1 and TH2 cytokines in a murine model of allergic dermatitis.* J Clin Invest, 1999. **103**(8): p. 1103-11.
27. Metcalfe, D.D., D. Baram, and Y.A. Mekori, *Mast cells.* Physiol Rev, 1997. **77**(4): p. 1033-79.
28. Moon, T.C., A.D. Befus, and M. Kulka, *Mast cell mediators: their differential release and the secretory pathways involved.* Front Immunol, 2014. **5**: p. 569.
29. Schwartz, L.B., et al., *Acid hydrolases and tryptase from secretory granules of dispersed human lung mast cells.* J Immunol, 1981. **126**(4): p. 1290-4.
30. Olszewski, M.B., et al., *TNF trafficking to human mast cell granules: mature chain-dependent endocytosis.* J Immunol, 2007. **178**(9): p. 5701-9.
31. de Paulis, A., et al., *Stem cell factor is localized in, released from, and cleaved by human mast cells.* J Immunol, 1999. **163**(5): p. 2799-808.
32. Stevens, R.L., et al., *Identification of chondroitin sulfate E proteoglycans and heparin proteoglycans in the secretory granules of human lung mast cells.* Proc Natl Acad Sci U S A, 1988. **85**(7): p. 2284-7.
33. Olivera, A. and J. Rivera, *An emerging role for the lipid mediator sphingosine-1-phosphate in mast cell effector function and allergic disease.* Adv Exp Med Biol, 2011. **716**: p. 123-42.
34. Gonzalez-Espinosa, C., et al., *Preferential signaling and induction of allergy-promoting lymphokines upon weak stimulation of the high affinity IgE receptor on mast cells.* J Exp Med, 2003. **197**(11): p. 1453-65.

35. Nakahashi-Oda, C., et al., *Apoptotic cells suppress mast cell inflammatory responses via the CD300a immunoreceptor.* J Exp Med, 2012. **209**(8): p. 1493-503.
36. Theoharides, T.C., et al., *Mast cells and inflammation.* Biochim Biophys Acta, 2012. **1822**(1): p. 21-33.
37. Irani, A.M., et al., *Deficiency of the tryptase-positive, chymase-negative mast cell type in gastrointestinal mucosa of patients with defective T lymphocyte function.* J Immunol, 1987. **138**(12): p. 4381-6.
38. Oskeritzian, C.A., et al., *Surface CD88 functionally distinguishes the MCTC from the MCT type of human lung mast cell.* J Allergy Clin Immunol, 2005. **115**(6): p. 1162-8.
39. Vassilatis, D.K., et al., *The G protein-coupled receptor repertoires of human and mouse.* Proc Natl Acad Sci U S A, 2003. **100**(8): p. 4903-8.
40. McNeil, B.D., et al., *Identification of a mast-cell-specific receptor crucial for pseudo-allergic drug reactions.* Nature, 2015. **519**(7542): p. 237-41.
41. Vibhuti, A., et al., *Distinct and shared roles of beta-arrestin-1 and beta-arrestin-2 on the regulation of C3a receptor signaling in human mast cells.* PLoS One, 2011. **6**(5): p. e19585.
42. Subramanian, H., et al., *beta-Defensins activate human mast cells via Mas-related gene X2.* J Immunol, 2013. **191**(1): p. 345-52.
43. Fujisawa, D., et al., *Expression of Mas-related gene X2 on mast cells is upregulated in the skin of patients with severe chronic urticaria.* J Allergy Clin Immunol, 2014. **134**(3): p. 622-633 e9.
44. Gloriam, D.E., R. Fredriksson, and H.B. Schioth, *The G protein-coupled receptor subset of the rat genome.* BMC Genomics, 2007. **8**: p. 338.
45. Tatemoto, K., et al., *Immunoglobulin E-independent activation of mast cell is mediated by Mrg receptors.* Biochem Biophys Res Commun, 2006. **349**(4): p. 1322-8.
46. Katritch, V., V. Cherezov, and R.C. Stevens, *Diversity and modularity of G protein-coupled receptor structures.* Trends Pharmacol Sci, 2012. **33**(1): p. 17-27.
47. Frossi, B., et al., *Rheostatic Functions of Mast Cells in the Control of Innate and Adaptive Immune Responses.* Trends Immunol, 2017. **38**(9): p. 648-656.
48. Shiota, N., et al., *Pathophysiological role of skin mast cells in wound healing after scald injury: study with mast cell-deficient W/W(V) mice.* Int Arch Allergy Immunol, 2010. **151**(1): p. 80-8.
49. Groschwitz, K.R., et al., *Mast cells regulate homeostatic intestinal epithelial migration and barrier function by a chymase/Mcpt4-dependent mechanism.* Proc Natl Acad Sci U S A, 2009. **106**(52): p. 22381-6.
50. Arifuzzaman, M., et al., *MRGPR-mediated activation of local mast cells clears cutaneous bacterial infection and protects against reinfection.* Sci Adv, 2019. **5**(1): p. eaav0216.
51. Irani, A.A., et al., *Two types of human mast cells that have distinct neutral protease compositions.* Proc Natl Acad Sci U S A, 1986. **83**(12): p. 4464-8.

52. Bankova, L.G., et al., *Maturation of mast cell progenitors to mucosal mast cells during allergic pulmonary inflammation in mice.* Mucosal Immunol, 2015. **8**(3): p. 596-606.
53. Dwyer, D.F., et al., *Expression profiling of constitutive mast cells reveals a unique identity within the immune system.* Nat Immunol, 2016. **17**(7): p. 878-87.
54. Thakurdas, S.M., et al., *The mast cell-restricted tryptase mMCP-6 has a critical immunoprotective role in bacterial infections.* J Biol Chem, 2007. **282**(29): p. 20809-15.
55. Piliponsky, A.M. and L. Romani, *The contribution of mast cells to bacterial and fungal infection immunity.* Immunol Rev, 2018. **282**(1): p. 188-197.
56. Malaviya, R. and S.N. Abraham, *Role of mast cell leukotrienes in neutrophil recruitment and bacterial clearance in infectious peritonitis.* J Leukoc Biol, 2000. **67**(6): p. 841-6.
57. Romani, L., *Immunity to fungal infections.* Nat Rev Immunol, 2011. **11**(4): p. 275-88.
58. Bassetti, M., et al., *Epidemiology, species distribution, antifungal susceptibility and outcome of nosocomial candidemia in a tertiary care hospital in Italy.* PLoS One, 2011. **6**(9): p. e24198.
59. Guery, B.P., et al., *Management of invasive candidiasis and candidemia in adult non-neutropenic intensive care unit patients: Part I. Epidemiology and diagnosis.* Intensive Care Med, 2009. **35**(1): p. 55-62.
60. Guery, B.P., et al., *Management of invasive candidiasis and candidemia in adult non-neutropenic intensive care unit patients: Part II. Treatment.* Intensive Care Med, 2009. **35**(2): p. 206-14.
61. Laxminarayan, R., et al., *Antibiotic resistance-the need for global solutions.* Lancet Infect Dis, 2013. **13**(12): p. 1057-98.
62. Diamond, G., et al., *The roles of antimicrobial peptides in innate host defense.* Curr Pharm Des, 2009. **15**(21): p. 2377-92.
63. Hancock, R.E. and G. Diamond, *The role of cationic antimicrobial peptides in innate host defences.* Trends Microbiol, 2000. **8**(9): p. 402-10.
64. Mahlapuu, M., et al., *Antimicrobial Peptides: An Emerging Category of Therapeutic Agents.* Front Cell Infect Microbiol, 2016. **6**: p. 194.
65. Shai, Y., *From innate immunity to de-novo designed antimicrobial peptides.* Curr Pharm Des, 2002. **8**(9): p. 715-25.
66. Yeaman, M.R. and N.Y. Yount, *Mechanisms of antimicrobial peptide action and resistance.* Pharmacol Rev, 2003. **55**(1): p. 27-55.
67. Subramanian, H., et al., *Mas-related gene X2 (MrgX2) is a novel G protein-coupled receptor for the antimicrobial peptide LL-37 in human mast cells: resistance to receptor phosphorylation, desensitization, and internalization.* J Biol Chem, 2011. **286**(52): p. 44739-49.
68. Koczulla, R., et al., *An angiogenic role for the human peptide antibiotic LL-37/hCAP-18.* J Clin Invest, 2003. **111**(11): p. 1665-72.
69. Hirsch, T., et al., *Human beta-defensin-3 promotes wound healing in infected diabetic wounds.* J Gene Med, 2009. **11**(3): p. 220-8.

70. Gupta, K., et al., *Activation of human mast cells by retrocyclin and protegrin highlight their immunomodulatory and antimicrobial properties.* Oncotarget, 2015. **6**(30): p. 28573-87.
71. Scott, R.W. and G.N. Tew, *Mimics of Host Defense Proteins; Strategies for Translation to Therapeutic Applications.* Curr Top Med Chem, 2017. **17**(5): p. 576-589.
72. Choi, S., et al., *De novo design and in vivo activity of conformationally restrained antimicrobial arylamide foldamers.* Proc Natl Acad Sci U S A, 2009. **106**(17): p. 6968-73.
73. Beckloff, N., et al., *Activity of an antimicrobial peptide mimetic against planktonic and biofilm cultures of oral pathogens.* Antimicrob Agents Chemother, 2007. **51**(11): p. 4125-32.
74. Yamada, K., et al., *Suppression of IgE-Independent Degranulation of Murine Connective Tissue-Type Mast Cells by Dexamethasone.* Cells, 2019. **8**(2).
75. Alkanfari, I., et al., *Naturally Occurring Missense MRGPRX2 Variants Display Loss of Function Phenotype for Mast Cell Degranulation in Response to Substance P, Hemokinin-1, Human beta-Defensin-3, and Icatibant.* J Immunol, 2018. **201**(2): p. 343-349.
76. Steinberg, D.A., et al., *Protegrin-1: a broad-spectrum, rapidly microbicidal peptide with in vivo activity.* Antimicrob Agents Chemother, 1997. **41**(8): p. 1738-42.
77. Yan, H. and R.E. Hancock, *Synergistic interactions between mammalian antimicrobial defense peptides.* Antimicrob Agents Chemother, 2001. **45**(5): p. 1558-60.
78. Ryan, L.K., et al., *Activity of potent and selective host defense peptide mimetics in mouse models of oral candidiasis.* Antimicrob Agents Chemother, 2014. **58**(7): p. 3820-7.
79. Kirshenbaum, A.S., et al., *Characterization of novel stem cell factor responsive human mast cell lines LAD 1 and 2 established from a patient with mast cell sarcoma/leukemia; activation following aggregation of FcepsilonRI or FcgammaRI.* Leuk Res, 2003. **27**(8): p. 677-82.
80. Ali, H., et al., *Regulation of stably transfected platelet activating factor receptor in RBL-2H3 cells. Role of multiple G proteins and receptor phosphorylation.* J Biol Chem, 1994. **269**(40): p. 24557-63.
81. Mrabet-Dahbi, S., et al., *Murine mast cells secrete a unique profile of cytokines and prostaglandins in response to distinct TLR2 ligands.* Exp Dermatol, 2009. **18**(5): p. 437-44.
82. Vukman, K.V., et al., *Mast cells cultured from IL-3-treated mice show impaired responses to bacterial antigen stimulation.* Inflamm Res, 2012. **61**(1): p. 79-85.
83. Hua, J., et al., *Activity of antimicrobial peptide mimetics in the oral cavity: I. Activity against biofilms of Candida albicans.* Mol Oral Microbiol, 2010. **25**(6): p. 418-25.

84. Hua, J., R.W. Scott, and G. Diamond, *Activity of antimicrobial peptide mimetics in the oral cavity: II. Activity against periopathogenic biofilms and anti-inflammatory activity.* Mol Oral Microbiol, 2010. **25**(6): p. 426-32.
85. Menzel, L.P., et al., *Potent in vitro and in vivo antifungal activity of a small molecule host defense peptide mimic through a membrane-active mechanism.* Sci Rep, 2017. **7**(1): p. 4353.
86. Scott, A., et al., *Evaluation of the ability of LL-37 to neutralise LPS in vitro and ex vivo.* PLoS One, 2011. **6**(10): p. e26525.
87. Saluja, R., M. Metz, and M. Maurer, *Role and relevance of mast cells in fungal infections.* Front Immunol, 2012. **3**: p. 146.
88. Saunte, D.M., et al., *Black yeast-like fungi in skin and nail: it probably matters.* Mycoses, 2012. **55**(2): p. 161-7.
89. Sauer, A., et al., *In vitro efficacy of antifungal treatment using riboflavin/UV-A (365 nm) combination and amphotericin B.* Invest Ophthalmol Vis Sci, 2010. **51**(8): p. 3950-3.
90. Thomas, P.A. and J. Kaliamurthy, *Mycotic keratitis: epidemiology, diagnosis and management.* Clin Microbiol Infect, 2013. **19**(3): p. 210-20.
91. Xie, Y., et al., *Mast Cell Activation Protects Cornea by Promoting Neutrophil Infiltration via Stimulating ICAM-1 and Vascular Dilation in Fungal Keratitis.* Sci Rep, 2018. **8**(1): p. 8365.
92. Gupta, K., et al., *Differential Regulation of Mas-Related G Protein-Coupled Receptor X2-Mediated Mast Cell Degranulation by Antimicrobial Host Defense Peptides and Porphyromonas gingivalis Lipopolysaccharide.* Infect Immun, 2017. **85**(10).
93. Manorak, W., et al., *Upregulation of Mas-related G Protein coupled receptor X2 in asthmatic lung mast cells and its activation by the novel neuropeptide hemokinin-1.* Respir Res, 2018. **19**(1): p. 1.
94. Babina, M., et al., *Allergic FcepsilonRI- and pseudo-allergic MRGPRX2-triggered mast cell activation routes are independent and inversely regulated by SCF.* Allergy, 2018. **73**(1): p. 256-260.
95. Di Nardo, A., et al., *Mast cell cathelicidin antimicrobial peptide prevents invasive group A Streptococcus infection of the skin.* J Immunol, 2008. **180**(11): p. 7565-73.
96. Yang, B., et al., *IL-27 Facilitates Skin Wound Healing through Induction of Epidermal Proliferation and Host Defense.* J Invest Dermatol, 2017. **137**(5): p. 1166-1175.
97. Kowalski, R.P., et al., *An Independent Evaluation of a Novel Peptide Mimetic, Brilacidin (PMX30063), for Ocular Anti-infective.* J Ocul Pharmacol Ther, 2016. **32**(1): p. 23-7.
98. Yoshino, N., et al., *Polymyxins as novel and safe mucosal adjuvants to induce humoral immune responses in mice.* PLoS One, 2013. **8**(4): p. e61643.
99. Reinholz, M., et al., *Pathogenesis and clinical presentation of rosacea as a key for a symptom-oriented therapy.* J Dtsch Dermatol Ges, 2016. **14 Suppl 6**: p. 4-15.

100. Schwab, V.D., et al., *Neurovascular and neuroimmune aspects in the pathophysiology of rosacea.* J Investig Dermatol Symp Proc, 2011. **15**(1): p. 53-62.
101. Moustafa, F.A., L.F. Sandoval, and S.R. Feldman, *Rosacea: new and emerging treatments.* Drugs, 2014. **74**(13): p. 1457-65.
102. Schauber, J. and R.L. Gallo, *Antimicrobial peptides and the skin immune defense system.* J Allergy Clin Immunol, 2008. **122**(2): p. 261-6.
103. Arck, P.C., et al., *Neuroimmunology of stress: skin takes center stage.* J Invest Dermatol, 2006. **126**(8): p. 1697-704.
104. Cevikbas, F., et al., *Neuroimmune interactions in allergic skin diseases.* Curr Opin Allergy Clin Immunol, 2007. **7**(5): p. 365-73.
105. Aroni, K., et al., *A study of the pathogenesis of rosacea: how angiogenesis and mast cells may participate in a complex multifactorial process.* Arch Dermatol Res, 2008. **300**(3): p. 125-31.
106. Buhl, T., et al., *Molecular and Morphological Characterization of Inflammatory Infiltrate in Rosacea Reveals Activation of Th1/Th17 Pathways.* J Invest Dermatol, 2015. **135**(9): p. 2198-208.
107. Helfrich, Y.R., et al., *Clinical, Histologic, and Molecular Analysis of Differences Between Erythematotelangiectatic Rosacea and Telangiectatic Photoaging.* JAMA Dermatol, 2015.
108. Muto, Y., et al., *Mast cells are key mediators of cathelicidin-initiated skin inflammation in rosacea.* J Invest Dermatol, 2014. **134**(11): p. 2728-2736.
109. Reich, A., A. Wojcik-Maciejewicz, and A.T. Slominski, *Stress and the skin.* G Ital Dermatol Venereol, 2010. **145**(2): p. 213-9.
110. Azimi, E. and E.A. Lerner, *Implications of MRGPRX2 in human and experimental cardiometabolic diseases.* Nat Rev Cardiol, 2017. **14**(2): p. 124.
111. Jin, H., et al., *Animal models of atopic dermatitis.* J Invest Dermatol, 2009. **129**(1): p. 31-40.
112. Takamori, A., et al., *Identification of inhibitory mechanisms in pseudo-allergy involving Mrgprb2/MRGPRX2-mediated mast cell activation.* J Allergy Clin Immunol, 2018.
113. Sulk, M., et al., *Distribution and expression of non-neuronal transient receptor potential (TRPV) ion channels in rosacea.* J Invest Dermatol, 2012. **132**(4): p. 1253-62.
114. Chen, Y., et al., *TRPV4 Moves toward Center-Fold in Rosacea Pathogenesis.* J Invest Dermatol, 2017. **137**(4): p. 801-804.
115. Mascarenhas, N.L., et al., *TRPV4 Mediates Mast Cell Activation in Cathelicidin-Induced Rosacea Inflammation.* J Invest Dermatol, 2017. **137**(4): p. 972-975.
116. Ashmole, I., et al., *The contribution of Orai(CRACM)1 and Orai(CRACM)2 channels in store-operated Ca2+ entry and mediator release in human lung mast cells.* PLoS One, 2013. **8**(9): p. e74895.
117. Ashmole, I., et al., *CRACM/Orai ion channel expression and function in human lung mast cells.* J Allergy Clin Immunol, 2012. **129**(6): p. 1628-35 e2.

118. Robas, N., E. Mead, and M. Fidock, *MrgX2 is a high potency cortistatin receptor expressed in dorsal root ganglion.* J Biol Chem, 2003. **278**(45): p. 44400-4.
119. Yamasaki, K., et al., *Increased serine protease activity and cathelicidin promotes skin inflammation in rosacea.* Nat Med, 2007. **13**(8): p. 975-80.
120. Woo, Y.R., et al., *Rosacea: Molecular Mechanisms and Management of a Chronic Cutaneous Inflammatory Condition.* Int J Mol Sci, 2016. **17**(9).
121. Heron, A. and D. Dubayle, *A focus on mast cells and pain.* J Neuroimmunol, 2013. **264**(1-2): p. 1-7.
122. Holowka, D., et al., *Roles for Ca2+ mobilization and its regulation in mast cell functions: recent progress.* Biochem Soc Trans, 2016. **44**(2): p. 505-9.
123. Baba, Y., et al., *Essential function for the calcium sensor STIM1 in mast cell activation and anaphylactic responses.* Nat Immunol, 2008. **9**(1): p. 81-8.
124. Choi, J.E., et al., *Botulinum toxin blocks mast cells and prevents rosacea like inflammation.* J Dermatol Sci, 2019. **93**(1): p. 58-64.
125. Kurkcuoglu, N. and F. Alaybeyi, *Substance P immunoreactivity in rosacea.* J Am Acad Dermatol, 1991. **25**(4): p. 725-6.
126. Steinhoff, M., et al., *Clinical, cellular, and molecular aspects in the pathophysiology of rosacea.* J Investig Dermatol Symp Proc, 2011. **15**(1): p. 2-11.
127. Green, D.P., et al., *A Mast-Cell-Specific Receptor Mediates Neurogenic Inflammation and Pain.* Neuron, 2019. **101**(3): p. 412-420 e3.
128. Meixiong, J., et al., *Activation of Mast-Cell-Expressed Mas-Related G-Protein-Coupled Receptors Drives Non-histaminergic Itch.* Immunity, 2019.
129. Wajdner, H.E., et al., *Orai and TRPC channel characterization in FcepsilonRI-mediated calcium signaling and mediator secretion in human mast cells.* Physiol Rep, 2017. **5**(5).
130. Subramanian, H., et al., *PMX-53 as a dual CD88 antagonist and an agonist for Mas-related gene 2 (MrgX2) in human mast cells.* Mol Pharmacol, 2011. **79**(6): p. 1005-13.
131. Azimi, E., V.B. Reddy, and E.A. Lerner, *Brief communication: MRGPRX2, atopic dermatitis and red man syndrome.* Itch (Phila), 2017. **2**(1).
132. Azimi, E., et al., *Substance P activates Mas-related G protein-coupled receptors to induce itch.* J Allergy Clin Immunol, 2017. **140**(2): p. 447-453 e3.
133. Okamura, Y., et al., *The dual regulation of substance P-mediated inflammation via human synovial mast cells in rheumatoid arthritis.* Allergol Int, 2017. **66S**: p. S9-S20.
134. Reddy, V.B., et al., *Mas-Related G-Protein Coupled Receptors and Cowhage-Induced Itch.* J Invest Dermatol, 2018. **138**(2): p. 461-464.
135. Grassin-Delyle, S., et al., *Expression and function of human hemokinin-1 in human and guinea pig airways.* Respir Res, 2010. **11**: p. 139.
136. Sumpter, T.L., et al., *Autocrine hemokinin-1 functions as an endogenous adjuvant for IgE-mediated mast cell inflammatory responses.* J Allergy Clin Immunol, 2015. **135**(4): p. 1019-30 e8.

137. Jin, L., *An update on innate defense molecules of human gingiva.* Periodontol 2000, 2011. **56**(1): p. 125-42.
138. Lumry, W.R., et al., *Randomized placebo-controlled trial of the bradykinin B(2) receptor antagonist icatibant for the treatment of acute attacks of hereditary angioedema: the FAST-3 trial.* Ann Allergy Asthma Immunol, 2011. **107**(6): p. 529-37.
139. Reddy, V.B., et al., *A single amino acid in MRGPRX2 necessary for binding and activation by pruritogens.* J Allergy Clin Immunol, 2017. **140**(6): p. 1726-1728.
140. Lansu, K., et al., *In silico design of novel probes for the atypical opioid receptor MRGPRX2.* Nat Chem Biol, 2017. **13**(5): p. 529-536.
141. Adzhubei, I., D.M. Jordan, and S.R. Sunyaev, *Predicting functional effect of human missense mutations using PolyPhen-2.* Curr Protoc Hum Genet, 2013. **Chapter 7**: p. Unit7 20.
142. Kircher, M., et al., *A general framework for estimating the relative pathogenicity of human genetic variants.* Nat Genet, 2014. **46**(3): p. 310-5.
143. Hauser, A.S., et al., *Pharmacogenomics of GPCR Drug Targets.* Cell, 2018. **172**(1-2): p. 41-54 e19.
144. Doyle, J.R., et al., *Naturally occurring HCA1 missense mutations result in loss of function: potential impact on lipid deposition.* J Lipid Res, 2013. **54**(3): p. 823-30.
145. Fischer, L., et al., *Functional relevance of naturally occurring mutations in adhesion G protein-coupled receptor ADGRD1 (GPR133).* BMC Genomics, 2016. **17**(1): p. 609.
146. Subramanian, H., K. Gupta, and H. Ali, *Roles of Mas-related G protein-coupled receptor X2 on mast cell-mediated host defense, pseudoallergic drug reactions, and chronic inflammatory diseases.* J Allergy Clin Immunol, 2016. **138**(3): p. 700-10.
147. Ali, H., *Emerging Roles for MAS-Related G Protein-Coupled Receptor-X2 in Host Defense Peptide, Opioid, and Neuropeptide-Mediated Inflammatory Reactions.* Adv Immunol, 2017. **136**: p. 123-162.
148. Gaudenzio, N., et al., *Different activation signals induce distinct mast cell degranulation strategies.* J Clin Invest, 2016. **126**(10): p. 3981-3998.
149. Karhausen, J. and S.N. Abraham, *How mast cells make decisions.* J Clin Invest, 2016. **126**(10): p. 3735-3738.
150. Katritch, V., V. Cherezov, and R.C. Stevens, *Structure-function of the G protein-coupled receptor superfamily.* Annu Rev Pharmacol Toxicol, 2013. **53**: p. 531-56.